Fig. 5.3-15(1) Calculated Water Quality in Case 6-1(Deepening the channels in 2010)(BOD) 5-68
Fig. 5.3-15(2) Calculated Water Quality in Case 6-1(Deepening the channels in 2010)(T-P) 5-69
Fig. 5.3-15(3) Calculated Water Quality in Case 6-1(Deepening the channels in 2010)(DO) 5-70
Fig. 5.3-16(1) Calculated Water Quality in Case 6-2(Deepening the channels in 2010)(BOD) 5-71
Fig. 5.3-16(2) Calculated Water Quality in Case 6-2(Deepening the channels in 2010)(DO) 5-72
Fig. 5.3-16(3) Calculated Water Quality in Case 6-2(Deepening the channels in 2010)(T-P) 5-73
Fig. 5.3-17(1) Calculated Water Quality in Case 6-3(BOD)(Filling up the channel sidelong the Governador) 5-74
Fig. 5.3-17(2) Calculated Water Quality in Case 6-3(DO)(Filling up the channel sidelong the Governador) 5-75
Fig. 5.3-17(3) Calculated Water Quality in Case 6-3(T-P)(Filling up the channel sidelong the Governador) 5-76
Fig. 5.3-18(1) Calculated Water Quality in Case 6-4(BOD)(Filling up the channel sidelong the Fundo) 5-77
Fig. 5.3-18(2) Calculated Water Quality in Case 6-4(DO)(Filling up the channel sidelong the Fundo) 5-78
Fig. 5.3-18(3) Calculated Water Quality in Case 6-4(T-P)(Filling up the channel sidelong the Fundo) 5-79
Fig. 5.4-1(1) External Load from Sub-Basin Groups 5-81
Fig. 5.4-1(2) External Load from Sub-Basin Groups 5-82
Fig. 5.4-2 Water Quality Change in each Block 5-83
Fig. 5.4-3(1) BOD Concentration and Variation in each Block 5-84
Fig. 5.4-3(2) DO Concentration and Variation in each Block 5-85
Fig. 5.4-3(3) T-P Concentration and Variation in each Block 5-86
Fig. 5.4-4(1) External Load from Sub-Basin Groups 5-88
Fig. 5.4-4(2) External Load from Sub-Basin Groups 5-89
Fig. 5.4-5 Water Quality Change in each Block 5-90
Fig. 5.4-6(1) BOD Concentration and Variation in each Block 5-91
Fig. 5.4-6(2) DO Concentration and Variation in each Block 5-92
Fig. 5.4-6(3) T-P Concentration and Variation in each Block 5-93
Fig. 5.4-7(1) External Load from Sub-Basin Groups 5-95
Fig. 5.4-7(2) External Load from Sub-Basin Groups 5-96
Fig. 5.4-8 Water Quality Change in each Block 5-97
Fig. 5.4-9(1) BOD Concentration and Variation in each Block 5-98
Fig. 5.4-9(2) T-P Concentration and Variation in each Block 5-99
Fig. 5.4-9(3) DO Concentration and Variation in each Block 5-100
Fig. 5.4-10 Water Quality Change in each Block 5-102
Fig. 5.4-11(1) BOD Concentration and Variation in each Block 5-103
Fig. 5.4-11(2) T-P Concentration and Variation in each Block 5-104
Fig. 5.4-11(3) DO Concentration and Variation in each Block 5-105
Fig. 5.4-12 Water Quality Change in each Block 5-107
Fig. 5.4-13(1) BOD Concentration and Variation in each Black 5-108
Fig. 5.4-13(2) T-P Concentration and Variation in each Black 5-109
Fig. 5.4-13(3) DO Concentration and Variation in each Black 5-110
Fig. 5.4-14 Water Quality Change in each Block 5-112
Fig. 5.4-15(1) BOD Concentration and Variation in each Block 5-113
Fig. 5.4-15(2) T-P Concentration and Variation in each Block 5-114
Fig. 5.4-15(3) DO Concentration and Variation in each Block 5-115

CHAPTER 1

NUMERICAL MODELING OF TIDAL CURRENT AND WATER QUALITY

1.1 Structure of the Numerical Simulation Model

A numerical simulation of water quality in the Guanabara Bay has carried out by the procedure of the flow-chart shown in Fig.1.1.-1. Numerical models are composed of three parts. The first is a "Hydrodynamic Model" showing a water circulation by tidal phenomena based on the result of the tidal current observation. The following water quality models are founded on this hydrodynamic model.

The second is a "Diffusion Model" for conservative substances such as salinity.
Generally, a diffusion model is used to estimate the water quality of conservative substances or substances being regarded as conservative. In the enclosed coastal seas, particularly in the water area rich in primary production and release from bottom sediment, an eutrophication model is better for the estimation of water quality. In this study, we used the diffusion model mainly to determine a diffusion coefficient.

The last is an "Eutrophication Model" which is one of a diffusion model and considers a release from bottom sediment as well as a primary production in the water and so on as described in detail later. We used this model for the estimation of water quality in the future and/or for the evaluation of measures.

These numerical simulation models were built on the basis of the results of the field observations and laboratory experiments.

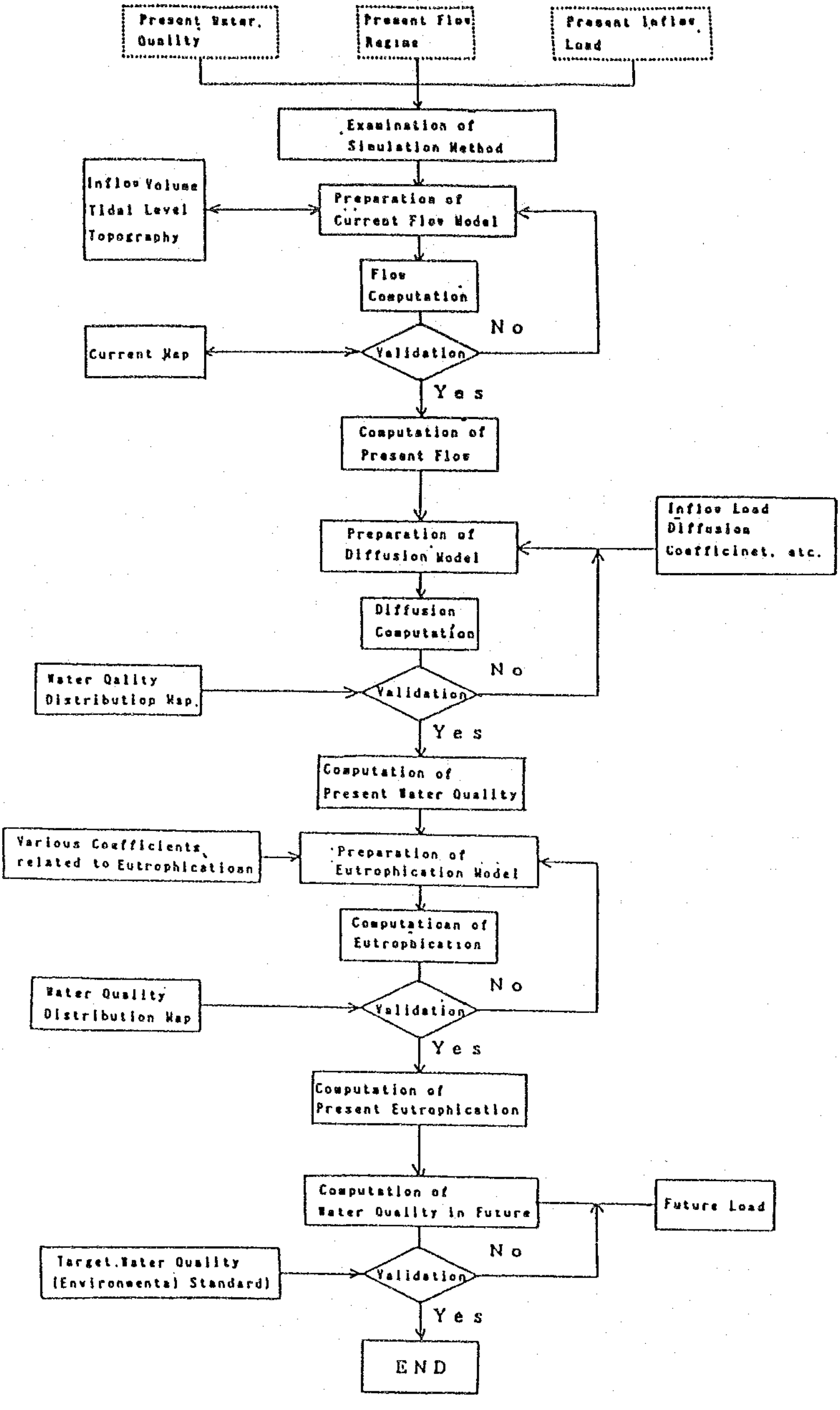

Fig. 1.1-1 Numerical Simulation of Water Quality Analysis

1.2 Hydrodynamic Model

The substances discharged into the bay move by advection and dispersion in the bay. On the reproduction of the flow in a model, an annual or seasonal mean flow is treated in general and various cases are considered with respect to the vertical distribution. In this study, we used a two-level model which can calculate vertical velocity component as well as two horizontal components. We suppose the upper layer as a photic layer.

The system of motion of water such as tidal current is governed by the mass conservation law and momentum conservation law, and is expressed by "Continuity Equation" and "Motion Equation". Tidal current can be estimated by solving these equation numerically. We start the calculation from high tide and solve velocity and water elevation of the calculating area every moment by giving the tidal height at the open boundary in this model. On practice, it needs the following procedure to solve them.

1) Vertical integration of three-dimensional governing equations
2) Converting to finite difference Equations

1.2.1 Governing Equation of Tidal Current

Governing Equation of Tidal Current

Governing Equations of tidal current are composed of the following three-dimensional "Continuity Equation" and "Navior-Stokes Equation".

$$\frac{\partial u}{\partial x}+\frac{\partial v}{\partial y}+\frac{\partial w}{\partial z}=0 \qquad (1)$$

$$\frac{\partial u}{\partial t}+u\frac{\partial u}{\partial x}+v\frac{\partial u}{\partial y}+w\frac{\partial u}{\partial z}=vf-\frac{1}{\rho}\frac{\partial p}{\partial x}+A_h\left(\frac{\partial^2 u}{\partial x^2}+\frac{\partial^2 u}{\partial y^2}\right)+A_v\frac{\partial^2 u}{\partial z^2} \qquad (2)$$

$$\frac{\partial v}{\partial t}+u\frac{\partial v}{\partial x}+v\frac{\partial v}{\partial y}+w\frac{\partial v}{\partial z}=-uf-\frac{1}{\rho}\frac{\partial p}{\partial y}+A_h\left(\frac{\partial^2 v}{\partial x^2}+\frac{\partial^2 v}{\partial y^2}\right)+A_v\frac{\partial^2 v}{\partial z^2} \qquad (3)$$

$$\frac{\partial w}{\partial t}+u\frac{\partial w}{\partial x}+v\frac{\partial w}{\partial y}+w\frac{\partial w}{\partial z}=-g-\frac{1}{\rho}\frac{\partial p}{\partial z}+A_h\left(\frac{\partial^2 w}{\partial x^2}+\frac{\partial^2 w}{\partial y^2}\right)+Az\frac{\partial^2 w}{\partial z^2} \qquad (4)$$

Where,

x,y	:	coordinate directions in the horizontal plane
z	:	coordinate direction in the vertical plane
u,v,w	:	velocity components in x,y,z direction
p	:	pressure
f	:	coriolis coefficient
Ah	:	horizontal eddy viscosity coefficient
Az	:	vertical eddy viscosity coefficient

1.2.2 Governing Equation of Tidal Current in Two-Level Model

Before discussing two-level model, we consider vertical integration about single layer model.

(1) Integration of Continuity Equation

Equation integered equation (1) from the bottom (z=-h) to the surface (z=ζ) is below:

$$\int_{-h}^{\zeta}\left(\frac{\partial u}{\partial x}+\frac{\partial v}{\partial y}\right)dz=-(w_{z=\zeta}-w_{z=-h}) \qquad (5)$$

And U, V are defined the averaged velocity of u, v from bottom to surface as follows:

$$(h+\zeta)U=\int_{-h}^{\zeta}udz,\qquad (h+\zeta)V=\int_{-h}^{\zeta}vdz \qquad (6)$$

The left side of equation (5) are given by a theorem of integration as follows:

$$\int_{-h}^{\zeta}\frac{\partial u}{\partial x}dz=\frac{\partial}{\partial x}\int_{-h}^{\zeta}udz-u\frac{\partial \zeta}{\partial x}-u\frac{\partial h}{\partial x} \qquad (7)$$

$$\int_{-h}^{\zeta}\frac{\partial v}{\partial y}dz=\frac{\partial}{\partial y}\int_{-h}^{\zeta}vdz-v\frac{\partial \zeta}{\partial y}-v\frac{\partial h}{\partial y} \qquad (8)$$

The kinematic boundary condition for the sea surface in the right side of equation (5) is

$$w_{z=\zeta}=\frac{d\zeta}{dt}=\frac{\partial \zeta}{\partial t}+u\frac{\partial \zeta}{\partial x}+v\frac{\partial \zeta}{\partial y} \qquad (9)$$

and the kinematic boundary condition for the sea bottom in the right side of equation (5) is

$$w_{z=-h}=-\frac{dh}{dt}=-u\frac{\partial h}{\partial x}-v\frac{\partial h}{\partial y}\ ,\ \frac{\partial h}{\partial t}=0 \qquad (10)$$

Continuity equation integrated for vertical direction is expressed as blow by substituting equation (7), (8), (9), (10) into equation (5) and by using averaged velocity for a vertical section U,V in equation (6).

$$\frac{\partial \zeta}{\partial t}+\frac{\partial\{(h+\zeta)U\}}{\partial x}+\frac{\partial\{(h+\zeta)V\}}{\partial y}=0 \qquad (11)$$

(2) Integration of Motion Equation

The scale of horizontal motion is much larger than vertical one in the flow of Long period wave such as tidal current. Therefore equation (4) is able to approximate as follow:

$$0=-\frac{1}{\rho}\frac{\partial p}{\partial z}-g \qquad (12)$$

And pressure P is given as equation (13) by integrating equation (12)

$$p=p_{0(z=\zeta)}+g\int_z^{\zeta}\rho dz=p_{0(z=\zeta)}+\rho g(\zeta-z) \qquad (13)$$

Under the assumption the horizontal variation of pressure is very small, $\frac{\partial p}{\partial x},\frac{\partial p}{\partial y}$ are given by equation (13) as follows:

$$-\frac{1}{\rho}\frac{\partial p}{\partial x}=-\frac{1}{\rho}\left\{g(\zeta-z)\frac{\partial \rho}{\partial x}+\rho g\frac{\partial \zeta}{\partial x}\right\}=-g\frac{\partial \zeta}{\partial x}$$

$$-\frac{1}{\rho}\frac{\partial p}{\partial y}=-\frac{1}{\rho}\left\{g(\zeta-z)\frac{\partial \rho}{\partial y}+\rho g\frac{\partial \zeta}{\partial y}\right\}=-g\frac{\partial \zeta}{\partial y} \qquad (14)$$

By substituting equation (14) into equation (2), (3). These equation is converted as follows:

$$\frac{\partial u}{\partial t}+u\frac{\partial u}{\partial x}+v\frac{\partial u}{\partial y}+w\frac{\partial u}{\partial z}=vf-g\frac{\partial \zeta}{\partial x}+A_h\left(\frac{\partial^2 u}{\partial x^2}+\frac{\partial^2 u}{\partial y^2}\right)+A_v\frac{\partial^2 u}{\partial z^2} \qquad (15)$$

$$\frac{\partial v}{\partial t}+u\frac{\partial v}{\partial x}+v\frac{\partial v}{\partial y}+w\frac{\partial v}{\partial z}=-uf-g\frac{\partial \zeta}{\partial y}+A_h\left(\frac{\partial^2 v}{\partial x^2}+\frac{\partial^2 v}{\partial y^2}\right)+A_v\frac{\partial^2 v}{\partial z^2} \qquad (16)$$

Discharge per unit width M, N are defined as follows:

$$M=\int_{-h}^{\zeta}udz=u(h+\zeta)\ ,\ N=\int_{-h}^{\zeta}vdz=v(h+\zeta) \qquad (17)$$

And each term is integrated by a theorem of integration as follows:

$$\int_{-h}^{\zeta}\frac{\partial u}{\partial t}dz=\frac{\partial}{\partial t}\int_{-h}^{\zeta}udz-u\frac{\partial \zeta}{\partial t}-u\frac{\partial h}{\partial t}\ ,\ \frac{\partial h}{\partial t}=0 \quad \text{------} \quad (18)$$

$$\int_{-h}^{\zeta}\frac{\partial (u^2)}{\partial x}dz=\frac{\partial}{\partial x}\int_{-h}^{\zeta}u^2dz-u^2\frac{\partial \zeta}{\partial x}-u^2\frac{\partial h}{\partial x} \quad \text{------} \quad (19)$$

$$\int_{-h}^{\zeta}\frac{\partial (uv)}{\partial y}dz=\frac{\partial}{\partial y}\int_{-h}^{\zeta}uvdz-uv\frac{\partial \zeta}{\partial y}-uv\frac{\partial h}{\partial y} \quad \text{------} \quad (20)$$

$$\int_{-h}^{\zeta}\frac{\partial (uw)}{\partial z}dz = (uw)_{z=\zeta}-(uw)_{z=-h} = u\left(\frac{\partial \zeta}{\partial t}+u\frac{\partial \zeta}{\partial x}+u\frac{\partial \zeta}{\partial y}\right)+u\left(u\frac{\partial h}{\partial x}+v\frac{\partial h}{\partial y}\right) \quad \text{------} \quad (21)$$

It is the same in y direction.
The term of vertical eddy viscosity is given by sea surface shear stress τ_s and bottom shear stress τ_b as follows:

$$A_v\int_{-h}^{\zeta}\frac{\partial^2 u}{\partial z^2}dz=A_v\left\{\left(\frac{\partial u}{\partial z}\right)_{z=\zeta}-\left(\frac{\partial u}{\partial z}\right)_{z=-h}\right\}=\frac{1}{\rho_w}(\tau_{sx}-\tau_{bx}) \quad \text{------} \quad (22)$$

$$A_v\int_{-h}^{\zeta}\frac{\partial^2 v}{\partial z^2}dz=A_v\left\{\left(\frac{\partial v}{\partial z}\right)_{z=\zeta}-\left(\frac{\partial v}{\partial z}\right)_{z=-h}\right\}=\frac{1}{\rho_w}(\tau_{sy}-\tau_{by}) \quad \text{------} \quad (23)$$

As the result, Continuity Equation and Motion Equations integrated vertically are shown as follows:

$$\frac{\partial \zeta}{\partial t}+\frac{\partial M}{\partial x}+\frac{\partial N}{\partial y}=0 \quad \text{------} \quad (24)$$

$$\frac{\partial M}{\partial t}+\frac{\partial (uM)}{\partial x}+\frac{\partial (vM)}{\partial y} = fN - g(\zeta+h)\frac{\partial \zeta}{\partial x}+A_h\left(\frac{\partial^2 M}{\partial x^2}+\frac{\partial^2 M}{\partial y^2}\right)+\frac{1}{\rho}(\tau_{sx}-\tau_{bx}) \quad \text{------} \quad (25)$$

$$\frac{\partial N}{\partial t}+\frac{\partial (uN)}{\partial x}+\frac{\partial (vN)}{\partial y} = -fM - g(\zeta+h)\frac{\partial \zeta}{\partial y}+A_h\left(\frac{\partial^2 N}{\partial x^2}+\frac{\partial^2 N}{\partial y^2}\right)+\frac{1}{\rho}(\tau_{sy}-\tau_{by}) \quad \text{------} \quad (26)$$

(3) Governing Equation of Two-Level Model

Layer is divided upper and lower as shown in Fig.1.2-1 to lead the governing equation of two-level model.
M_1, N_1, M_2, N_2 are defined the discharge per unit width in upper and lower layer as follows:

$$M_1=\int_{-h}^{\zeta} u_1 dz = u_1(h_1+\zeta) \quad , \quad N_1=\int_{-h}^{\zeta} v_1 dz = v_1(h_1+\zeta) \qquad (28)$$

$$M_2=\int_{-h}^{-h1} u_2 dz = u_2 h_2 \ , \ N_2=\int_{-h}^{-h1} v_2 dz = v_2 h_2$$

Where,

h_1, h_2 : thickness of upper layer and lower layer respectively

u_1, v_1, u_2, v_2: depth averaged horizontal velocity

w : vertical velocity at the interface between upper and lower layer.

Continuity Equation are given by equation (33), (34) from equation (28) and the motion between upper and lower layer are expressed by vertical velocity w in two-level model.

The advection term in both layer of z direction in Motion Equation are shown as follows:

$$\int_{-h1}^{\zeta} \frac{\partial (uw)}{\partial z} dz = (uw)_{z=\zeta} - (uw)_{z=-h1} \qquad (29)$$

$$\int_{-h}^{-h1} \frac{\partial (uw)}{\partial z} dz = (uw)_{z=-h1} - (uw)_{z=-h}$$

The term at z=ζ, z=-h in equation (21) are wiped out by other terms, and only the term at $z=-h_1$ remain.
It is the same in y direction.
Vertical eddy viscosity term are expressed as follows:

$$A_v=\int_{-h1}^{\zeta} \frac{\partial^2 u}{\partial z^2} dz = A_v\left\{\left(\frac{\partial u}{\partial z}\right)_{z=\zeta} - \left(\frac{\partial u}{\partial z}\right)_{z=-h1}\right\} = \frac{1}{\rho_w}(\gamma_{sx}-\gamma_{ix}) \qquad (30)$$

$$A_v=\int_{-h}^{-h1} \frac{\partial^2 u}{\partial z^2} dz = A_v\left\{\left(\frac{\partial u}{\partial z}\right)_{z=-h1} - \left(\frac{\partial u}{\partial z}\right)_{z=h}\right\} = \frac{1}{\rho_w}(\gamma_{ix}-\gamma_{bx})$$

It is the same in y direction.
Here surface shear stress is not considered in Tidal Current.
Bottom shear stress are given as follows:

$$\tau_{bx}=\gamma_b{}^2 u_2\sqrt{u_2{}^2+v_2{}^2} \qquad (31)$$

$$\tau_{by}=\gamma_b{}^2 v_2\sqrt{u_2{}^2+v_2{}^2}$$

and shear stress at the interface between both layers are defined as follows:

$$\tau_{ix}=\gamma_i{}^2 (u_1-u_2)\sqrt{(u_1-u_2)^2+(v_1-v_2)^2} \qquad (32)$$

$$\tau_{iy}=\gamma_i{}^2 (v_1-v_2)\sqrt{(u_1-u_2)^2+(v_1-v_2)^2}$$

As the result, Governing Equations of two-level model are given by equation (33) - (38).

[Continuity Equation]

Upper Layer:

$$\frac{\partial \zeta}{\partial t}=w-\frac{\partial M_1}{\partial x}-\frac{\partial N_1}{\partial y} \qquad (33)$$

Lower layer:

$$w=-\frac{\partial M_2}{\partial x}-\frac{\partial N_2}{\partial y} \qquad (34)$$

[Motion Equation]

Upper Layer:

x-direction

$$\frac{\partial M_1}{\partial t}+\frac{\partial (u_1M_1)}{\partial x}+\frac{\partial (v_1M_1)}{\partial y}-(u.w)_{z=h1}=fN_1-g(\zeta+h_1)\frac{\partial \zeta}{\partial x}+A_h(\zeta+h_1)\left(\frac{\partial^2 u_1}{\partial x^2}+\frac{\partial^2 u_1}{\partial y^2}\right)-\gamma_i{}^2(u_1-u_2)\sqrt{(u_1-u_2)^2+(v_1-v_2)^2} \qquad (35)$$

y-direction

$$\frac{\partial N_1}{\partial t}+\frac{\partial (u_1N_1)}{\partial x}+\frac{\partial (v_1N_1)}{\partial y}-(v.w)_{z=h1}=-fM_1-g(\zeta+h_1)\frac{\partial \zeta}{\partial y}+A_h(\zeta+h_1)\left(\frac{\partial^2 v_1}{\partial x^2}+\frac{\partial^2 v_1}{\partial y^2}\right)-\gamma_i{}^2(v_1-v_2)\sqrt{(u_1-u_2)^2+(v_1-v_2)^2} \qquad (36)$$

Lower Layer:

x－direction

$$\frac{\partial M_2}{\partial t}+\frac{\partial (u_2M_2)}{\partial x}+\frac{\partial (v_2M_2)}{\partial y}+(u_*w)_{z=h1}= fN_2-gh_2\frac{\partial \zeta}{\partial x}+A_hh_2\left(\frac{\partial^2u_2}{\partial x^2}+\frac{\partial^2u_2}{\partial y^2}\right) \qquad (37)$$

$$+\gamma_i^2(u_1-u_2)\sqrt{(u_1-u_2)^2+(v_1-v_2)^2} -\gamma_b^2u_2\sqrt{u_2^2+v_2^2}$$

y－direction

$$\frac{\partial N_2}{\partial t}+\frac{\partial (u_2N_2)}{\partial x}+\frac{\partial (v_2N_2)}{\partial y}+(v_*w)_{z=h1}=-fM_2-gh_2\frac{\partial \zeta}{\partial y}+A_hh_2\left(\frac{\partial^2v_2}{\partial x^2}+\frac{\partial^2v_2}{\partial y^2}\right) \qquad (38)$$

$$+\gamma_i^2(v_1-v_2)\sqrt{(u_1-u_2)^2+(v_1-v_2)^2} -\gamma_b^2v_2\sqrt{u_2^2+v_2^2}$$

The parameters which contain asterrisk indicate that

$u_*=u_2$, $v_*=v_2$ for $w>0$,

$u_*=u_1$, $v_*=v_1$ for $w>0$,

respectively.

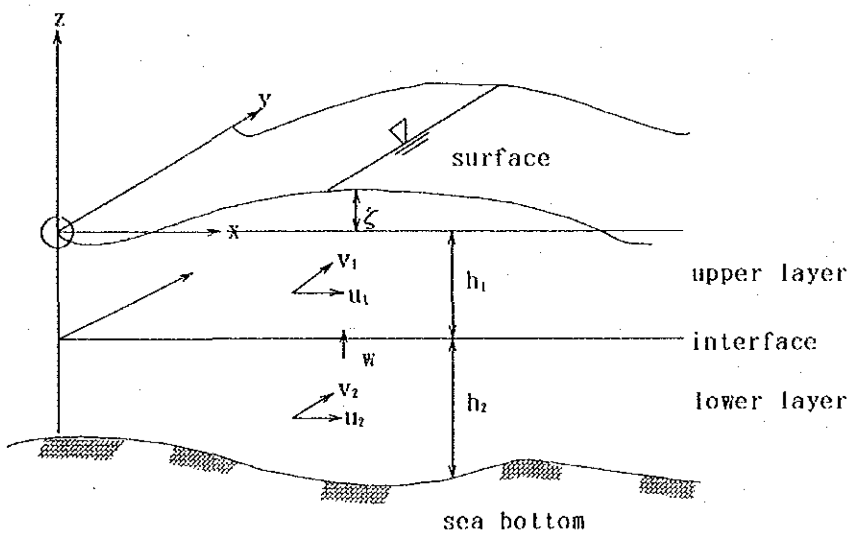

Fig. 1. 2-1 Definition of parameters in Two-level Model

Parameters appeared in each equation are explained as shown in Fig.1.2-1 and as follows:

M_1, N_1: discharge per unit width in x, y direction of upper layer

M_2, N_2: discharge per unit width in x, y direction of lower layer

u_1, v_1: *horizontal velocity components of seawater circulation in upper layer*

u_2, v_2: horizontal velocity components of seawater circulation in lower layer

w : vertical velocity components of seawater circulation in the interface between the upper layer and lower layer

ζ : water surface elevation

h_1 : thickness of upper layer

h_2 : thickness of lower layer

g : acceleration due to gravity

f : coliolis coefficient

A_h : horizontal eddy viscosity coefficient

r_i^2 : *inner friction coefficient in the interface* between the upper layer and lower layer

r_b^2 : bottom friction coefficient

1.2.3 Finite Difference Equation

Governing equation of two-level model are converted to finite difference equation below.
This model uses a finite difference method by an explicit method and upwind scheme for advection terms, and the calculation points are shown in Fig.1.2-1.

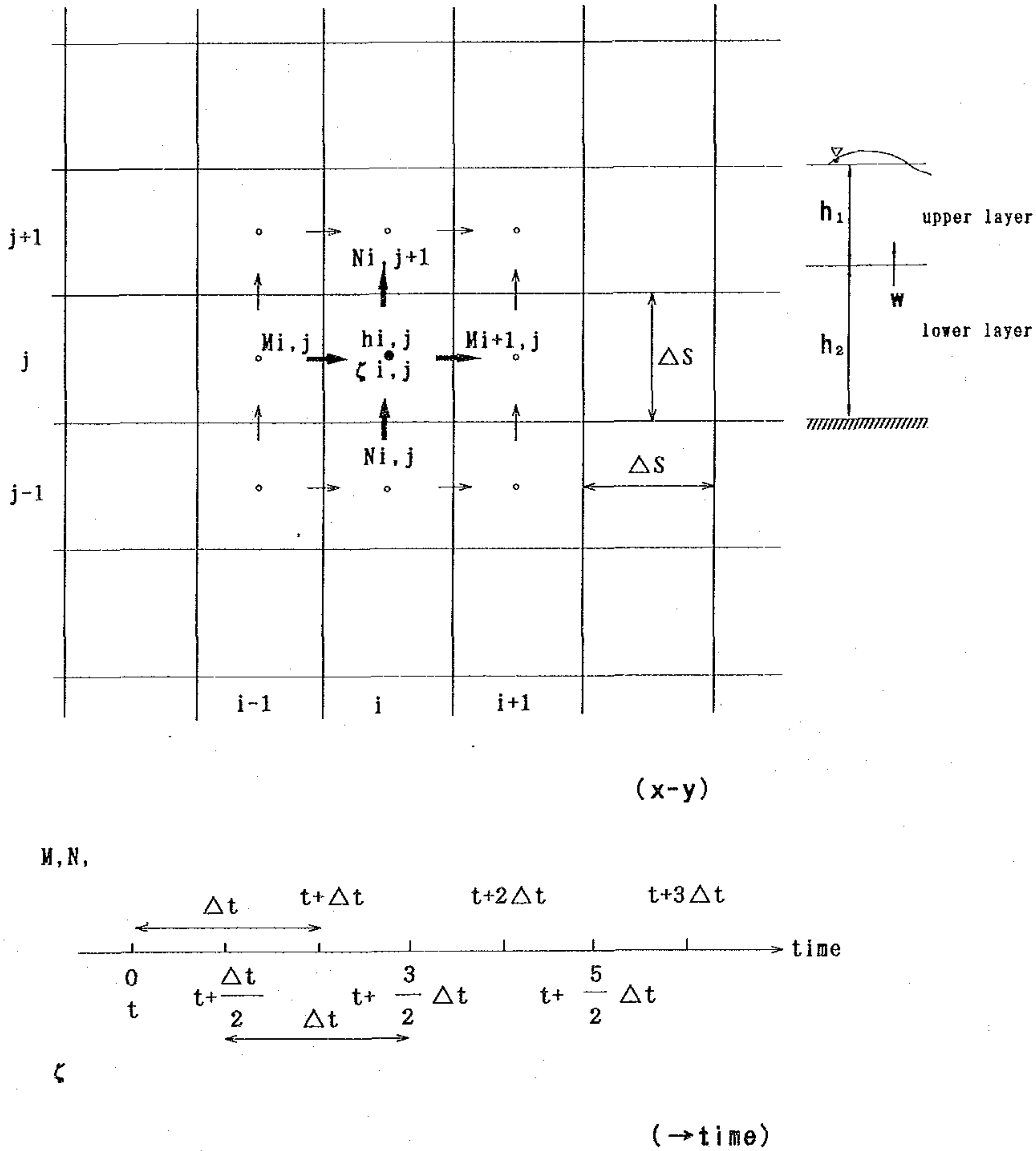

Fig. 1. 2-1 Definition of Calculation Points

(1) Finite Difference Equation of Continuity Equation

Upper Layer:

Equation (33) is converted to equation (39).

$$\frac{\partial \zeta}{\partial t} = w - \frac{\partial M_1}{\partial x} - \frac{\partial N_1}{\partial y}$$

$$\frac{\partial \zeta}{\partial t} = \frac{\zeta_{i,j}(t+\Delta t/2) - \zeta_{i,j}(t-\Delta t/2)}{\Delta t}$$

$$\frac{\partial M_1}{\partial x} = \frac{M_{1\,i+1,j} - M_{1\,i,j}}{\Delta s}$$

$$\frac{\partial N_1}{\partial y} = \frac{N_{1\,i,j+1} - N_{1\,i,j}}{\Delta s}$$

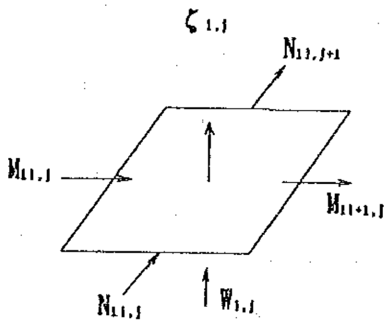

Therefore,

$$\zeta_{i,j}(t+\Delta t/2) = \zeta_{i,j}(t-\Delta t/2) + \Delta t\{w_{i,j} - [(M_{1\,i+1,j} - M_{1\,i,j}) + (N_{1\,i,j+1} - N_{1\,i,j})]\} \quad \text{———} \quad (39)$$

Lower layer:

Equation (34) is converted to equation (40).

$$w = -\frac{\partial M_2}{\partial x} - \frac{\partial N_2}{\partial y}$$

$$\frac{\partial M_2}{\partial x} = \frac{M_{2\,i+1,j} - M_{2\,i,j}}{\Delta s}$$

$$\frac{\partial N_2}{\partial y} = \frac{N_{2\,i,j+1} - N_{2\,i,j}}{\Delta s}$$

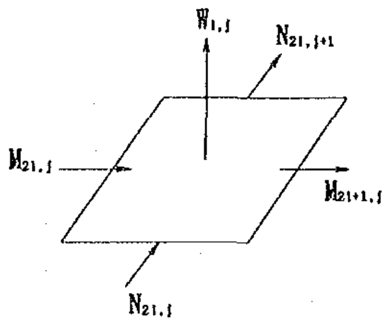

Therefore,

$$W_{i,j} = -[(M_{2\,i+1,j} - M_{2\,i,j}) + (N_{2\,i,j+1} - N_{2\,i,j})]/\Delta s \quad \text{———} \quad (40)$$

(2) Finite Difference Equation of Motion Equation

Equation (35) is divided eight terms shown as follows:

$$\underbrace{\frac{\partial M_1}{\partial t}}_{①}+\underbrace{\frac{\partial(u_1M_1)}{\partial x}}_{②}+\underbrace{\frac{\partial(v_1M_1)}{\partial y}}_{③}-\underbrace{(uw)_{z=h1}}_{④}=\underbrace{fN_1}_{⑤}-\underbrace{g(\zeta+h_1)\frac{\partial\zeta}{\partial x}}_{⑥}+\underbrace{A_h(\zeta+h_1)\left(\frac{\partial^2u_1}{\partial x^2}+\frac{\partial^2u_1}{\partial y^2}\right)}_{⑦}$$

$$\underbrace{-\gamma_i^2(u_1-u_2)\sqrt{(u_1-u_2)^2+(v_1-v_2)^2}}_{⑧}$$

① : $\frac{\partial M_1}{\partial t}=\{M_{1i,j}(t+\Delta t)-M_{1i,j}(t)\}/\Delta t$ ——— (41)

② : $\frac{\partial(u_1M_1)}{\partial x}=\{(u_1M_1)_{i+1/2,j}-(u_1M_1)_{i-1/2,j}\}/\Delta s$

$\left\{\frac{1}{2}(M_{1i+1,j}+M_{1i,j})u_{1i,j}-\frac{1}{2}(M_{1i,j}+M_{1i-1,j})u_{1i-1,j}\right\}/\Delta s$ for $M_1>0$

$\left\{\frac{1}{2}(M_{1i+1,j}+M_{1i,j})u_{1i+1,j}-\frac{1}{2}(M_{1i,j}+M_{1i-1,j})u_{1i,j}\right\}/\Delta s$ for $M_1<0$

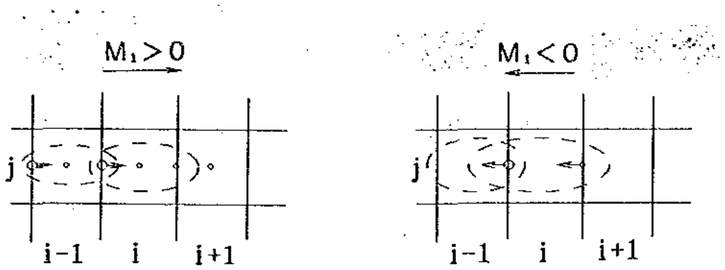

This term is stated with two cases as follows:

$$\frac{\partial(u_1M_1)}{\partial x}=\frac{1}{2\Delta s}\{(M_{1i+1,j}+M_{1i,j})u_{1i/i+1,j}-(M_{1i,j}+M_{1i-1,j})u_{1i-1/i,j}\} \quad (42)$$

③ : $\frac{\partial(v_1M_1)}{\partial y}=\frac{\partial(v_1(\zeta+h_1)u_1)}{\partial y}=\frac{\partial}{\partial y}(u_1N_1)=\{(u_1M_1)_{i,j+1/2}-(u_1N_1)_{i,j-1/2}\}/\Delta s$

$\left\{\frac{1}{2}(N_{1i,j+1}+N_{1i-1,j+1})u_{1i,j}-\frac{1}{2}(N_{1i,j}+N_{1i-1,j})u_{1i,j-1}\right\}/\Delta s$ for $N_1>0$

$\left\{\frac{1}{2}(N_{1i,j+1}+N_{1i-1,j+1})u_{1i,j+1}-\frac{1}{2}(N_{1i,j}+N_{1i-1,j})u_{1i,j}\right\}/\Delta s$ for $N_1<0$

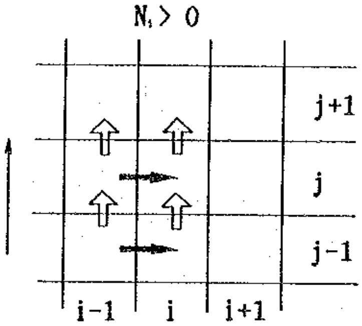

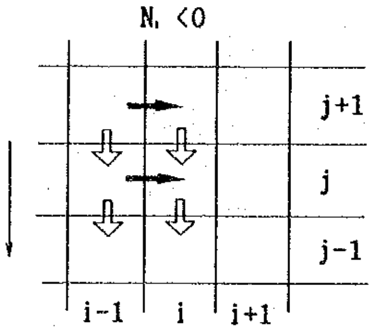

This term is stated with two cases as follows:

$$\frac{\partial (u_1 N_1)}{\partial y} = \frac{1}{2\Delta s}\{(N_{1i,j+1}+N_{1i-1,j+1})u_{1i,j/j+1}-(N_{1i,j}+N_{1i-1,j})u_{1i,j-1/j}\} \quad (43)$$

$$④ : -(uW) = -\frac{1}{2}(W_{i-1,j}+W_{i,j})u_{*i,j} \quad (44)$$

$$-\frac{1}{2}(W_{i-1,j}+W_{i,j})u_{2i,j} \qquad \text{for } W>0$$

$$-\frac{1}{2}(W_{i-1,j}+W_{i,j})u_{1i,j} \qquad \text{for } W<0$$

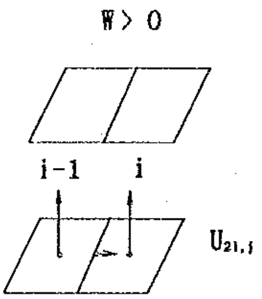

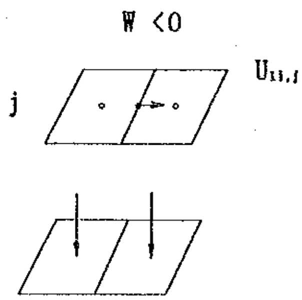

$$⑤ : fN_1 = \frac{f}{4}(N_{1i,j}+N_{1i,j+1}+N_{1i-1,j+1}+N_{1i-1,j}) \quad (45)$$

$$⑥ : -g(\zeta+h_1)\frac{\partial \zeta}{\partial x} = -\frac{g}{2}(\zeta_{i-1,j}+\zeta_{i,j}+h_{1i-1,j}+h_{1i,j})\frac{\zeta_{i,j}-\zeta_{i-1,j}}{\Delta x} \quad (46)$$

$$⑦ : A_h(\zeta+h_1)\left(\frac{\partial^2 u_1}{\partial x^2}+\frac{\partial^2 u_1}{\partial y^2}\right) = A_h\left(\frac{\partial^2 M_1}{\partial x^2}+\frac{\partial^2 M_1}{\partial y^2}\right)$$

$$\frac{\partial^2 M_1}{\partial x^2} = \frac{1}{\Delta s}\left(\frac{M_{1\,i+1,\,j}-M_{1\,i,\,j}}{\Delta s} - \frac{M1_{i,\,j}-M1_{i-1,\,j}}{\Delta s}\right) = \frac{1}{\Delta s^2}(M_{1\,i+1,\,j}-2M_{1\,i,\,j}+M_{1\,i-1,\,j}) \quad \cdots \quad (47)$$

$$\frac{\partial^2 M_1}{\partial y^2} = \frac{1}{\Delta s}\left(\frac{M_{1\,i,\,j+1}-M_{1\,i,\,j}}{\Delta s} - \frac{M_{1\,i,\,j}-M_{1\,i,\,j-1}}{\Delta s}\right) = \frac{1}{\Delta s^2}(M_{1\,i,\,j+1}-2M_{1\,i,\,j}+M_{1\,i,\,j-1}) \quad \cdots \quad (48)$$

$$⑧ : -\gamma_i^2(u_1-u_2)\sqrt{(u_1-u_2)^2+(v_1-v_2)^2} = -\gamma_i^2 UU\sqrt{UU^2+VV^2} \quad \text{———} \quad (49)$$

$$UU = (u_{1\,i,\,j}-u_{2\,i,\,j})$$

$$VV = \frac{1}{4}\{(v_{1\,i,\,j}-v_{2\,i,\,j})+(v_{1\,i,\,j+1}-v_{2\,i,\,j+1})+(v_{1\,i-1,\,j+1}-v_{2\,i-1,\,j+1})+(v_{1\,i-1,\,j}-v_{2\,i-1,\,j})\}$$

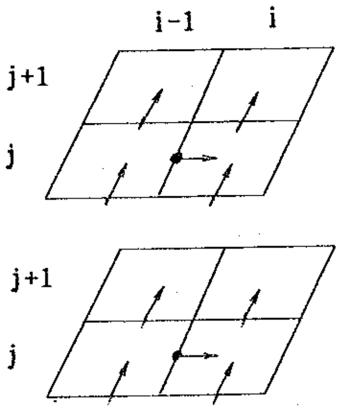

It is the same in y-direction of upper layer stated equation (36).

Lower Layer:

Equation (37) is divided nine terms shown as follows:

$$\underbrace{\frac{\partial M_2}{\partial t}}_{①}+\underbrace{\frac{\partial (u_2M_2)}{\partial x}}_{②}+\underbrace{\frac{\partial (v_2M_2)}{\partial y}}_{③}+\underbrace{(uw)_{z=h1}}_{④}=\underbrace{fN_2}_{⑤}\underbrace{-gh_2\frac{\partial \zeta}{\partial x}}_{⑥}\underbrace{+A_hh_2\left(\frac{\partial^2u_2}{\partial x^2}+\frac{\partial^2u_2}{\partial y^2}\right)}_{⑦}$$

$$\underbrace{+\gamma_i{}^2(u_1-u_2)\sqrt{(u_1-u_2)^2+(v_1-v_2)^2}}_{⑧}\ \underbrace{-\gamma_b{}^2u_2\sqrt{u_2{}^2+v_2{}^2}}_{⑨}$$

$$① : \frac{\partial M_2}{\partial t}=\{M_{2i,j}(t+\Delta t)-M_{2i,j}(t)\}/\Delta t \tag{50}$$

$$② : \frac{\partial (u_2M_2)}{\partial x}=\{(u_2M_2)_{i+1/2,j}-(u_2M_2)_{i-1/2,j}\}/\Delta s$$

$$\left\{\frac{1}{2}(M_{2i+1,j}+M_{2i,j})u_{2i,j}-\frac{1}{2}(M_{2i,j}+M_{2i-1,j})u_{2i-1,j}\right\}/\Delta s \qquad \text{for } M_2>0$$

$$\left\{\frac{1}{2}(M_{2i+1,j}+M_{2i,j})u_{2i+1,j}-\frac{1}{2}(M_{2i,j}+M_{2i-1,j})u_{2i,j}\right\}/\Delta s \qquad \text{for } M_2<0$$

This term is stated with two cases as follows:

$$\frac{\partial (u_2M_2)}{\partial x}=\frac{1}{2\Delta s}\{(M_{2i+1,j}+M_{2i,j})u_{2i/i+1,j}-(M_{2i,j}+M_{2i-1,j})u_{2i-1/i,j}\} \tag{51}$$

$$③ : \frac{\partial (v_2M_2)}{\partial y}=\frac{\partial (v_2h_2u_2)}{\partial y}=\frac{\partial}{\partial y}(u_2N_2)=\{(u_2N_2)_{i,j+1/2}-(u_2N_2)_{i,j-1/2}\}/\Delta s$$

$$\left\{\frac{1}{2}(N_{2i,j+1}+N_{2i-1,j+1})u_{2i,j}-\frac{1}{2}(N_{2i,j}+N_{2i-1,j})u_{2i,j-1}\right\}/\Delta s \qquad \text{for } N_2>0$$

$$\left\{\frac{1}{2}(N_{2i,j+1}+N_{2i-1,j+1})u_{2i,j+1}-\frac{1}{2}(N_{2i,j}+N_{2i-1,j})u_{2i,j}\right\}/\Delta s \qquad \text{for } N_2<0$$

This term is stated with two cases as follows:

$$\frac{\partial (u_2N_2)}{\partial y}=\frac{1}{2\Delta s}\{(N_{2i,j+1}+N_{2i-1,j+1})u_{2i,j/j+1}-(N_{2i,j}+N_{2i-1,j})u_{2i,j-1/j}\} \tag{52}$$

$$④ : (uW) = \frac{1}{2}(W_{i-1,j}+W_{i,j})u_{*i,j} \quad (53)$$

$$\frac{1}{2}(W_{i-1,j}+W_{i,j})u_{2i,j} \quad \text{for} \quad W>0$$

$$\frac{1}{2}(W_{i-1,j}+W_{i,j})u_{1i,j} \quad \text{for} \quad W<0$$

$$⑤ : fN_2 = \frac{f}{4}(N_{2i,j}+N_{2i,j+1}+N_{2i-1,j+1}+N_{2i-1,j}) \quad (54)$$

$$⑥ : -gh_2\frac{\partial \zeta}{\partial x} = -\frac{g}{2}(h_{2i-1,j}+h_{2i,j})\frac{\zeta_{i,j}-\zeta_{i-1,j}}{\Delta x} \quad (55)$$

$$⑦ : A_h h_2\left(\frac{\partial^2 u_2}{\partial x^2}+\frac{\partial^2 u_2}{\partial y^2}\right) = A_h\left(\frac{\partial^2 M_2}{\partial x^2}+\frac{\partial^2 M_2}{\partial y^2}\right)$$

$$\frac{\partial^2 M_2}{\partial x^2} = \frac{1}{\Delta s}\left(\frac{M_{2i+1,j}-M_{2i,j}}{\Delta s} - \frac{M_{2i,j}-M_{2i-1,j}}{\Delta s}\right) = \frac{1}{\Delta s^2}(M_{2i+1,j}-2M_{2i,j}+M_{2i-1,j}) \quad (56)$$

$$\frac{\partial^2 M_2}{\partial y^2} = \frac{1}{\Delta s}\left(\frac{M_{2i,j+1}-M_{2i,j}}{\Delta s} - \frac{M_{2i,j}-M_{2i,j-1}}{\Delta s}\right) = \frac{1}{\Delta s^2}(M_{2i,j+1}-2M_{2i,j}+M_{2i,j-1}) \quad (57)$$

$$⑧ : \gamma_i{}^2(u_1-u_2)\sqrt{(u_1-u_2)^2+(v_1-v_2)^2} = \gamma_i{}^2 UU\sqrt{UU^2+VV^2} \quad (58)$$

$$UU = (u_{1i,j}-u_{2i,j})$$

$$VV = \frac{1}{4}\{(v_{1i,j}-v_{2i,j})+(v_{1i,j+1}-v_{2i,j+1})+(v_{1i-1,j+1}-v_{2i-1,j+1})+(v_{1i-1,j}-v_{2i-1,j})\}$$

$$⑨ : \gamma_b{}^2 u_2\sqrt{u_2{}^2+v_2{}^2} = \gamma_i{}^2 u_{2i,j}\sqrt{u_{2i,j}{}^2+(v_{2i,j}+v_{2i,j+1}+v_{2i,j+1}+v_{2i-1,j+1}+v_{2i-1,j})^2/16} \quad (59)$$

It is the same in y-direction of lower layer stated equation (38).
As the result, the finite difference equations of two-level model are stated by uniting equation (39) - (59) as follows:

[Continuity Equation]

Upper Layer

$$\zeta_{i,j}(t+\Delta t/2) = \zeta_{i,j}(t-\Delta t/2) + \Delta t\{w_{i,j}-[(M_{1i+1,j}-M_{1i,j})+(N_{1i,j+1}-N_{1i,j})]/\Delta s\} \quad \text{—} \quad (60)$$

Lower Layer

$$w_{i,j} = -\{(M_{2i+1,j} - M_{2i,j}) + (N_{2i,j+1} - N_{2i,j})\}/\Delta s \quad \text{———} \quad (61)$$

[Motion Equation]

Upper Layer X-direction

$$\begin{aligned}
M_{1i,j}(t+\Delta t) = M_{1i,j}(t) & -\frac{\Delta t}{2\Delta s}\{(M_{1i+1,j}+M_{1i,j})u_{1i/i+1,j}-(M_{1i,j}+M_{1i-1,j})u_{1i-1/i,j}\} \\
& -\frac{\Delta t}{2\Delta s}\{(N_{1i,j+1}+N_{1i-1,j+1})u_{1i,j/j+1}-(N_{1i,j}+N_{1i-1,j})u_{1i,j-1/j}\} \\
& +\frac{\Delta t}{2}(w_{i-1,j}+w_{i,j})u_{*i,j}+\frac{f}{4}\Delta t(N_{1i,j}+N_{1i-1,j}+N_{1i-1,j-1}+N_{1i,j-1}) \\
& -\frac{g\Delta t}{2\Delta s}(\zeta_{i-1,j}+\zeta_{i,j}+h_{1i-1,j}+h_{1i,j})(\zeta_{i,j}-\zeta_{i-1,j}) \\
& +\left(\frac{\Delta t}{\Delta s^2}\right)A_h(M_{1i+1,j}+M_{1i-1,j}+M_{1i,j+1}+M_{1i,j-1}-4M_{1i,j}) \\
& -\Delta t\gamma_i{}^2 UU_1\sqrt{UU_1{}^2+VV_1{}^2} \quad \text{———} \quad (62)
\end{aligned}$$

Upper Layer Y-direction

$$\begin{aligned}
N_{1i,j}(t+\Delta t) = N_{1i,j}(t) & -\frac{\Delta t}{2\Delta s}\{(M_{1i+1,j}+M_{1i+1,j-1})v_{1i/i+1,j}-(M_{1i,j}+M_{1i,j-1})v_{1i-1/i,j}\} \\
& -\frac{\Delta t}{2\Delta s}\{(N_{1i,j+1}+N_{1i,j})v_{1i,j/j+1}-(N_{1i,j}+N_{1i,j-1})v_{1i,j-1/j}\} \\
& +\frac{\Delta t}{2}(w_{i,j}+w_{i,j-1})v_{*i,j}+\frac{f}{4}\Delta t(M_{1i,j}+M_{1i,j-1}+M_{1i+1,j-1}+M_{1i+1,j}) \\
& -\frac{g\Delta t}{2\Delta s}(\zeta_{i,j}+\zeta_{i,j-1}+h_{1i,j}+h_{1i,j-1})(\zeta_{i,j}-\zeta_{i,j-1}) \\
& +\left(\frac{\Delta t}{\Delta s^2}\right)A_h(N_{1i+1,j}+N_{1i-1,j}+N_{1i,j+1}+N_{1i,j-1}-4N_{1i,j}) \\
& -\Delta t\gamma_i{}^2 VV_2\sqrt{UU_2{}^2+VV_2{}^2} \quad \text{———} \quad (63)
\end{aligned}$$

Where,

$UU_1 = u_{1i,j} - u_{2i,j}$

$$VV_1=\frac{1}{4}\{(v_{1i,j}-v_{2i,j})+(v_{1i,j+1}-v_{2i,j+1})+(v_{1i-1,j+1}-v_{2i-1,j+1})+(v_{1i-1,j}-v_{2i-1,j})\}$$

$$UU_2=\frac{1}{4}\{(u_{1i,j}-u_{2i,j})+(u_{1i,j-1}-u_{2i,j-1})+(u_{1i+1,j-1}-u_{2i+1,j-1})+(u_{1i+1,j}-u_{2i+1,j})\}$$

$$VV_2=v_{1i,j}-v_{2i,j}$$

$u_*=u_2$, $v_*=v_2$ for $w\geqq 0$ $u_*=u_1$, $v_*=v_1$ for $w<0$

Lower Layer X-direction

$$M_{2i,j}(t+\Delta t)=M_{2i,j}(t)-\frac{\Delta t}{2\Delta s}\{(M_{2i+1,j}+M_{2i,j})u_{2i/i+1,j}-(M_{2i,j}+M_{2i-1,j})u_{2i-1/i,j}\}$$

$$-\frac{\Delta t}{2\Delta s}\{(N_{2i,j+1}+N_{2i-1,j+1})u_{2i,j/j+1}-(N_{2i,j}+N_{2i-1,j})u_{2i,j-1/j}\}$$

$$+\frac{\Delta t}{2}(w_{i-1,j}+w_{i,j})u_{*i,j}+\frac{f}{4}\Delta t(N_{2i,j}+N_{2i-1,j}+N_{2i-1,j-1}+N_{2i,j-1})$$

$$-\frac{g\Delta t}{2\Delta s}(h_{2i-1,j}+h_{2i,j})(\zeta_{i,j}-\zeta_{i-1,j})$$

$$+\left(\frac{\Delta t}{\Delta s^2}\right)A_h(M_{2i+1,j}+M_{2i-1,j}+M_{2i,j+1}+M_{2i,j-1}-4M_{2i,j})$$

$$+\Delta t\gamma_i{}^2UU_1\sqrt{UU_1{}^2+VV_1{}^2}$$

$$+\Delta t\gamma_b{}^2u_2i,j\sqrt{u_{2i,j}{}^2+(v_{2i,j}+v_{2i,j+1}+v_{2i-1,j+1}+v_{2i-1,j})^2/16} \quad \text{——— (64)}$$

Lower Layer Y-direction

$$N_{2i,j}(t+\Delta t)=N_{2i,j}(t)-\frac{\Delta t}{2\Delta s}\{(M_{2i+1,j}+M_{2i+1,j-1})v_{2i/i+1,j}-(M_{2i,j}+M_{2i,j-1})v_{2i-1/i,j}\}$$

$$-\frac{\Delta t}{2\Delta s}\{(N_{2i,j+1}+N_{2i,j})v_{2i,j/j+1}-(N_{2i,j}+N_{2i,j-1})v_{2i,j-1/j}\}$$

$$+\frac{\Delta t}{2}(w_{i,j}+w_{i,j-1})v_{*i,j}+\frac{f}{4}\Delta t(M_{2i,j}+M_{2i,j-1}+M_{2i+1,j-1}+M_{2i+1,j})$$

$$-\frac{g\Delta t}{2\Delta s}(h_{2i,j}+h_{2i,j-1})(\zeta_{i,j}-\zeta_{i,j-1})$$

$$+\left(\frac{\Delta t}{\Delta s^2}\right)A_h(N_{2i+1,j}+N_{2i-1,j}+N_{2i,j+1}+N_{2i,j-1}-4N_{2i,j})$$

$$+\Delta t\gamma_i{}^2VV_2\sqrt{UU_2{}^2+VV_2{}^2}$$

$$+\Delta t\gamma_b{}^2v_2i,j\sqrt{(u_{2i,j}+u_{2i,j+1}+u_{2i-1,j+1}+u_{2i-1,j})^2/16+v_{2i,j}{}^2} \quad \text{——— (65)}$$

Where,

$$UU_1=u_{1i,j}-u_{2i,j}$$

$$VV_1=\frac{1}{4}\{(v_{1i,j}-v_{2i,j})+(v_{1i,j+1}-v_{2i,j+1})+(v_{1i-1,j+1}-v_{2i-1,j+1})+(v_{1i-1,j}-v_{2i-1,j})\}$$

$$UU_2=\frac{1}{4}\{(u_{1\,i,\,j}-u_{2\,i,\,j})+(u_{1\,i,\,j-1}-u_{2\,i,\,j-1})+(u_{1\,i+1,\,j-1}-u_{2\,i+1,\,j-1})+(u_{1\,i+1,\,j}-u_{2\,i+1,\,j})\}$$

$$VV_2=v_{1\,i,\,j}-v_{2\,i,\,j}$$

$u_*=u_2$, $v_*=v_2$ for $w\geqq 0$ $u_*=u_1$, $v_*=v_1$ for $w<0$

1.3 Diffusion Model

1.3.1 Governing Equation

Basic equation for two-level diffusion model for conservative substances are expressed below. The concentration of water quality at each time can be calculated by solving these equations using a finite difference method.

Upper Layer :

$$\underbrace{\frac{\partial C_1 \cdot D_1}{\partial t}}_{\text{time variation}} = \underbrace{-\frac{\partial}{\partial x}(C_1 \cdot u_1 \cdot D_1) - \frac{\partial}{\partial y}(C_1 \cdot v_1 \cdot D_1)}_{\text{horizontal advection}} + \underbrace{\frac{\partial}{\partial x}\left(K_h D_1 \frac{\partial C_1}{\partial x}\right) + \frac{\partial}{\partial y}\left(K_h D_1 \frac{\partial C_1}{\partial y}\right)}_{\text{horizontal dispersion}}$$

$$\underbrace{+ w \cdot C^* - K_z (C_1 - C_2)}_{\text{vertical advection \& dispersion}} \quad \underbrace{+ L}_{\text{external load}} \qquad \text{------} \quad (66)$$

Lower Layer :

$$\underbrace{\frac{\partial C_2 \cdot D_2}{\partial t}}_{\text{time variation}} = \underbrace{-\frac{\partial}{\partial x}(C_2 \cdot u_2 \cdot D_2) - \frac{\partial}{\partial y}(C_2 \cdot v_2 \cdot D_2)}_{\text{horizontal advection}} + \underbrace{\frac{\partial}{\partial x}\left(K_h D_2 \frac{\partial C_2}{\partial x}\right) + \frac{\partial}{\partial y} K_h D_2 \frac{\partial C_2}{\partial y})}_{\text{horizontal dispersion}}$$

$$\underbrace{- w \cdot C^* + K_z (C_1 - C_2)}_{\text{vertical advection \& dispersion}} \qquad \text{------} \quad (67)$$

Parameters appeared in each equation are explained as follows:

C_1 : salinity concentration in upper layer

C_2 : salinity concentration in lower layer

L : external load

D_1 : thickness of upper layer

D_2 : thickness of lower layer

u_1, v_1 : horizontal velocity components of seawater circulation in upper layer calculated by Tidal Current Model

u_2, v_2 : horizontal velocity cimponents of seawater circulation in lower layer calculated by Tidal Current Model

w : vertical velocity components of seawater circulation in the interface between the upper layer and lower layer calculated by Tidal Current Model

K_h : horizontal dispersion coefficient

K_z : vertical dispersion coefficient

The parameters which contain asterisk indicate that

$$C^* = C_2 \quad \text{for } w \geqq 0,$$
$$C^* = C_1 \quad \text{for } w < 0,$$

respectively.

1.3.2 Finite Difference Equation

Finite difference equation of two-level diffusion model converted from equation (66) and (67) is expressed by equation (68) and (69) in upper and lower layer respectively.

Upper Layer

$$
\begin{aligned}
D_1C_1(t+\Delta t) &= D_1C_1(t) \\
&- \frac{\Delta t}{\Delta s}(M_{1\,i+1,\,j}C_{1\,i/i+1,\,j} - M_{1\,i,\,j}C_{1\,i-1/i,\,j} + N_{1\,i,\,j+1}C_{1\,i,\,j/j+1} - N_{1\,i,\,j}C_{1\,i,\,j/j-1}) \\
&+ \frac{\Delta t K_h}{2(\Delta s)^2}\{(D_{1\,i+1,\,j}+D_{1\,i,\,j})(C_{1\,i+1,\,j}-C_{2\,i,\,j}) - (D_{1\,i,\,j}+D_{1\,i-1,\,j})(C_{1\,i,\,j}-C_{1\,i-1,\,j}) \\
&+ (D_{1\,i,\,j+1}+D_{1\,i,\,j})(C_{1\,i,\,j+1}-C_{1\,i,\,j}) - (D_{1\,i,\,j}+D_{1\,i,\,j-1})(C_{1\,i,\,j}-C_{1\,i,\,j-1})\} \\
&+ \Delta t\{wC_{2/1\,i,\,j} - K_z(C_{1\,i,\,j}-C_{2\,i,\,j})\}\ (+\Delta t L) \qquad (68)
\end{aligned}
$$

Lower Layer

$$
\begin{aligned}
D_2C_2(t+\Delta t) &= D_2C_2(t) \\
&- \frac{\Delta t}{\Delta s}(M_{2\,i+1,\,j}C_{2\,i/i+1,\,j} - M_{2\,i,\,j}C_{2\,i-1/i,\,j} + N_{2\,i,\,j+1}C_{2\,i,\,j/j+1} - N_{2\,i,\,j}C_{2\,i,\,j/j-1}) \\
&+ \frac{\Delta t K_h}{2(\Delta s)^2}\{(D_{2\,i+1,\,j}+D_{2\,i,\,j})(C_{2\,i+1,\,j}-C_{2\,i,\,j}) - (D_{2\,i,\,j}+D_{2\,i-1,\,j})(C_{2\,i,\,j}-C_{2\,i-1,\,j}) \\
&+ (D_{2\,i,\,j+1}+D_{2\,i,\,j})(C_{2\,i,\,j+1}-C_{2\,i,\,j}) - (D_{2\,i,\,j}+D_{2\,i,\,j-1})(C_{2\,i,\,j}-C_{2\,i,\,j-1})\} \\
&+ \Delta t\{-wC_{2/1\,i,\,j} + K_z(C_{1\,i,\,j}-C_{2\,i,\,j})\} \qquad (69)
\end{aligned}
$$

where, the expression such as i/i+1 indicates the upwind scheme.

1.4 Eutrophication Model

On the formulation of a nutrient cycle between seawater and sediment, we assumed the follows:

(1) The system controlling the process of a nutrient cycle is treated as a growth and a decomposition between PO_4-P(Phosphate Phosphorus) and O-P(Organic Phosphorus), and DO(Dissolved Oxygen) and organic matters increase corresponding to the amount of primary production.

(2) As indices, COD(Chemical Oxygen Demand) and BOD(Biological Oxygen Demand) are used for the concentration of organic matters, and PO_4-P, O-P and DO are also used.

(3) The area is vertically divided into two layers of a photic later (upper layer) and a non-photic layer(lower layer). The growth of phytoplankton occurs only in the photic layer.

(4) COD, DO and nutrient salts vary through the process of growth, decomposition, settling and release etc. as well as inflow from rivers (Fig.1.4-1).

(5) COD, DO and nutrient salts vary by advection and dispersion due to tidal current.

1.4.1 Governing Equation

The time variation in two-level model is expressed as the following equations and the concentration of water quality at each time can be calculated by solving these equations using a finite difference method.

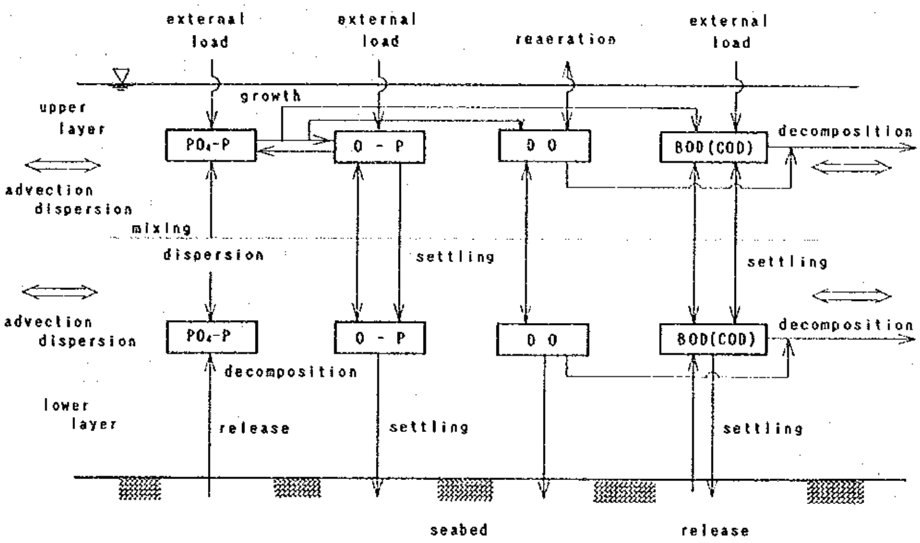

Fig. 1.4-1 Nutrient Cycle Model

O−P

Upper layer :

$$\underbrace{\frac{\partial OP_1 \cdot D_1}{\partial t}}_{\text{time variation}} = \underbrace{-\frac{\partial}{\partial x}(OP_1 \cdot u_1 \cdot D_1) - \frac{\partial}{\partial y}(OP_1 \cdot v_1 \cdot D_1)}_{\text{horizontal advection}} + \underbrace{\frac{\partial}{\partial x}\left(K_h D_1 \frac{\partial OP_1}{\partial x}\right) + \frac{\partial}{\partial y}\left(K_h D_1 \frac{\partial OP_1}{\partial y}\right)}_{\text{horizontal dispersion}}$$

$$\underbrace{+ w \cdot OP^* - K_z(OP_1 - OP_2)}_{\text{vertical advection \& dispersion}} \underbrace{+ G \cdot OPP_1 \cdot D_1}_{\text{growth}} \underbrace{- B_1^P \cdot OP_1 \cdot D_1}_{\text{decomposition}} \underbrace{- S_1^P \cdot OP_1}_{\text{settling}}$$

$$\underbrace{+ L_{OP}}_{\text{external load}}$$

Lower layer :

$$\underbrace{\frac{\partial OP_2 \cdot D_2}{\partial t}}_{\text{time variation}} = \underbrace{-\frac{\partial}{\partial x}(OP_2 \cdot u_2 \cdot D_2) - \frac{\partial}{\partial y}(OP_2 \cdot v_2 \cdot D_2)}_{\text{horizontal advection}} + \underbrace{\frac{\partial}{\partial x}\left(K_h D_2 \frac{\partial OP_2}{\partial x}\right) + \frac{\partial}{\partial y}\left(K_h D_2 \frac{\partial OP_2}{\partial y}\right)}_{\text{horizontal dispersion}}$$

$$\underbrace{- w \cdot OP^* + K_z(OP_1 - OP_2)}_{\text{vertical advection \& dispersion}} \underbrace{- B_2^P \cdot OP_2 \cdot D_2}_{\text{decomposition}} \underbrace{+ S_1^P \cdot OP_1 - S_2^P \cdot OP_2}_{\text{settling}}$$

O−P (Inner Production)

Upper layer :

$$\underbrace{\frac{\partial OPP_1 \cdot D_1}{\partial t}}_{\text{time variation}} = \underbrace{-\frac{\partial}{\partial x}(OPP_1 \cdot u_1 \cdot D_1) - \frac{\partial}{\partial y}(OPP_1 \cdot v_1 \cdot D_1)}_{\text{horizontal advection}} + \underbrace{\frac{\partial}{\partial x}\left(K_h D_1 \frac{\partial OPP_1}{\partial x}\right) + \frac{\partial}{\partial y}\left(K_h D_1 \frac{\partial OPP_1}{\partial y}\right)}_{\text{horizontal dispersion}}$$

$$\underbrace{+ w \cdot OPP^* - K_z(OPP_1 - OPP_2)}_{\text{vertical advection \& dispersion}} \underbrace{+ G \cdot OPP_1 \cdot D_1}_{\text{growth}} \underbrace{- B_1^P \cdot OPP_1 \cdot D_1}_{\text{decomposition}} \underbrace{- S_1^P \cdot OPP_1}_{\text{settling}}$$

Lower layer :

$$\underbrace{\frac{\partial OPP_2 \cdot D_2}{\partial t}}_{\text{time variation}} = \underbrace{-\frac{\partial}{\partial x}(OPP_2 \cdot u_2 \cdot D_2) - \frac{\partial}{\partial y}(OPP_2 \cdot v_2 \cdot D_2)}_{\text{horizontal advection}} + \underbrace{\frac{\partial}{\partial x}\left(K_h D_2 \frac{\partial OPP_2}{\partial x}\right) + \frac{\partial}{\partial y}\left(K_h D_2 \frac{\partial OPP_2}{\partial y}\right)}_{\text{horizontal dispersion}}$$

$$\underbrace{- w \cdot OPP^* + K_z(OPP_1 - OPP_2)}_{\text{vertical advection \& dispersion}} \underbrace{- B_2^P \cdot OPP_2 \cdot D_2}_{\text{decomposition}} \underbrace{+ S_1^P \cdot OPP_1 - S_2^P \cdot OPP_2}_{\text{settling}}$$

PO_4–P

Upper layer :

$$\underbrace{\frac{\partial IP_1 \cdot D_1}{\partial t}}_{\text{time variation}} = \underbrace{-\frac{\partial}{\partial x}(IP_1 \cdot u_1 \cdot D_1) - \frac{\partial}{\partial y}(IP_1 \cdot v_1 \cdot D_1)}_{\text{horizontal advection}} + \underbrace{\frac{\partial}{\partial x}\left(K_h D_1 \frac{\partial IP_1}{\partial x}\right) + \frac{\partial}{\partial y}\left(K_h D_1 \frac{\partial IP_1}{\partial y}\right)}_{\text{horizontal dispersion}}$$

$$\underbrace{+ w \cdot IP^* - K_z(IP_1 - IP_2)}_{\text{vertical advection \& dispersion}} \underbrace{- G \cdot OPP_1 \cdot D_1}_{\text{growth}} \underbrace{+ B_1^P \cdot OP_1 \cdot D_1}_{\text{decomposition}} \underbrace{+ L_{IP}}_{\text{external load}}$$

lower layer :

$$\underbrace{\frac{\partial IP_2 \cdot D_2}{\partial t}}_{\text{time variation}} = \underbrace{-\frac{\partial}{\partial x}(IP_2 \cdot u_2 \cdot D_2) - \frac{\partial}{\partial y}(IP_2 \cdot v_2 \cdot D_2)}_{\text{horizontal advection}} + \underbrace{\frac{\partial}{\partial x}\left(K_h D_2 \frac{\partial IP_2}{\partial x}\right) + \frac{\partial}{\partial y}\left(K_h D_2 \frac{\partial IP_2}{\partial y}\right)}_{\text{horizontal dispersion}}$$

$$\underbrace{- w \cdot IP^* + K_z(IP_1 - IP_2)}_{\text{vertical advection \& dispersion}} \underbrace{+ B_2^P \cdot OP_2 \cdot D_2}_{\text{decomposition}} \underbrace{+ R_{IP}}_{\text{release}}$$

COD

Upper layer :

$$\underbrace{\frac{\partial COD_1 \cdot D_1}{\partial t}}_{\text{time variation}} = \underbrace{-\frac{\partial}{\partial x}(COD_1 \cdot u_1 \cdot D_1) - \frac{\partial}{\partial y}(COD_1 \cdot V_1 \cdot D_1)}_{\text{horizontal advection}} + \underbrace{\frac{\partial}{\partial x}\left(K_h D_1 \frac{\partial COD_1}{\partial x}\right) + \frac{\partial}{\partial y}\left(K_h D_1 \frac{\partial COD_1}{\partial y}\right)}_{\text{horizontal dispersion}}$$

$$\underbrace{+ w \cdot COD^* - K_z(COD_1 - COD_2)}_{\text{vertical advection \& dispersion}} \underbrace{+ \beta \cdot G \cdot OPP_1 \cdot D_1}_{\text{growth}} \underbrace{- B_1^C \cdot COD_1 \cdot D_1}_{\text{decomposition}} \underbrace{- S_1^C \cdot COD_1}_{\text{settling}}$$

$$\underbrace{+ L_{COD}}_{\text{external load}}$$

Lower layer :

$$\underbrace{\frac{\partial COD_2 \cdot D_2}{\partial t}}_{\text{time variation}} = \underbrace{-\frac{\partial}{\partial x}(COD_2 \cdot u_2 \cdot D_2) - \frac{\partial}{\partial y}(COD_2 \cdot V_2 \cdot D_2)}_{\text{horizontal advection}} + \underbrace{\frac{\partial}{\partial x}\left(K_h D_2 \frac{\partial COD_2}{\partial x}\right) + \frac{\partial}{\partial y}\left(K_h D_2 \frac{\partial COD_2}{\partial y}\right)}_{\text{horizontal dispersion}}$$

$$+\underbrace{w\cdot COD^{*} - K_z(COD_1 - COD_2)}_{\text{vertical advection \& dispersion}} \underbrace{- B_2^{C}\cdot COD_2\cdot D_2}_{\text{decomposition}} + \underbrace{S_1^{C}\cdot COD_1 - S_2^{C}\cdot COD_2}_{\text{settling}}$$

$$+\underbrace{R_{COD}}_{\text{release}}$$

BOD

Upper layer :

$$\underbrace{\frac{\partial BOD_1\cdot D_1}{\partial t}}_{\text{time variation}} = \underbrace{-\frac{\partial}{\partial x}(BOD_1\cdot u_1\cdot D_1) - \frac{\partial}{\partial y}(BOD_1\cdot V_1\cdot D_1)}_{\text{horizontal advection}} + \underbrace{\frac{\partial}{\partial x}\left(K_h D_1 \frac{\partial BOD_1}{\partial x}\right) + \frac{\partial}{\partial y}\left(K_h D_1 \frac{\partial BOD_1}{\partial y}\right)}_{\text{horizontal dispersion}}$$

$$+\underbrace{w\cdot BOD^{*} - K_z(BOD_1 - BOD_2)}_{\text{vertical advection \& dispersion}} + \underbrace{\delta\cdot G\cdot OPP_1\cdot D_1}_{\text{growth}} - \underbrace{B_1^{B}\cdot BOD_1\cdot D_1}_{\text{decomposition}} - \underbrace{S_1^{B}\cdot BOD_1}_{\text{settling}}$$

$$+\underbrace{L_{BOD}}_{\text{external load}}$$

Lower layer :

$$\underbrace{\frac{\partial BOD_2\cdot D_2}{\partial t}}_{\text{time variation}} = \underbrace{-\frac{\partial}{\partial x}(BOD_2\cdot u_2\cdot D_2) - \frac{\partial}{\partial y}(BOD_2\cdot V_2\cdot D_2)}_{\text{horizontal advection}} + \underbrace{\frac{\partial}{\partial x}\left(K_h D_2 \frac{\partial BOD_2}{\partial x}\right) + \frac{\partial}{\partial y}\left(K_h D_2 \frac{\partial BOD_2}{\partial y}\right)}_{\text{horizontal dispersion}}$$

$$+\underbrace{w\cdot BOD^{*} - K_z(BOD_1 - BOD_2)}_{\text{vertical advection \& dispersion}} \underbrace{- B_2^{B}\cdot BOD_2\cdot D_2}_{\text{decomposition}} + \underbrace{S_1^{B}\cdot BOD_1 - S_2^{B}\cdot BOD_2}_{\text{settling}}$$

$$+\underbrace{R_{BOD}}_{\text{release}}$$

DO

Upper layer :

$$\underbrace{\frac{\partial DO_1\cdot D_1}{\partial t}}_{\text{time variation}} = \underbrace{-\frac{\partial}{\partial x}(DO_1\cdot u_1\cdot D_1) - \frac{\partial}{\partial y}(DO_1\cdot v_1\cdot D_1)}_{\text{horizontal advection}} + \underbrace{\frac{\partial}{\partial x}\left(K_h D_1 \frac{\partial DO_1}{\partial x}\right) + \frac{\partial}{\partial y}\left(K_h D_1 \frac{\partial DO_1}{\partial y}\right)}_{\text{horizontal dispersion}}$$

$$+\underline{w \cdot DO^{*} - K_z(DO_1 - DO_2)} \quad + \underline{\gamma \cdot G \cdot OPP_1 \cdot D_1} - \underline{B_1^{O} \cdot COD_1 \cdot D_1}$$

vertical advection & dispersion   growth   decomposition

$$+\underline{A(HOWA - DO_1)}$$

reaeration

Lower layer :

$$\underline{\frac{\partial DO_2 \cdot D_2}{\partial t}} = \underline{-\frac{\partial}{\partial x}(DO_2 \cdot u_2 \cdot D_2) - \frac{\partial}{\partial y}(DO_2 \cdot v_2 \cdot D_2)} + \underline{\frac{\partial}{\partial x}(K_h D_2 \frac{\partial DO_2}{\partial x}) + \frac{\partial}{\partial y}(K_h D_2 \frac{\partial DO_2}{\partial y})}$$

time variation   horizontal advection   horizontal dispersion

$$-\underline{w \cdot DO^{*} + K_z(DO_1 - DO_2)} \quad - \underline{B_2^{O} \cdot COD_2 \cdot D_2} - \underline{DB}$$

vertical advection & dispersion   decomposition   uptake by sediment

Parameters appeared in each equation are explained as follows:

OP_1 : O-P concentration in upper layer

OPP_1 : O-P(Inner Production) concentration in upper layer

IP_1 : PO_4-P concentration in upper layer

COD_1 : COD concentration in upper layer

BOD_1 : BOD concentration in upper layer

DO_1 : DO concentration in upper layer

OP_2 : O-P concentration in lower layer

OPP_2 : O-P(Inner Production) concentration in lower layer

IP_2 : PO_4-P concentration in lower layer

COD_2 : COD concentration in lower layer

BOD_2 : BOD concentration in lower layer

DO_2 : DO concentration in lower layer

D_1 : thickness of upper layer

D_2 : thickness of lower layer

G : growth rate of phytoplankton

B_1^{P} : O-P decomposition rate in upper layer

B_1^{C} : COD decomposition rate in upper layer

B_1^{B} : BOD decomposition rate in upper layer

B_1^{O} : DO uptake rate by decomposition in upper layer

S_1^{P} : O-P settling rate in upper layer

S_1^{C} : COD settling rate in upper layer

S_1^B : BOD settling rate in upper layer
B_2^P : O-P decomposition rate in lower layer
B_2^C : COD decomposition rate in lower layer
B_2^B : BOD decomposition rate in lower layer
B_2^O : DO uptake rate by decomposition in lower layer
S_2^P : O-P settling rate in lower layer
S_2^C : COD settling rate in lower layer
S_2^B : BOD settling rate in lower layer
R_{IP} : PO_4-P release rate
R_{COD} : COD release rate
R_{BOD} : BOD release rate
L_{OP} : O-P external load
L_{IP} : PO_4-P external load
L_{COD} : COD external load
L_{BOD} : BOD external load
DB : oxygen uptake rate by seabed sediment
A : reaeration constant
HOWA : saturated oxygen concentration
β : COD conversion factor from O-P
δ : BOD conversion factor from O-P
γ : DO conversion factor from O-P
u_1, v_1 : horizontal velocity components of seawater circulation in upper layer calculated by Tidal Current Model
u_2, v_2 : horizontal velocity components of seawater circulation in lower layer calculated by Tidal Current Model
w : vertical velocity components of seawater circulation in the interface between the upper layer and lower layer calculated by Tidal Current Model
K_h : horizontal dispersion coefficient
K_z : vertical dispersion coefficient

The parameters which contain asterisk indicate that

$OP^*=OP_2$, $OPP^*=OPP_2$, $IP^*=IP_2$, $COD^*=COD_2$, $BOD^*=BOD_2$, $DO^*=DO_2$ for $w \geqq 0$,
$OP^*=OP_1$, $OPP^*=OPP_1$, $IP^*=IP_1$, $COD^*=COD_1$, $BOD^*=BOD_1$, $DO^*=DO_1$ for $w < 0$,

respectively.

1.4.2 Finite Difference Equation

The method of converting to finite difference equations in the eutrophication model is same as that in the diffusion model mentioned above.

CHAPTER 2

RESULTS OF VERIFICATION TESTS

2.1 Review of Field Surveys and Laboratory Tests on Water Quality

Through this study, many field surveys and laboratory tests were performed. Most of their results are useful for the numerical simulation models as input data and verification data as follows;

(1) Pollution Sources and Runoff Loads

River discharge → Hydrodynamic Model, Diffusion Model, Eutrophication Model

Runoff load → Eutrophication Model

(2) Tidal Current and Tidal height → Hydrodynamic Model

(3) Water Quality in the Bay → Diffusion Model, Eutrophication Model

(4) Release Test and Oxygen Consumption Test → Eutrophication Model

(5) Primary Production Test → Eutrophication Model

(6) Sedimentation Test → Eutrophication Model

In these results, the distributions of water quality in DO, T-P, PO_4-P, O-P, COD and BOD are shown in Fig.2.1-1 to Fig.2.1-6 as verification data of numerical simulation models.

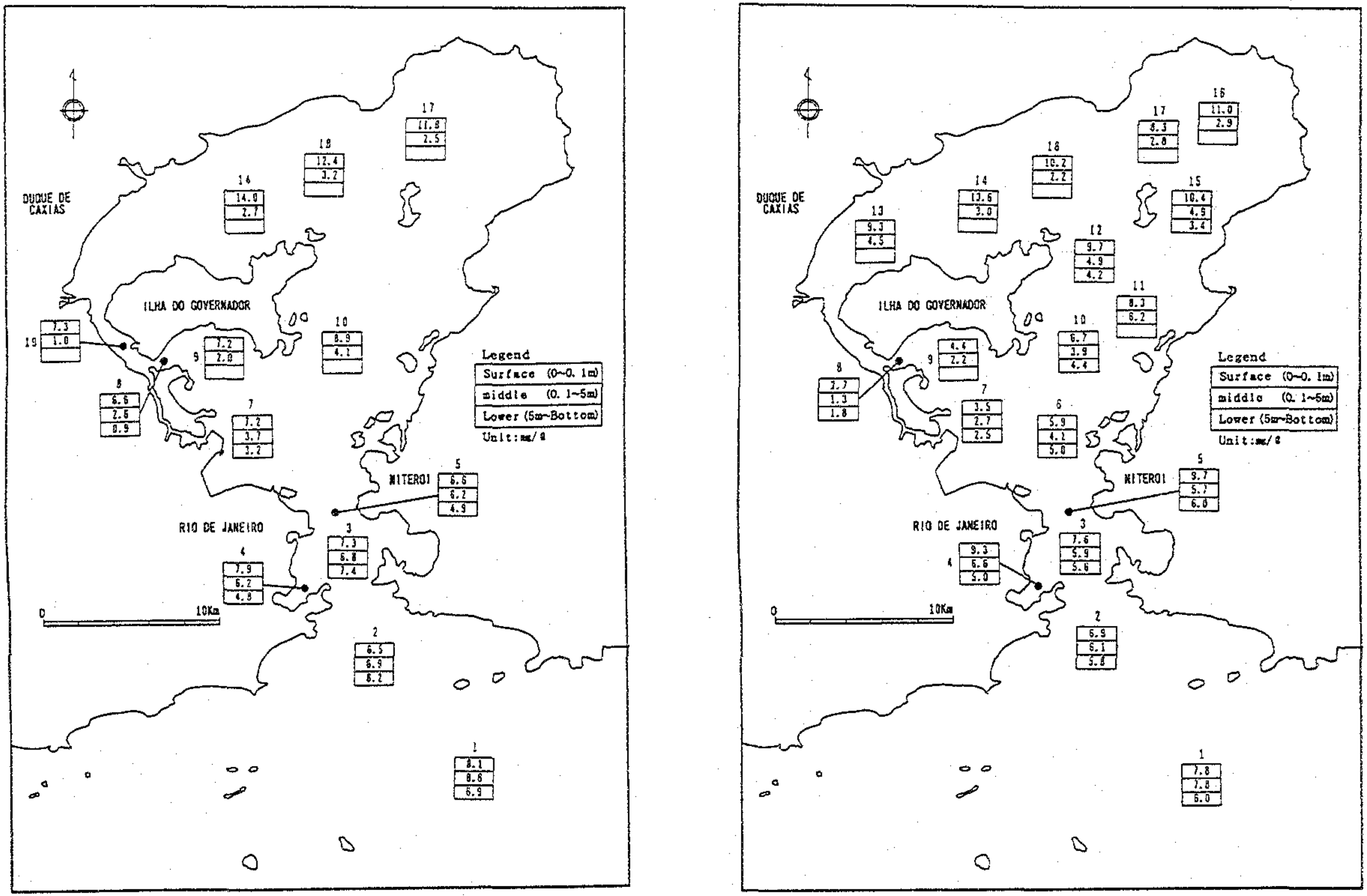

Rainy Season

Dry Season

Fig. 2.1-1 Observed Water Quality Distribusion (DO)

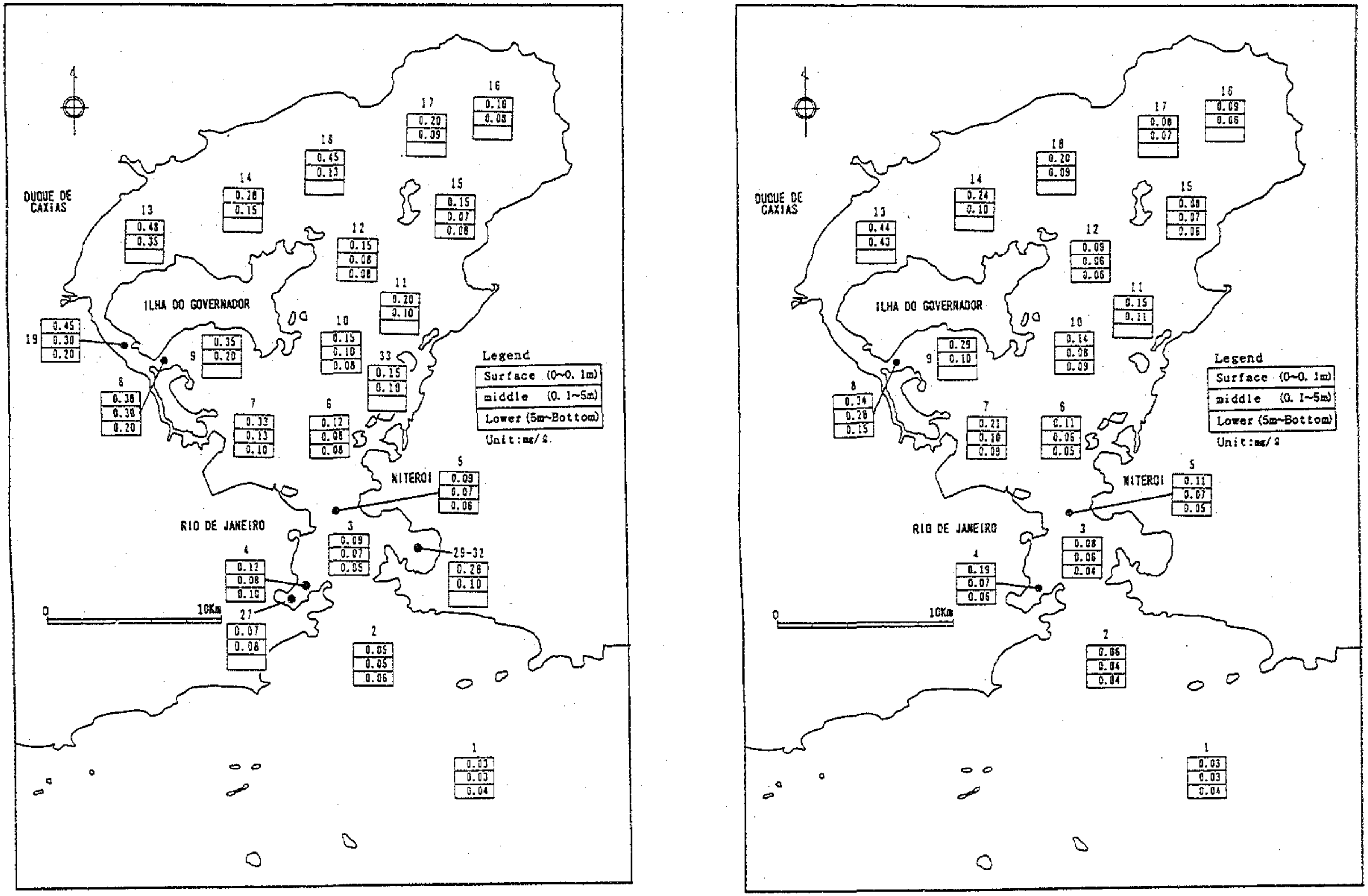

Rainy Season

Dry Season

Fig. 2.1-2 Observed Water Quality Distribusion (T-P)

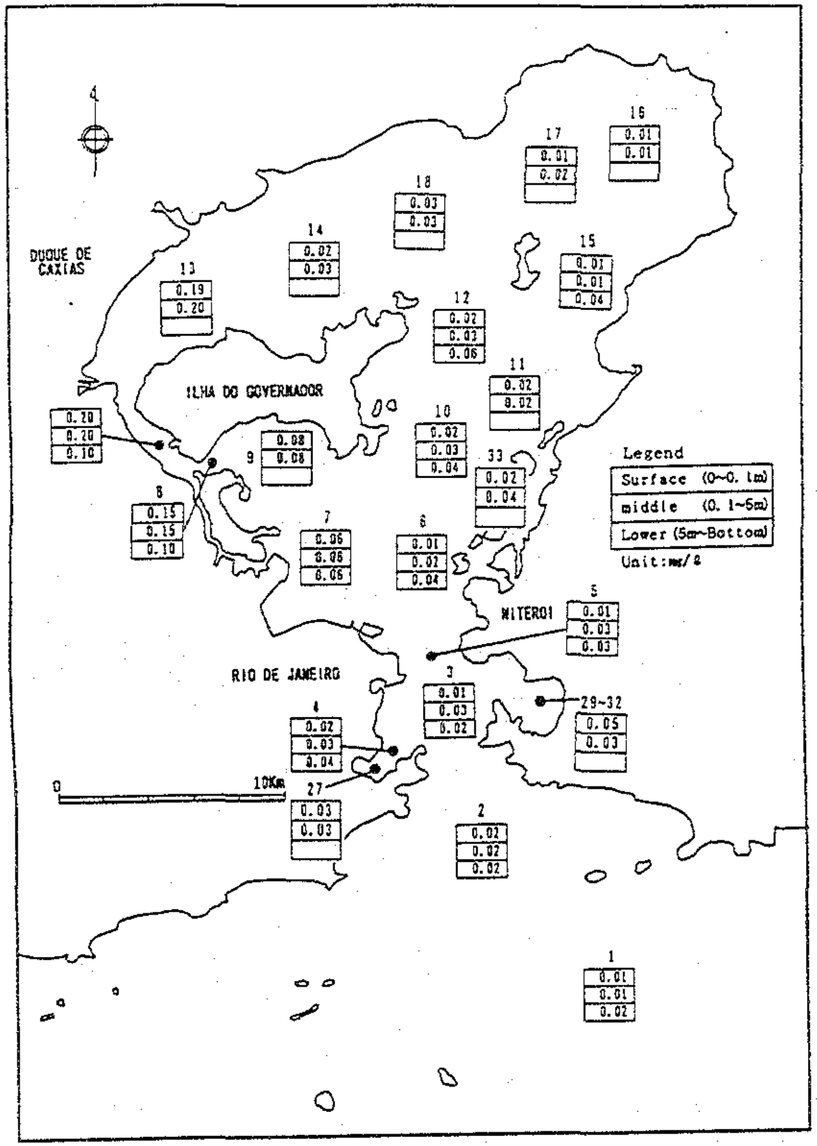

Rainy Season

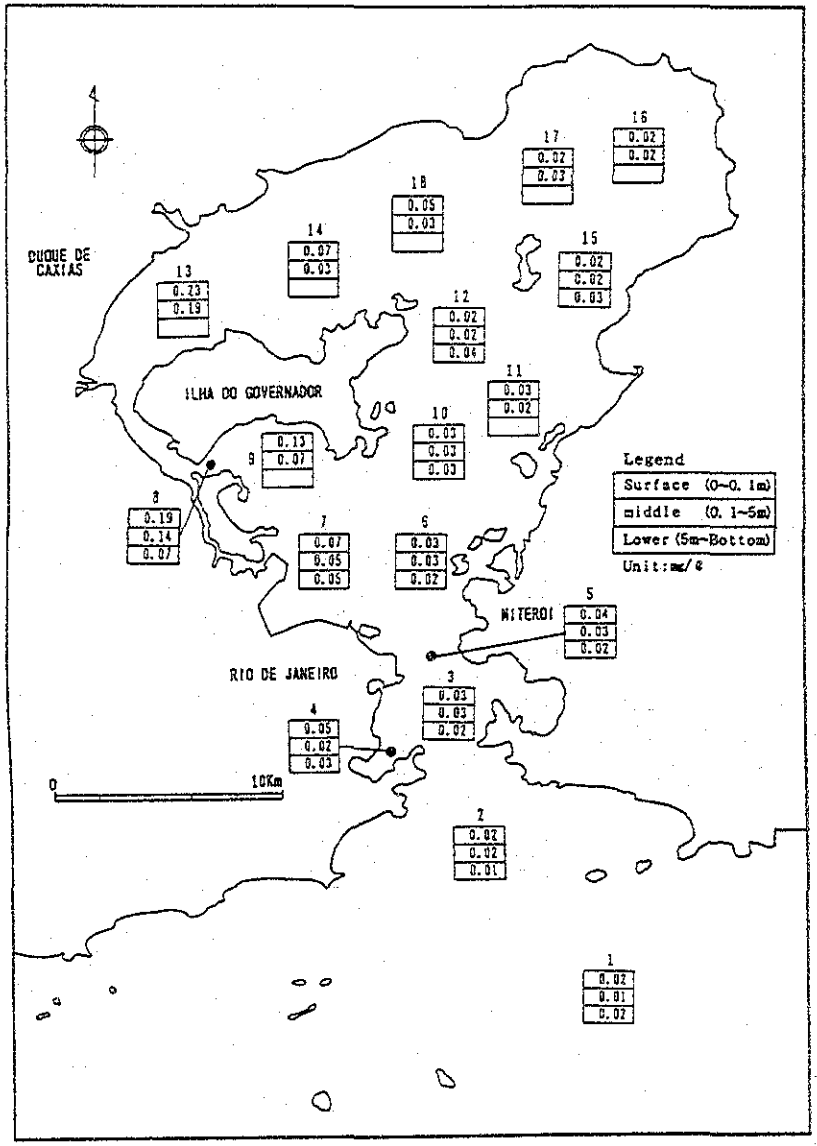

Dry Season

Fig. 2.1-3 Observed Water Quality Distribusion (PO_4-P)

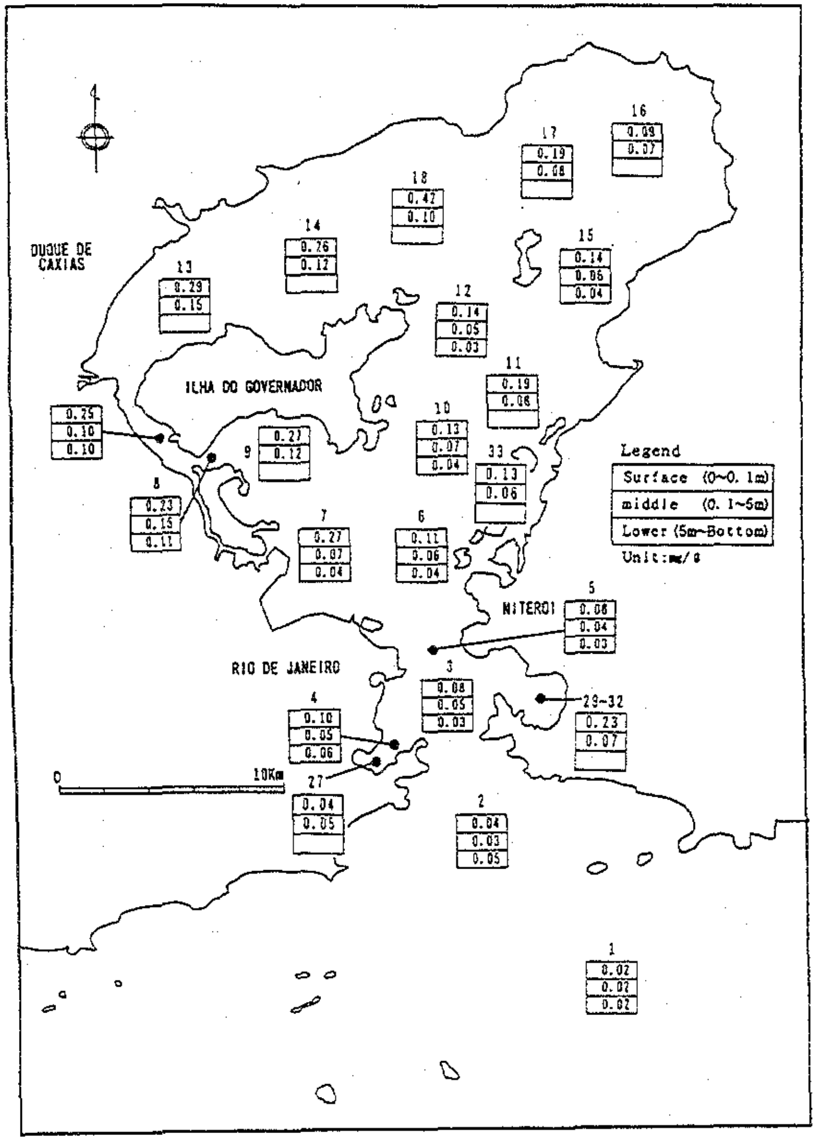

Rainy Season

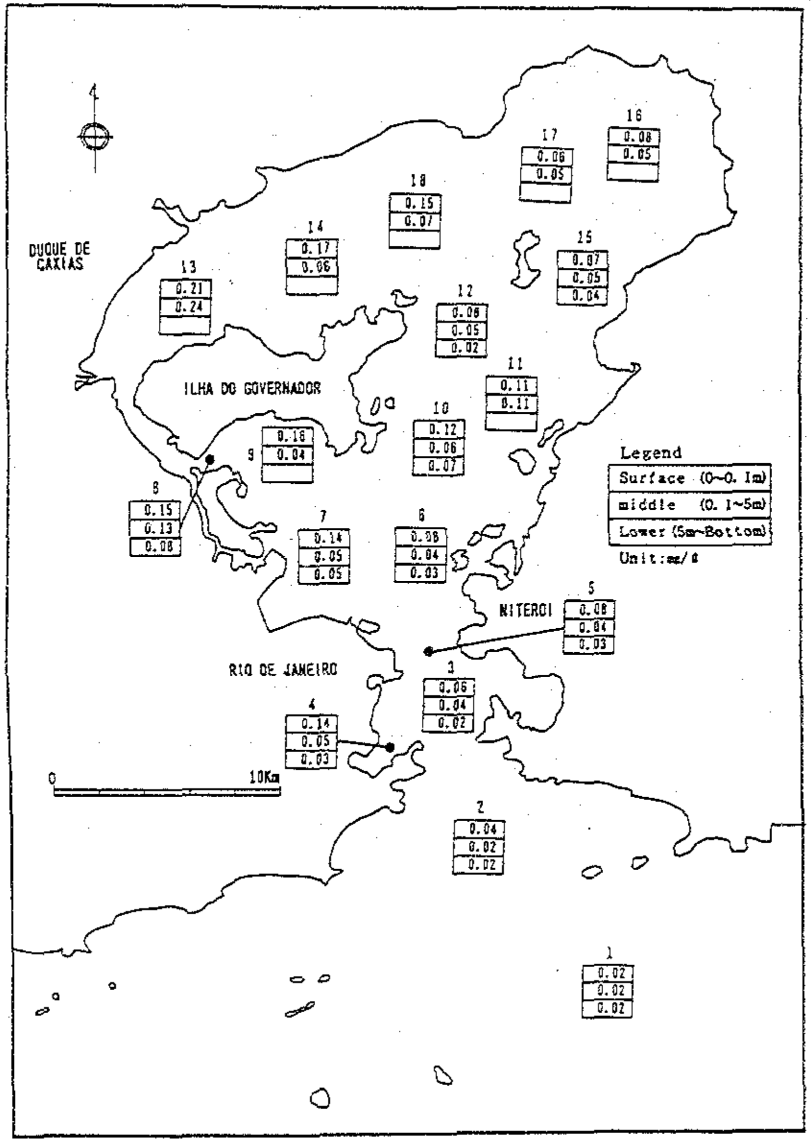

Dry Season

Fig. 2.1-4 Observed Water Quality Distribusion (O-P)

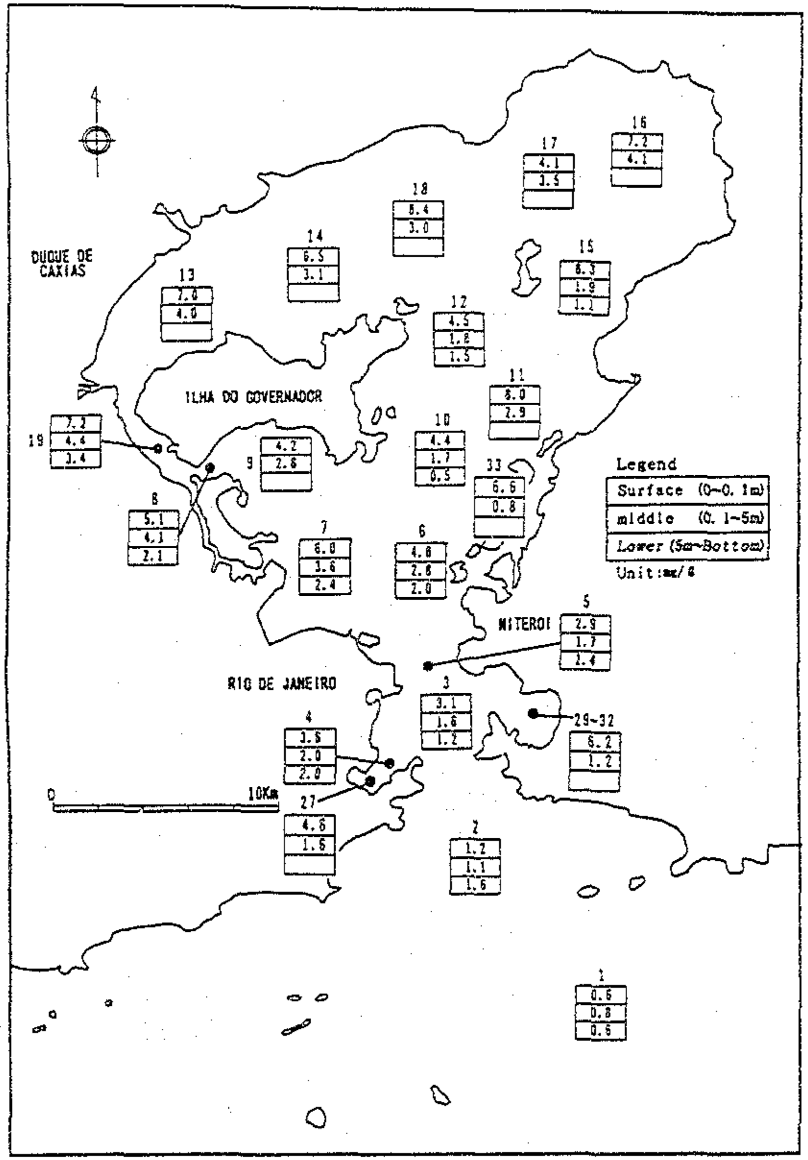

Rainy Season

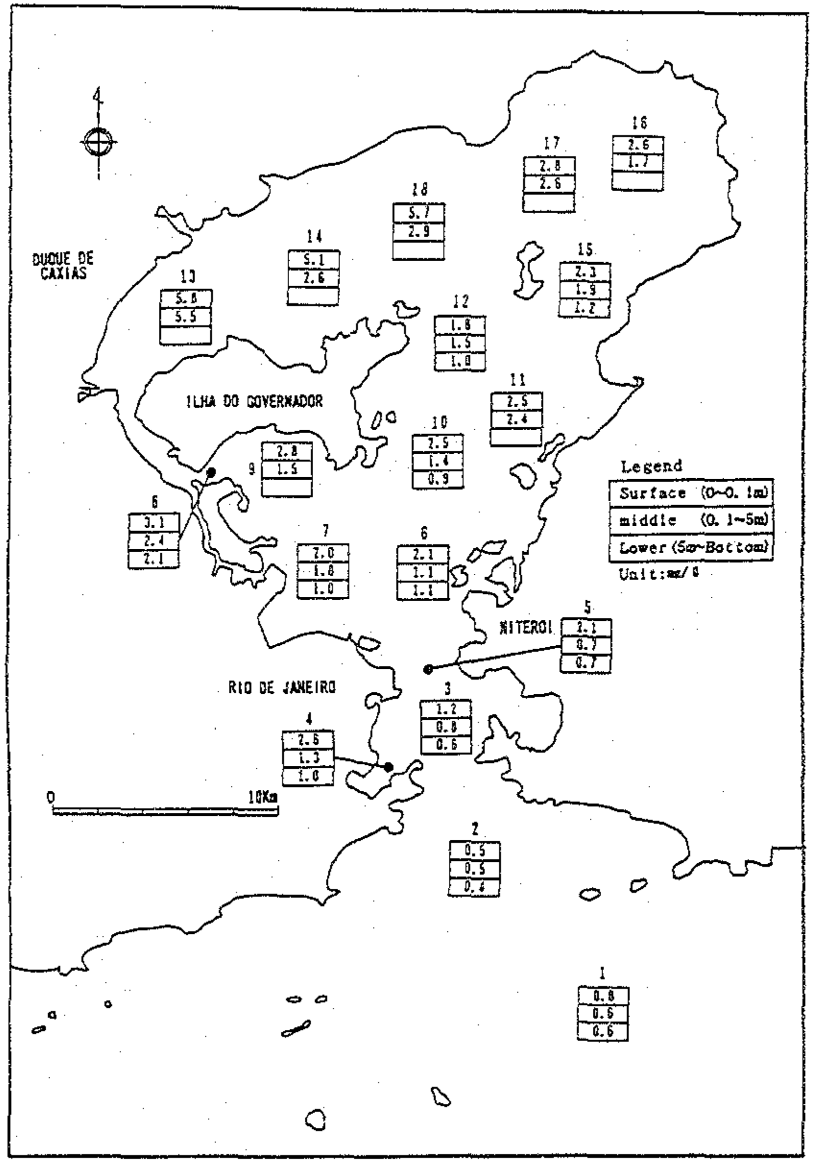

Dry Season

Fig. 2.1-5 Observed Water Quality Distribusion (COD_{MN})

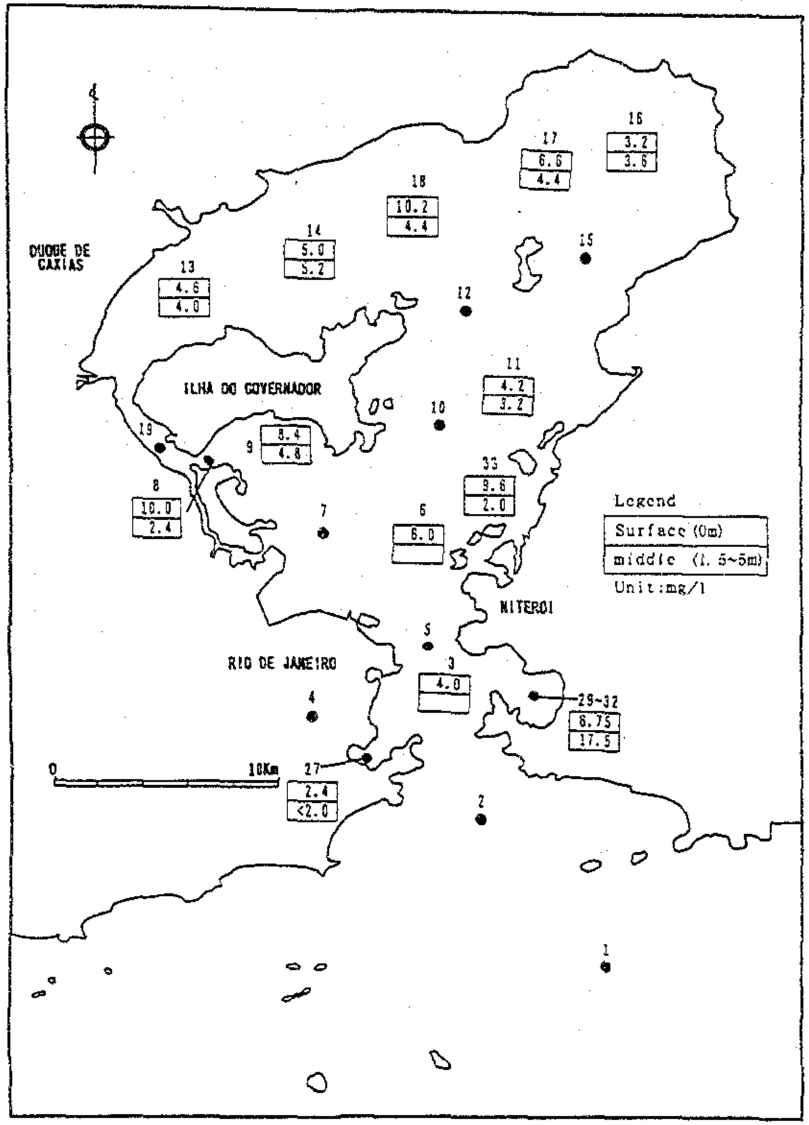

Rainy Season

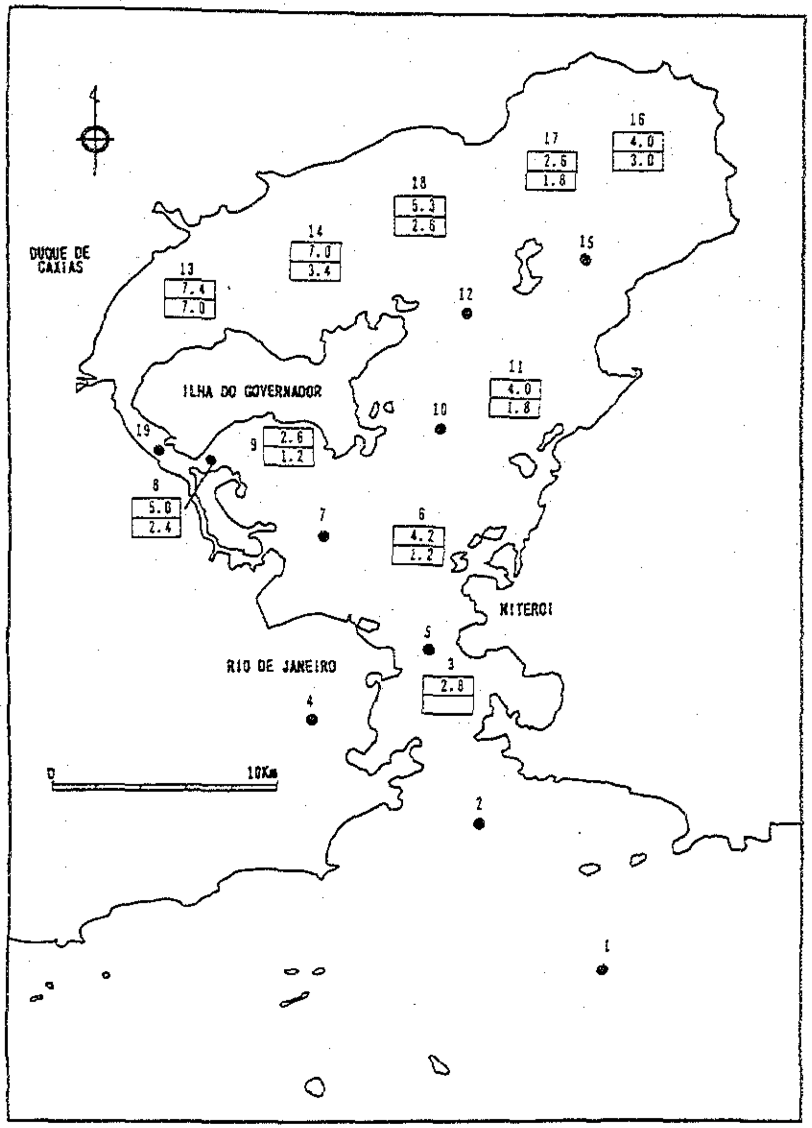

Dry Season

Fig. 2.1-6 Observed Water Quality Distribusion (BOD)

2.2 Calculation Indices

On the assumption mentioned in the previous chapter, we calculated the following indices by the numerical simulation in this study.

Hydrodynamic	:	Two horizontal velocity components both in upper layer and lower layer.
Diffusion Model	:	Salinity for calibration of dispersion coefficient.
Eutrophication Model	:	BOD and COD for the concentration of organic matters. DO for the amount of dissolved oxygen. PO_4-P and O-P as nutrient salts.

On the formulation of an eutrophication model, there are much arguments about tracers. Phosphorus and nitrogen compounds are the most important nutrients which control seawater pollution by organics. The content of phosphorus and nitrogen in organics is generally kept in a certain ratio, but this ratio differs between species of organisms or the stage of their growth. Therefore, the nutrient budget is determined by both phosphorus and nitrogen.

The structure of the prediction model, however, becomes more complicated if both phosphorus and nitrogen behaviors are formulated. Thus, the nutrient cycle treated by only phosphorus is preferentially applied to the model for the reason that the phosphorus would be a limiting factor to a nutrient cycle in an eutrophic bay from Fig.2.2-1 showing the correlation between N and P ratio both in water and in algae. Details can be referred to the chapter about Aquatic Organisms.

	Seston	Water
N	0.132 +4.92 x P	0.562 +4.42P
R	0.89	0.77
Sample Number	48	49

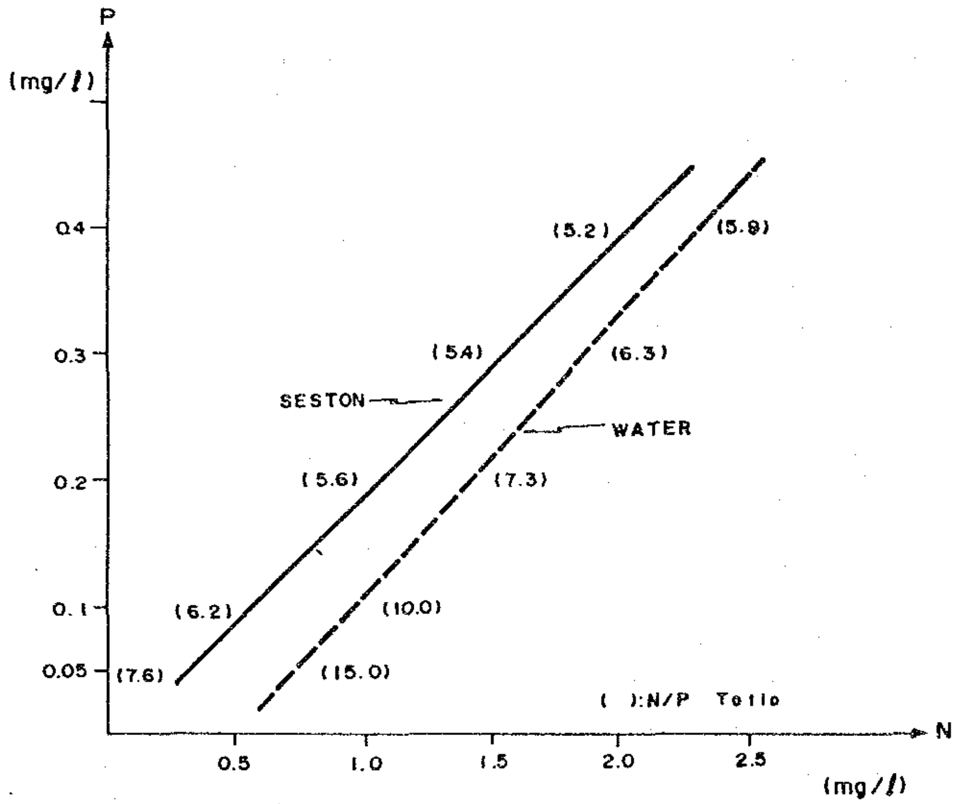

Fig. 2. 2-1 N and P Ratio in Water and in Seston

2.3 Calculation Conditions

2.3.1 Hydrodynamic Model

The calculation of tidal currents in the Guanabara Bay was performed for the area shown in Fig.2.3.1 using a two-level model with 500 meters lattice interval on the mean spring tides.

Calculation conditions applied in the hydrodynamic model are summarized in Table 2.3-1.

Table 2.3-1 Calculation condition for Hydrodynamic Model

Item	Condition
Target Season	Dry season, Rain season, Annual Mean
Model	Two-Level Model
Lattice Interval	500m
Calculation Area	Fig.2.3-1
Topography	Fig.2.3-2
Tidal Condition	M_2+S_2
Mean Water Level	M.S.L
Thickness of Upper Layer	3.0m
Time Step	15 sec
Horizontal Eddy Viscosity	10^4 cm^2/s
Bottom Friction Coefficient	0.0026
Inner Friction Coefficient	0.001
Acceleration Due to Gravity	9.8 m/s^2
Coriolis Coefficient	$-5.64*10^{-5}$
Open Boundary Condition	The tidal height at all open boundaries are 45cm and the difference between the eastern and western boundary is 1.38°
Calculation time	for 5 tidal repetition

a) Lattice Interval

Lattice Interval was determined in view of the accuracy of reproduction of topography and the ability of computer.

b) Topography

Topography of the Guanabara bay shown in fig.2.3-2 was read by the existing chart.

c) Tidal Condition

In the Guanabara Bay, semi-diurnal tides such as M_2 and S_2 constituents are predominant and it is thought tidal current caused by them influence upon the water quality in the bay.

Therefore, we simulated tidal current under the mean spring tide.

d) Thickness of Upper Layer

This value is based on the observed results of the vertical profile of σ_t and transparency as shown in Fig.2.3.3 and Fig.2.3-4.

Here, we supposed the thickness of the upper layer as a photic layer. Generally, there is a correlation between the transparency (T) and the compensation depth (C_D), that is C_D=2.5 x T.

e) Time Step

Time interval for the hydrodynamic model by explicit finite difference method is determined by the following equation;

$$dt \geqq ds/\sqrt{(2gh_{max})}$$

f) Coriolis Coefficient

Coriolis coefficient is determined by the following equation;

$$f = 2\omega \sin\phi$$

ω: phase velocity of rotation of the earth

ϕ: latitude

g) Open Boundary Condition

The open boundary conditions are given by tidal height and phase lag. The harmonic constants at Santa Cruz in the mouth of the Guanabara Bay and Ilha Guaiba located 92km west from the Guanabara Bay, as shown in Table 2.3-2, were used to determine open boundary conditions.

Table 2.3-2 Tidal Harmonic Constants for Simulation Model

	Height (cm)		Phase lag (degree)	
Point	M2	S2	M2+S2	G(°)
Ilha Guaiba	32.9	19.2	52.1	86.96
Santa Cruz	31.6	17.4	49.0	83.00

The difference between the phase lag of Ilha Guaiba and Santa Cruz is 3.9°, and the distance of these two points is about 92km. By establishing a simulation range of 32km at the open boundary, a phase lag difference of 1.38° was estimated between the east and west open boundaries. The height of the tides was established as 0.45m at all open boundaries, thus the height of the tides at Santa Cruz is 0.49m, and the amplitude of constituents is M2 and S2.

h) Calculation Time

Calculation time means the time required to be stabilized the calculated result.

In general this value is about from 3 to 5 tidals in the case of tidal current calculation. In this study this value determined 5 tidals after the confirmation in pre-calculation.

i) other coefficients

We set the values using in the sea area generally.

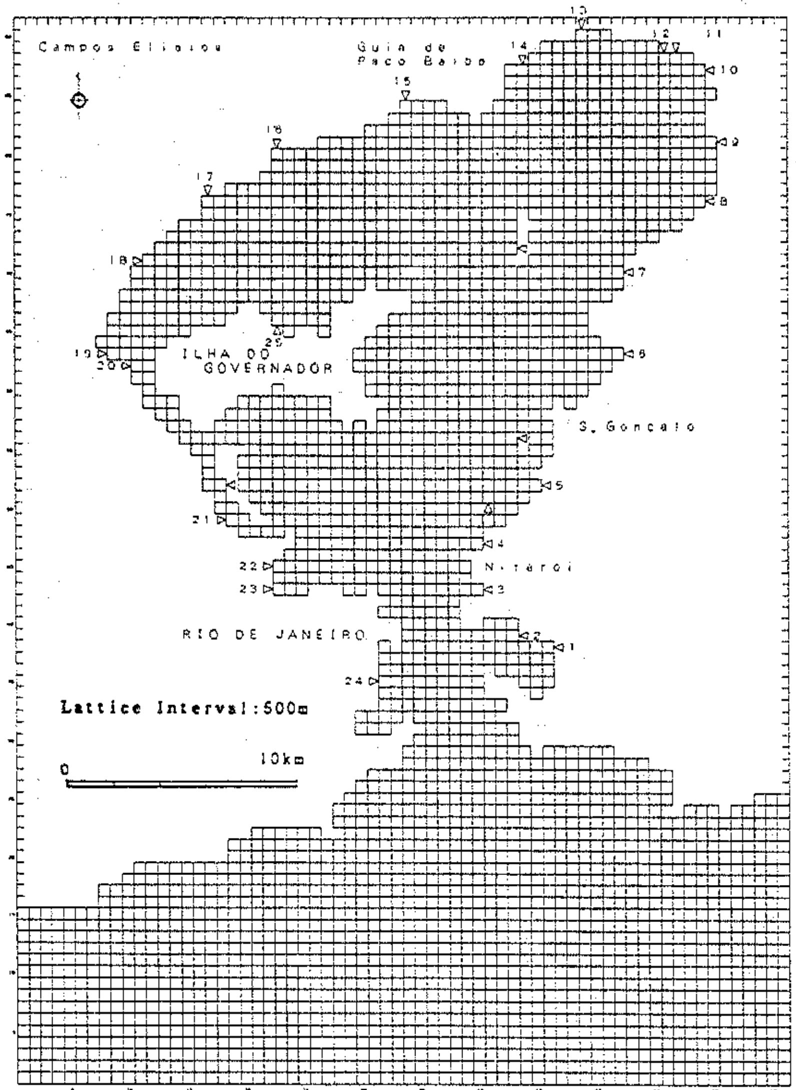

Fig. 2. 3-1 Simulation Lattice Map and River Inflow Points

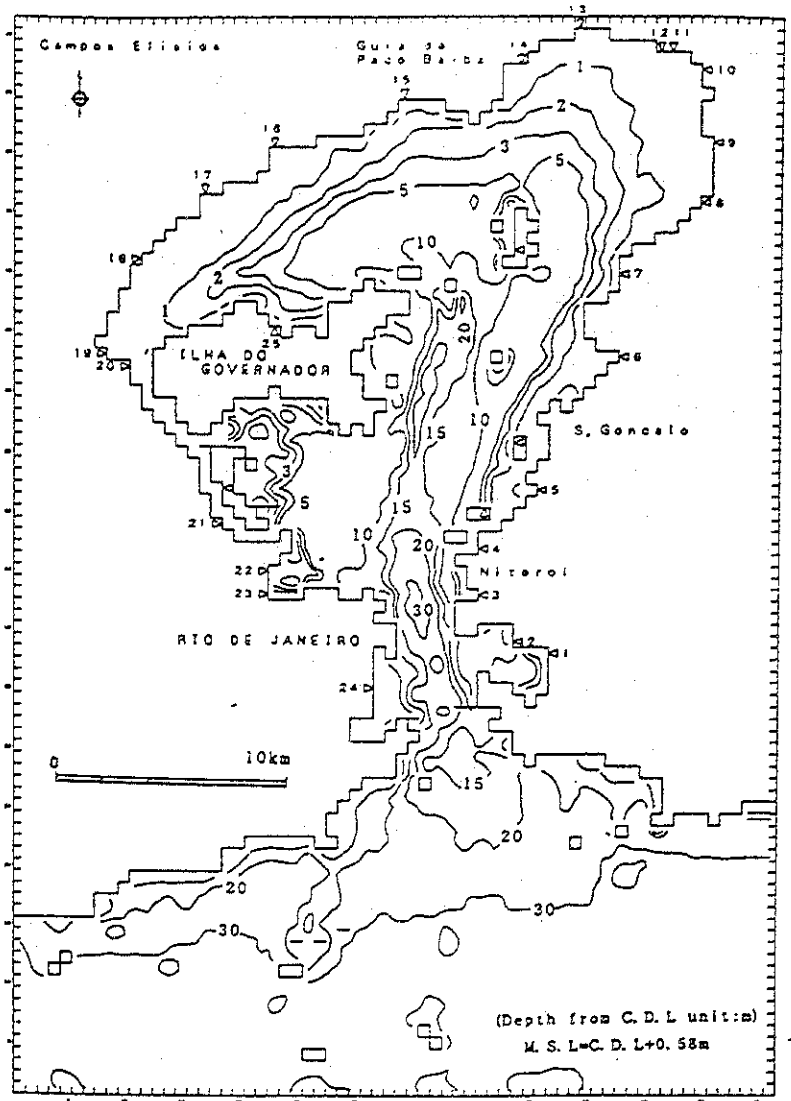

Fig. 2. 3-2 Water Depths used for simulation Model

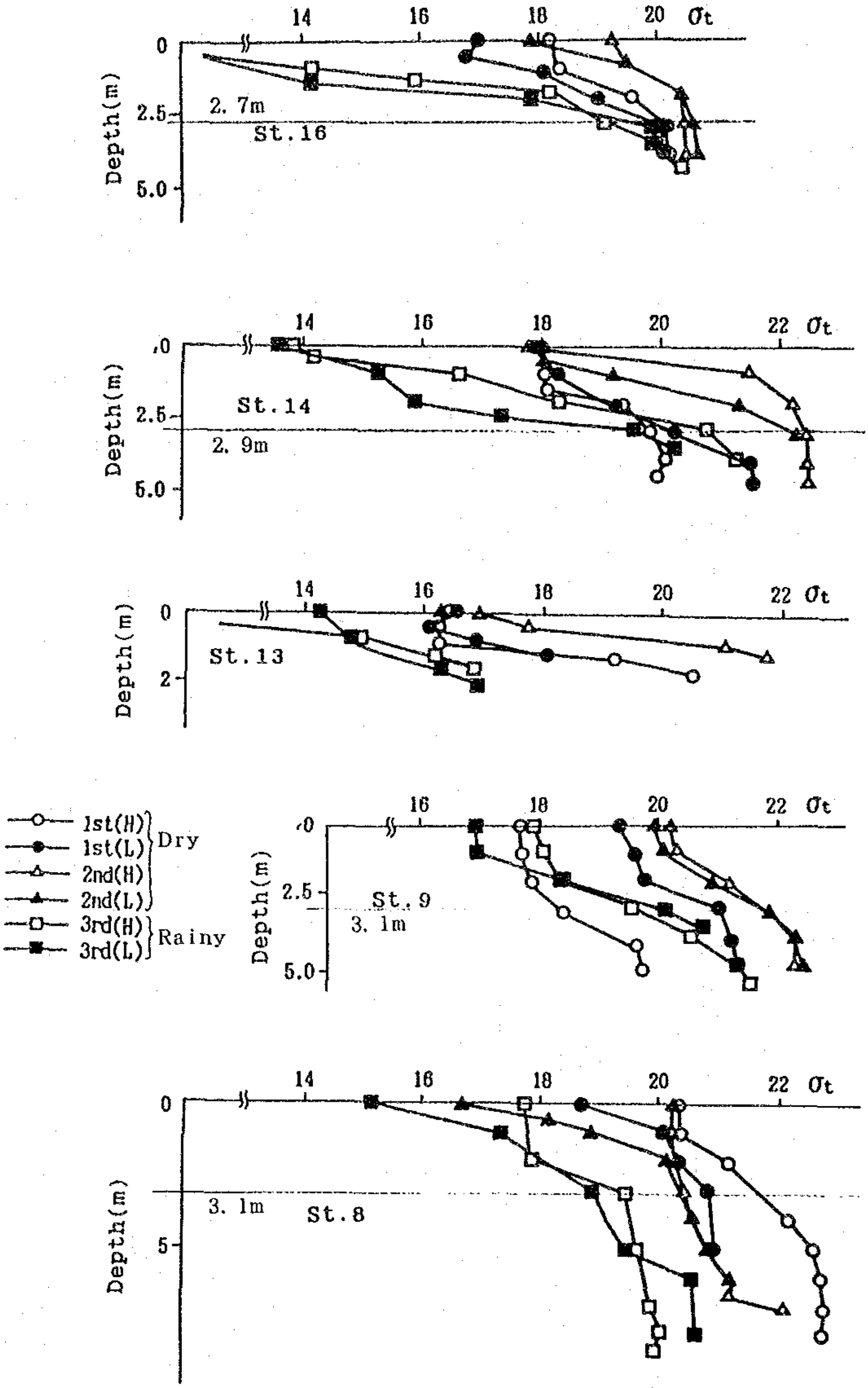

Fig. 2. 3-3(1) **Vertical Distribution of Sigma-t** (1)

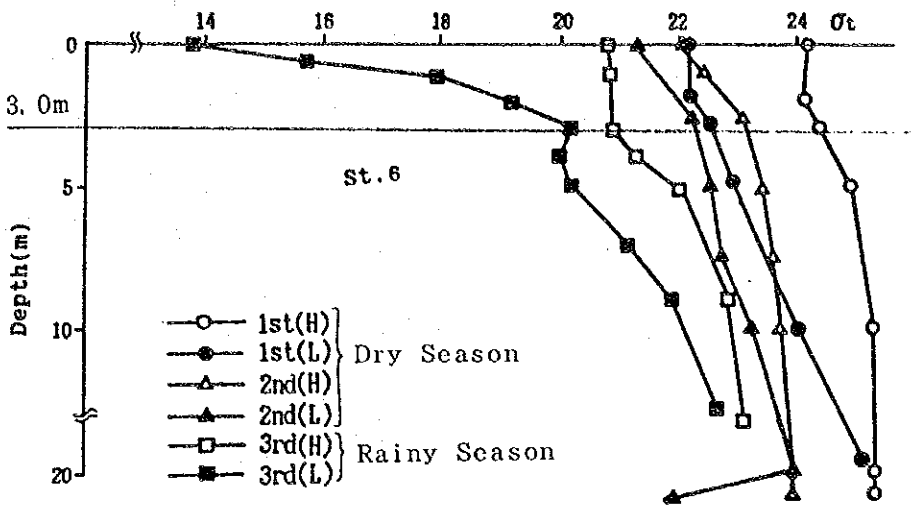

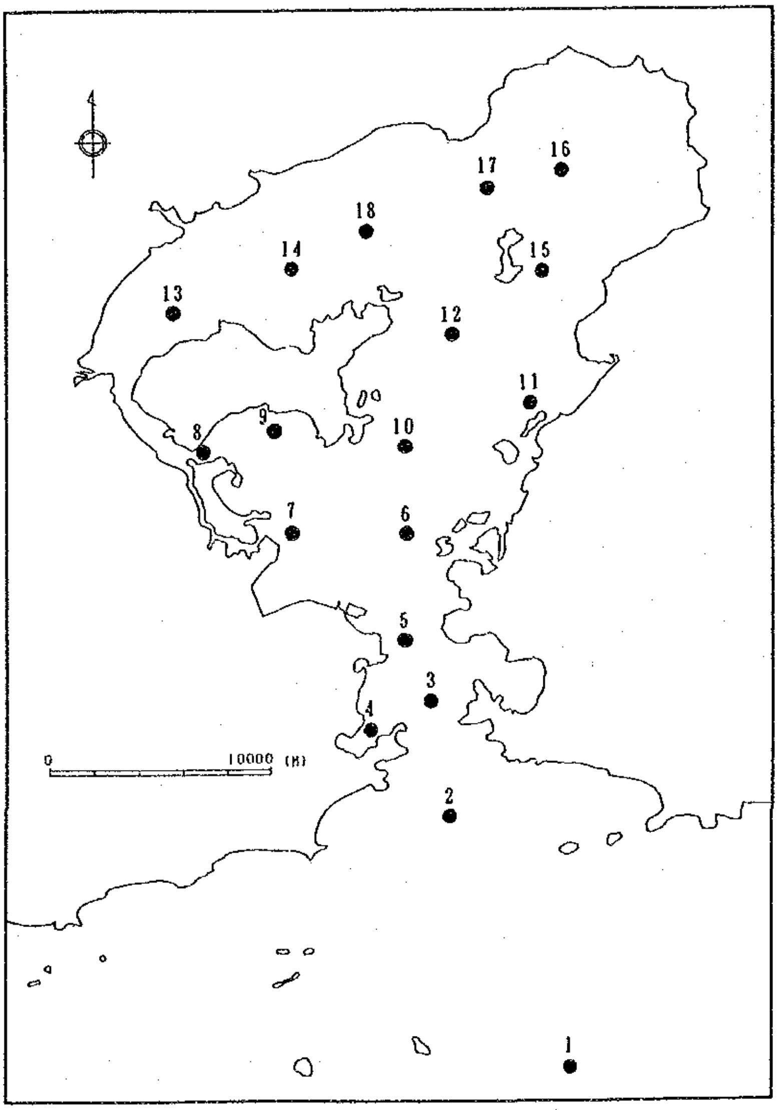

Fig. 2. 3-3(2) **Vertical Distribution of Sigma-t** (2)

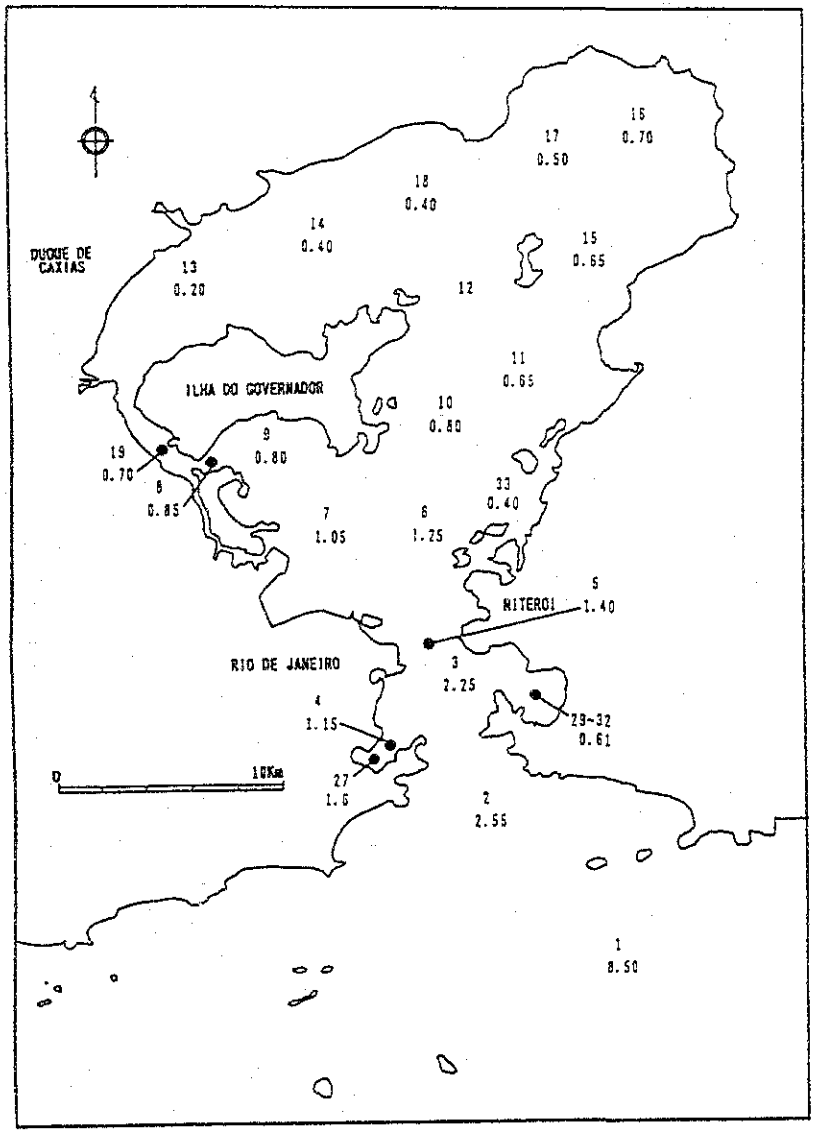

Rainy Season

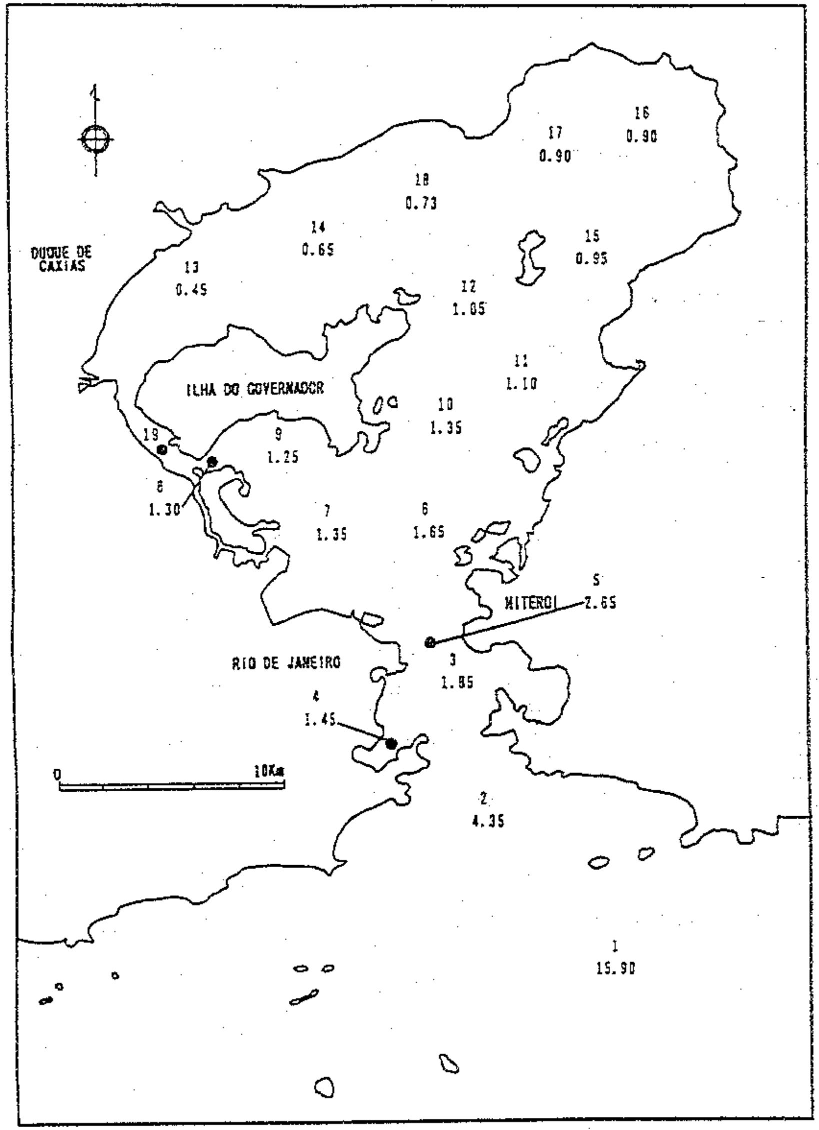

Dry Season

Fig. 2.3-4 Observed Water Quality Distribusion (Transparency)

2.3.2 Diffusion Model

The calculation for the diffusion or dispersion of conservative substances in the bay was performed to determine the dispersion coefficients using a salinity as a conservative substance both in the dry season and the rainy season.

Calculation conditions applied in the diffusion model are summarized in Table 2.3-3.

Table 2.3-3 Calculation Condition for Diffusion Model

Item	Condition
Target Season	Dry season, Rain season
Index	Salinity
Tidal Condition	M_2+S_2
Thickness of Upper Layer	3.0m
Computational Area	Fig.2.3-1
Horizontal Dispersion Coefficient	Fig.2.3-5
Vertical Dispersion Coefficient	0.0 cm^2-s
Discharge of Rivers	Table 11.1-4
Initial Value	Inner of the bay 30 Outer of the bay 35
Open Boundary Concentration	35
Time Step	150 second
Computation Time	for 120 tidal repetition

a) Target Season

Through the observation of the distribution of salinity in the bay, there is the obvious difference between dry season and rainy season.

To raise accuracy we calculated both seasons.

b) Horizontal Dispersion Coefficient

We finally set the horizontal dispersion coefficient as shown in Fig.2.3-5. The value in the almost area is

$1.0x10^6$ cm^2/s except the eastern costal area, in which it is smaller because of complex of topography.
Therefore, we set $1.0 \times 10^4 cm^2/s$ in Jurujuba bay and $5.0x10^4$ cm^2/s in the part of eastern area through the cariblation tests.

c) *Vertical Dispersion Coefficient*

We usually use about $0.001cm^2/s$ as vertical dispersion coefficient. But vertical velocity is overestimated compared with observed vertical distribution of salinity. Therefore, we set it as $0.0cm^2/s$.
Regarding the vertical dispersion coefficient, we set zero on an assumption that the vertical movement is controlled by a vertical advection.

d) Discharge of Rivers

Discharge of rivers for simulation is determined by the results of field survey as shown in Table 2.3-5 later.

e) Initial Value

The initial values for the distribution of concentration were given with the concentrations observed.

Moreover, we practiced a pre-calculation using the above concentration for the period of 120 tidals and the result of the pre-calculation was used as an initial value for the final calculation.

f) Open Boundary Concentration

The concentration at the open boundaries was given with the concentrations observed at the outside of the bay (St.1).

g) Computation Time

It takes about 120 tidals to stabilize the calculated results because the residence time in Guanabara Bay is thought about 60 days.
This was confirmed by the pre-calculation.

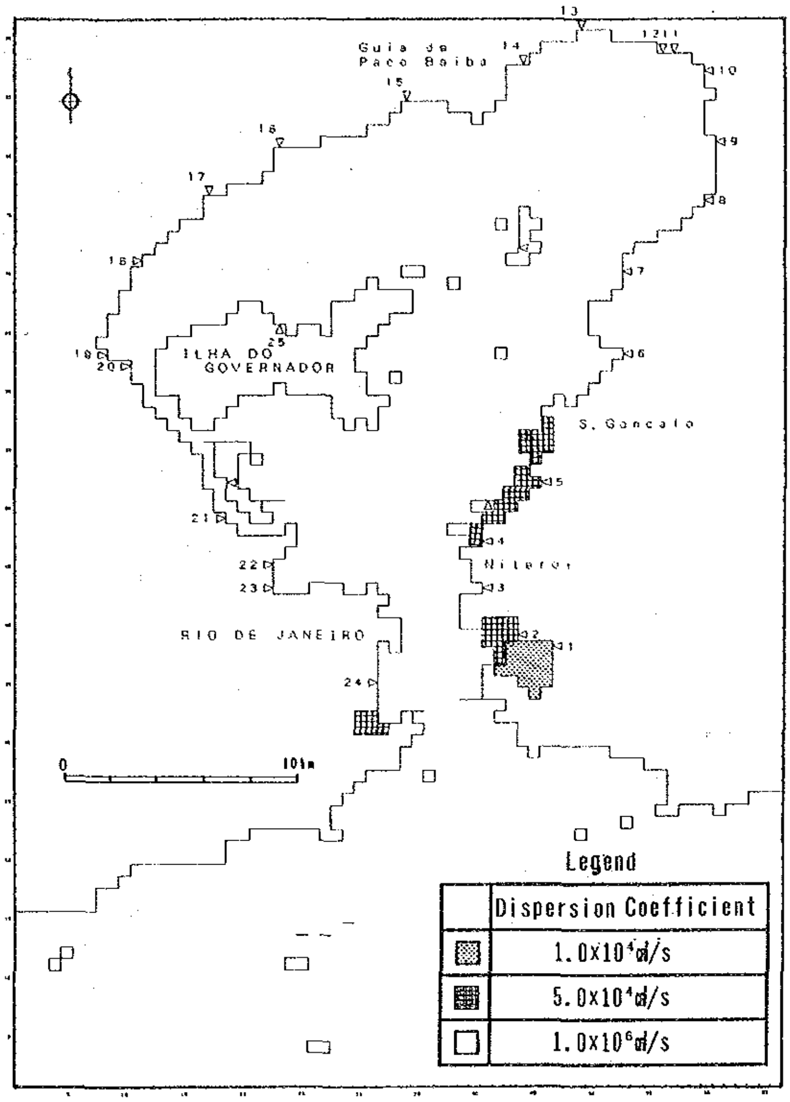

Fig. 2. 3-5 Dispersion Coefficient used for Simulation

2.3.3 Eutrophication Model

On the calculation for the concentration of organic matters and/or nutrient salts considering eutrophic phenomena, it needs to determine the values for various parameters referring to the observation data in the field and the existing literatures.

The method and criteria for the determination of parameters are described below and calculation conditions applied in the eutrophication model are summarized in Table 2.3-4.

Table 2.3-4(1) Calculation Condition for Eutrophication Model

Item		sign	value
Target season			Dry season, Rainy season, Annual mean
Index			COD, BOD, O-p, PO_4-P, DO
Computational area			Fig.2.3-1
Tidal condition			M_2+S_2
Thickness of upper			3.0m
growth rate (1/day)		G	0.70*(IP_1/0.012+IP_1)
Growth rate constant		μmax	0.700
P04-P Semi-saturation constant		k_{IP}	0.012
decomposition rate (1/day)			
upper	O-P	B_1^P	0.10
	COD	B_1^C	0.10
	BOD	B_1^B	0.10
lower	O-P	B_2^P	0.10
	COD	B_2^C	0.10
	BOD	B_2^B	0.10
DO uptake rate by decomposition(1/day)			
upper		B_1^O	0.60
lower		B_2^O	0.60
settling rate (1-day)			
upper	O-P	S_1^P	0.30
	COD	S_1^C	0.30
	BOD	S_1^B	0.30
lower	O-P	S_2^P	0.45
	COD	S^C	0.45
	BOD	S_2^B	0.45

Table 2.3-4(2) Calculation Condition for Eutrophication Model

Item	sign	value
release rate ($mg/m^2/day$)		Fig.2.3-8
COD	R_{COD}	167.0
BOD	R_{BOD}	262.0
PO_4-P	R_{IP}	11.0 ~ 20.0
DO uptake rate by sediment ($mg/m^2/day$)	DB	690.0 ~ 1670
reaeration constant (1/day)	A	0.8
saturated DO concentration (mg/l)	HOWA	6.8
conversion factor		
COD/O-P	β	16.4
BOD/O-P	δ	25.6
DO/O-P	γ	143
Horizontal dispersion coefficient	K_H	Fig.2.3-5 ($1.0x10^4$ ~ $1.0x10^6$ cm^2/s)
Vertical dispersion coefficient	K_z	0.0 cm^2/s
external load	L_{COD} L_{BOD} L_{IP}	Table 2.3-5
initial value		The value based on the observation
Open boundary condition		Open boundary concentration is fixed as shown below COD 0.6mg/l BOD 1.0mg/l PO4-P 0.02mg/l O-P 0.02mg/l DO 7.8mg/l
time step		120 second
computation time		for 120 tidal repetition

a) Thickness of the Upper Layer

This was discussed in the section of conditions for Hydraulic Model calculation.

b) Growth Rate

The growth rate of phytoplankton is expressed as the increase of O-P in the model and BOD (COD) is increased corresponding to the amount of O-P.

Generally, the growth rate of phytoplankton can be determined in relation to water temperature, light intensity and concentration of nutrient salts such as N and P, and the growth rate of O-P (G) can be expressed with the concentration of PO_4-P (IP) as follows if we suppose water temperature and light intensity as a constant;

$$G = \mu_{max} \times IP / (K_{IP}+IP)$$

μ_{max} : maximum specific growth rate of O-P

IP : concentration of PO_4-P

K_{IP} : semi-saturation constant of PO_4-P

The value of μ_{max} was 0.70 through the calibration in comparison with the results of primary production experiments and that of K_{IP} was 0.012 according to the experiment for Oscillatoria.

We set these values as a constant for both seasons of dry season and rainy season because of no data for both seasons, though there is a possibility of change in both seasons.

Fig.2.3-6 shows the growth rate variation according to PO4-P concentration and Fig.2.3-7 shows the correlation between Transparency and T-P concentration.

It is thought the amount of primary production is extremely small comparing with external PO4-P loads in western area. Therefore, we decreased the amount of production of O-P in proportion to the ratio of the transparency calculated T-P concentration to the thickness of upper layer (3m).

c) Decomposition Rate

The decomposition is considered on BOD(COD) and on the process from O-P to PO_4-P in the model. Generally, the decomposition rate changes depending on the water temperature. the variation of temperature, however, does not be considered in the model and we do not have any data about it in Brazil. Therefore, we set constant value shown in Table 2.3-4 as decomposition rate through calibration tests, referring to the following data obtained in Japan.

COD: 0.01 to 0.1 (1/day)

O-P: 0.01 to 0.2 (1/day)

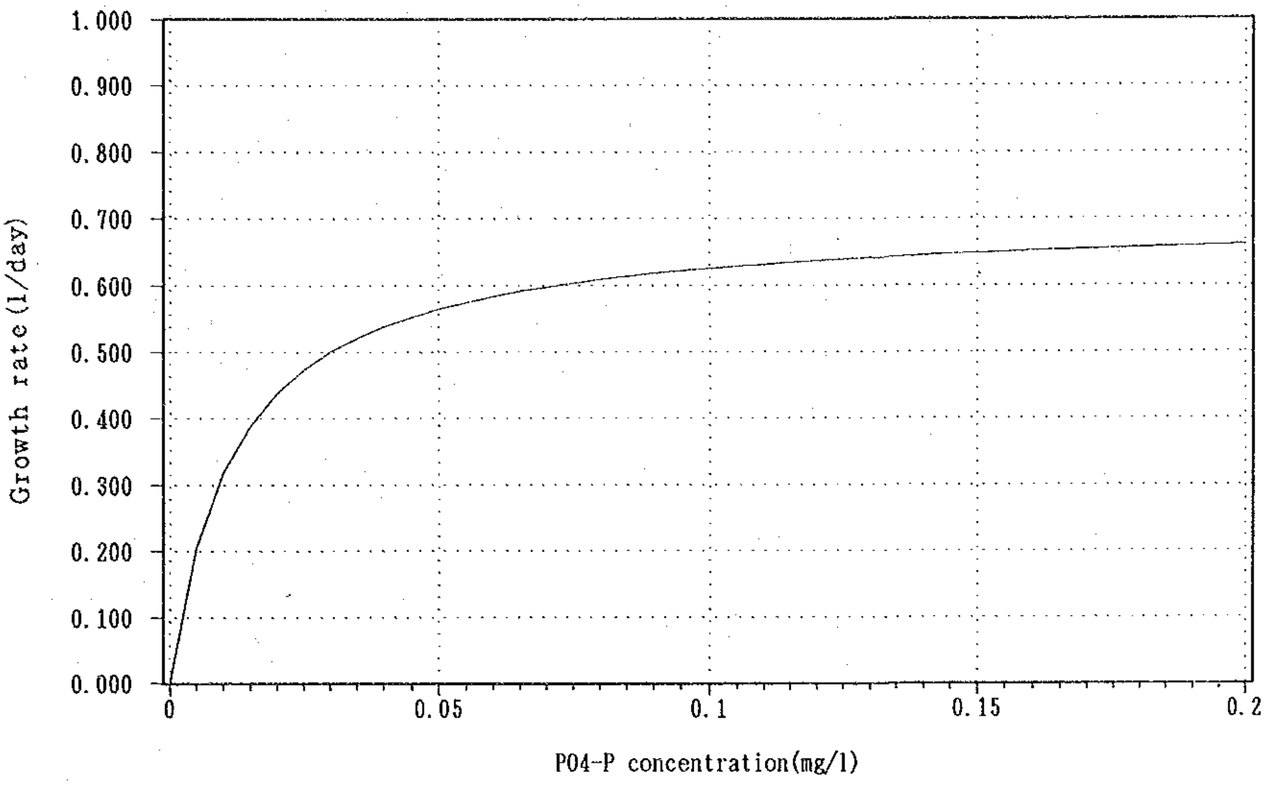

Fig. 2. 3-6 Correlation between PO_4-P and Growth Rate used for Simulation

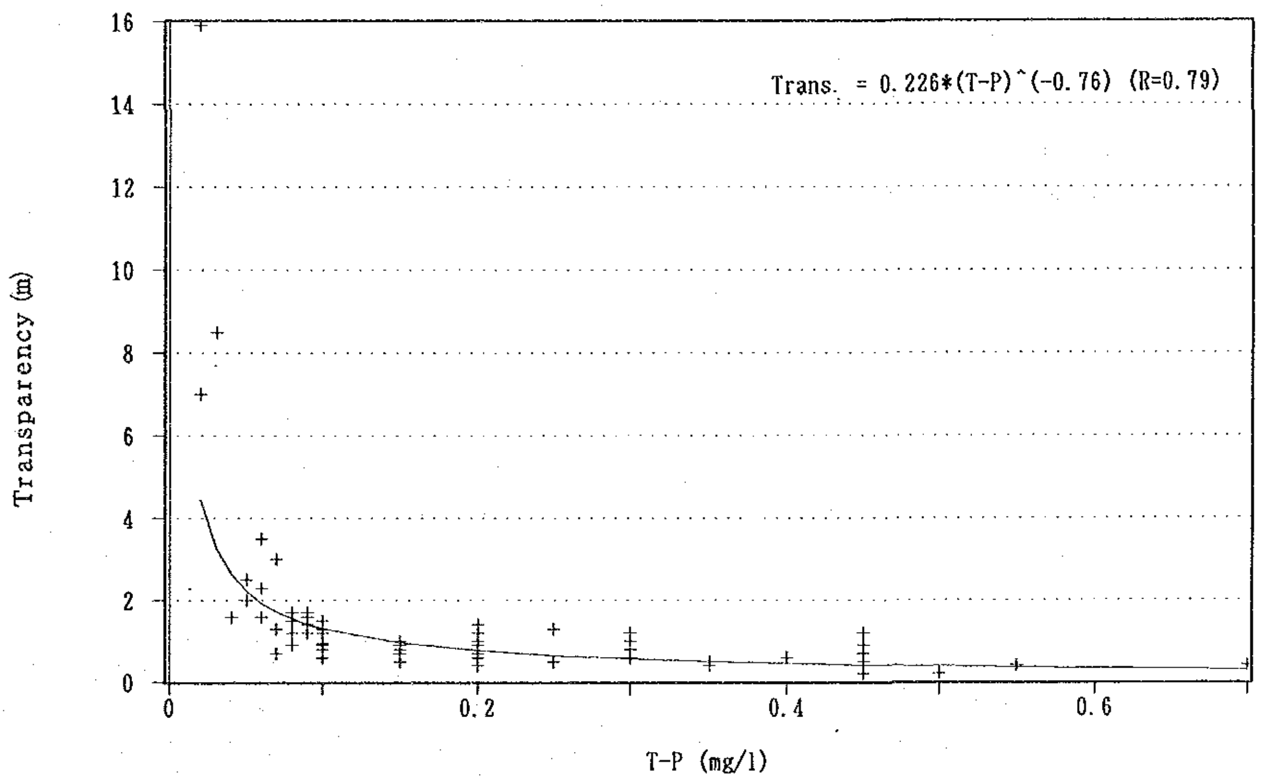

Fig. 2. 3-7 Correlation between T-P and Transparency throuh the Observation

d) Settling Velocity

The settling is considered on O-P and BOD (COD) in the model. Generally, the settling amount is in proportion to the concentration.

We set constant value shown in Table 2.3-4 as settling velocity in the model through calibration tests, referring to the result of the experiment.

e) Release Rate

The release rate from sediments is determined as a function of water temperature, DO concentration and sediment's characteristics itself.
We set the value based on the results of the experiment as shown in Fig.2.3-8. In the outside of the bay, we assumed the release rate zero.

f) Conversion Factor

The ratio of BOD to O-P(BOD/O-P) were determined by the correlation between BOD and O-P concentration in the seasurface through the observation as shown in Fig.2.3-9.
The ratio of COD to O-P(COD/O-P) were determined by Fig.2.3-10 (same as BOD/O-P).
We set 25.6 as the ratio of BOD to O-P and 16.4 as the ratio of COD to O-P.
The ratio of DO to O-P (DO/O-P) can be obtained by the following chemical equation which is well known as chemical reactions by photosynthesis;

$$106CO_2+16HNO_3+H_3PO_4+122H_2O=(CH_2O)_{106}(NH_3)_{16}H_3PO_4+138O_2$$

$$DO/O\text{-}P=138 \times O/P=138 \times 16 \times 2 \div 31 \fallingdotseq 143$$

g) Parameters concerned with DO

(1) Uptake Rate by Decomposition

Uptake rate by Decomposition is given as the rate against the amount of BOD decomposition.
This value was estimated at 0.1 to 10 by the ratio of thinning in the analyzing BOD concentration and we finally set 0.6 through calibration tests.

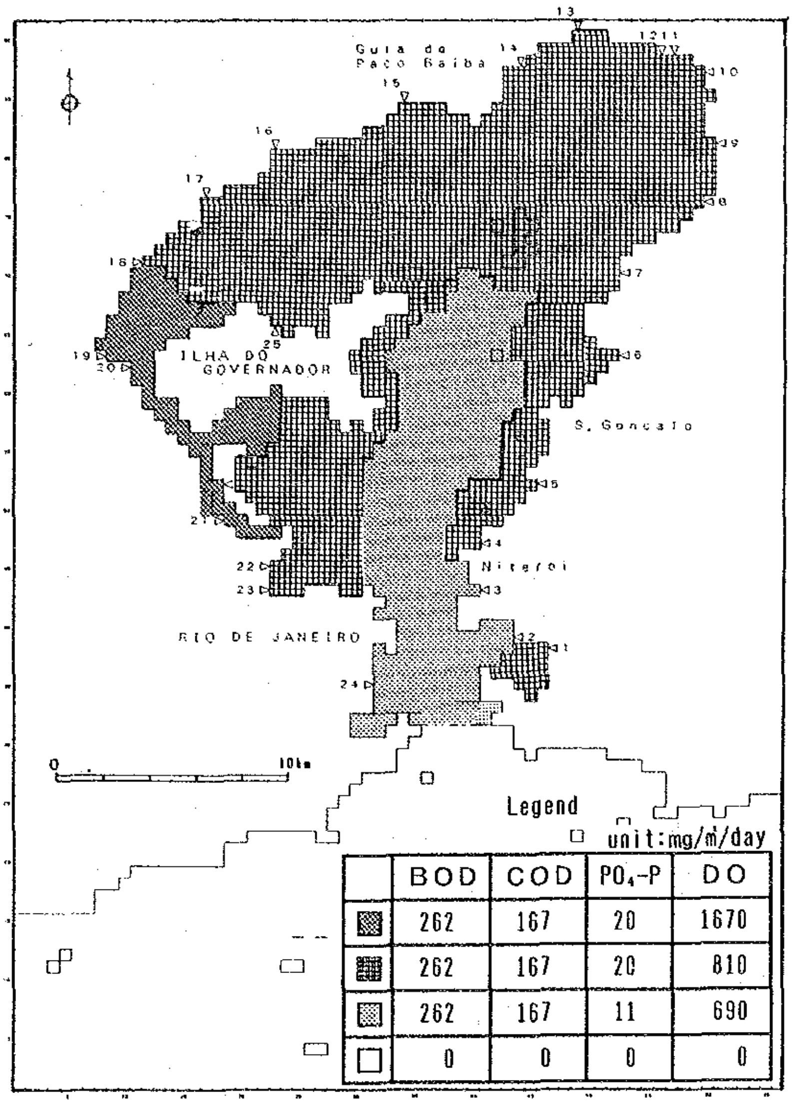

	BOD	COD	PO_4-P	DO
(dense hatch)	262	167	20	1670
(grid hatch)	262	167	20	810
(light dots)	262	167	11	690
(blank)	0	0	0	0

Fig. 2. 3-8 Release Rate and DO Consumption Rate by sediment used for Simulation

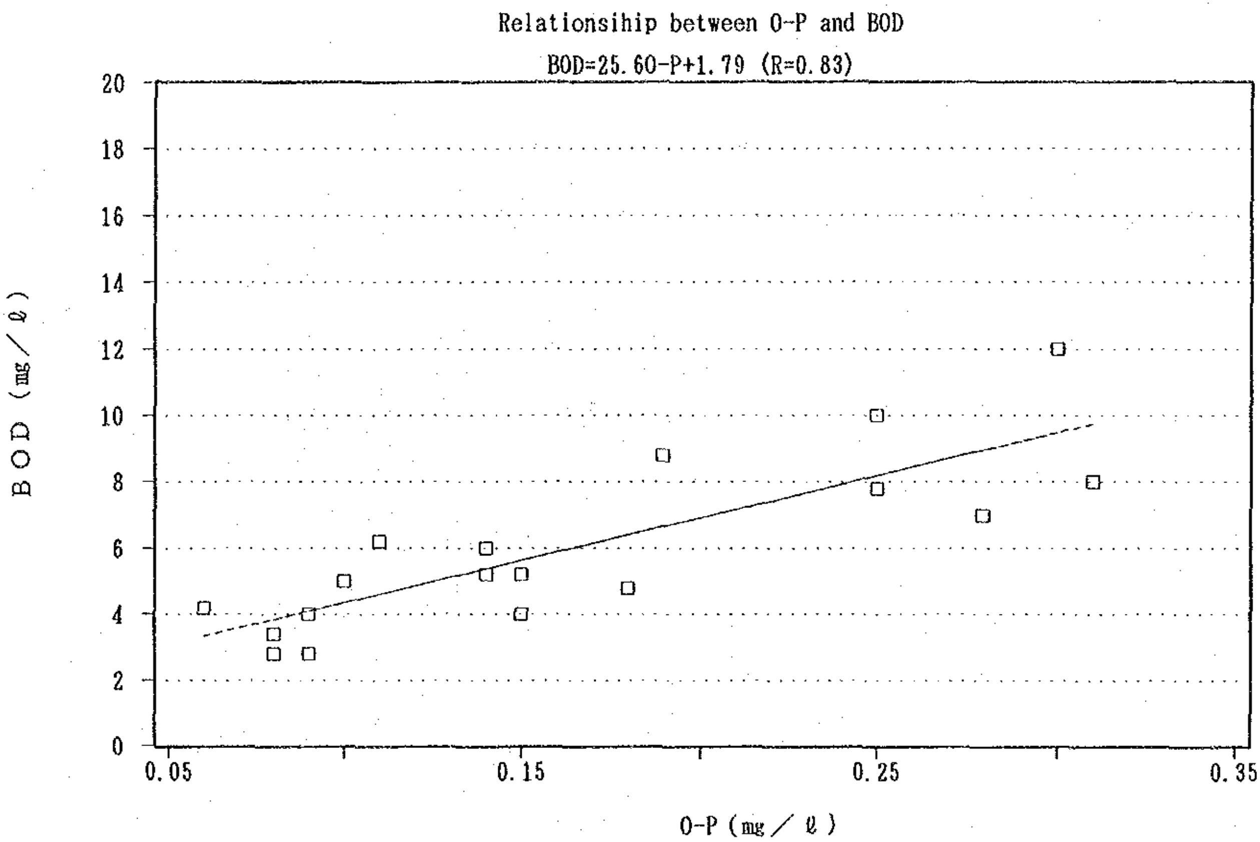

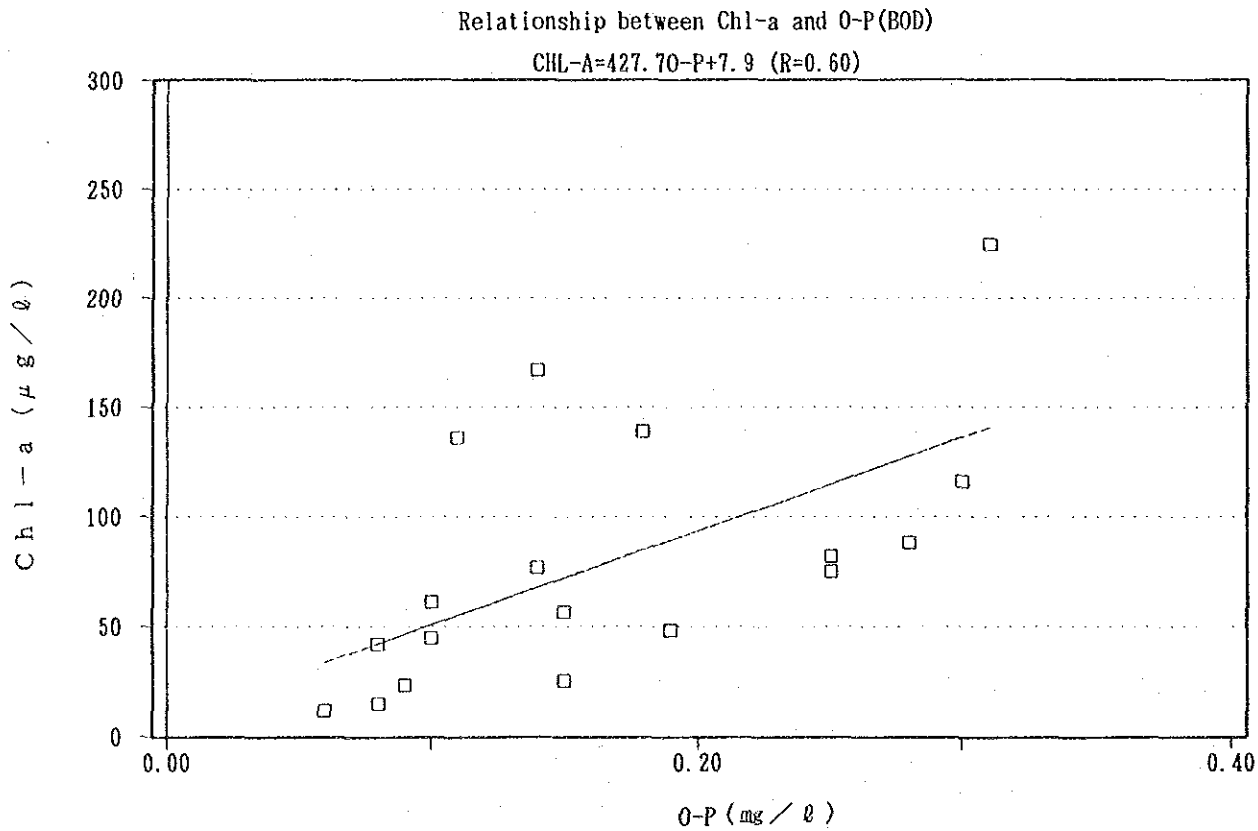

Fig. 2.3-9 Correlation between BOD, O-P and Chl-a in Upper Layer through the Observation

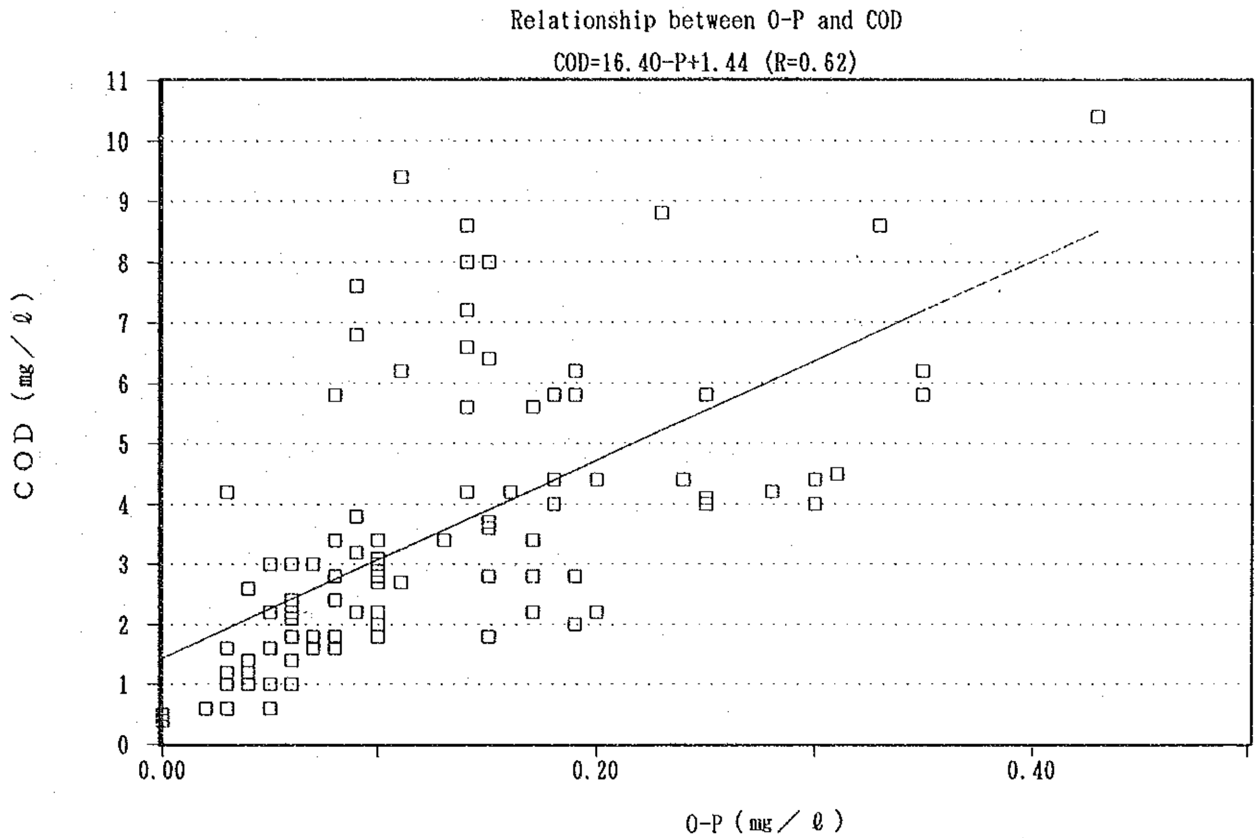

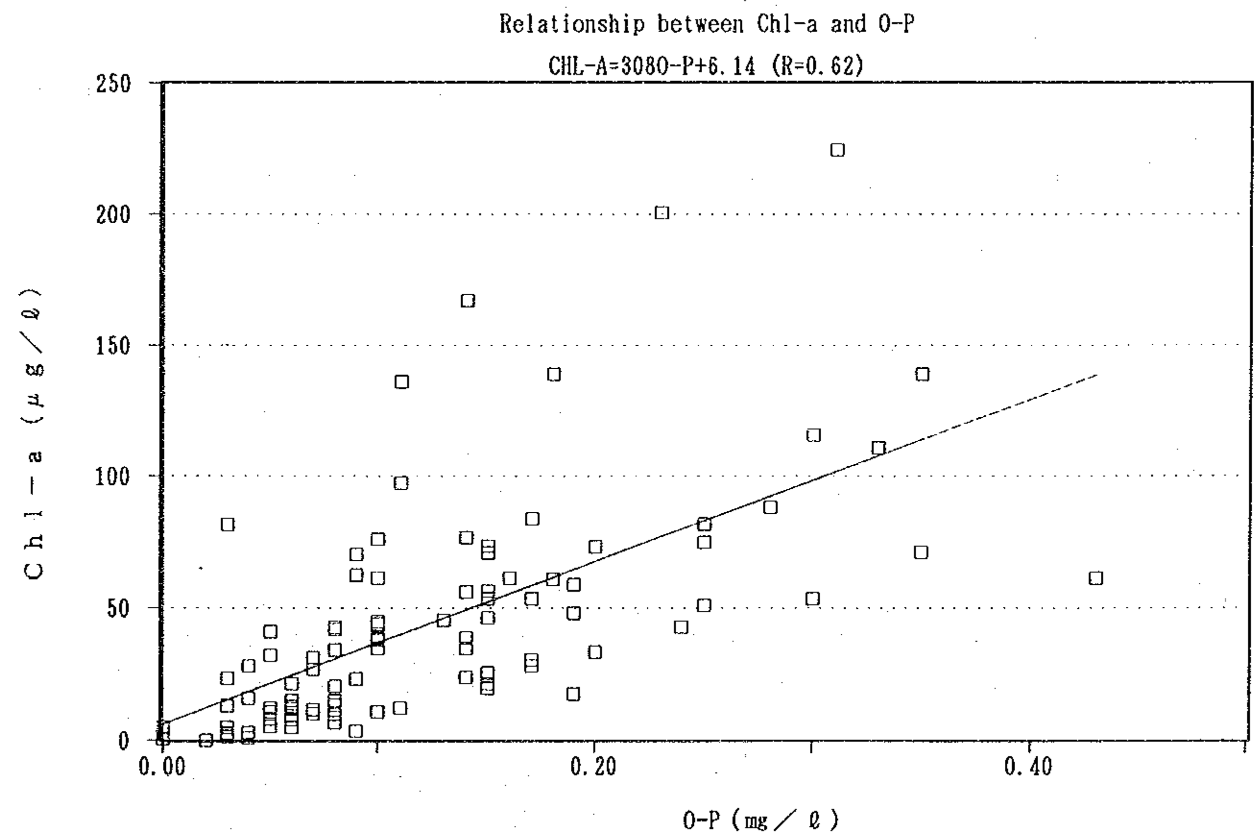

Fig. 2.3-10 Correlation between COD, O-P and Chl-a in Upper Layer through the Observation

(2) Uptake Rate by Sediment

We set 690~810 mg/m^2/day except the western area as the uptake rate by sediment, which was obtained by the experiment as shown in Fig.2.3-8.

In the western area, we set a value two times of the above (1670), considering low DO concentration observed in the area and the fact that uptake rate by sediment is approximately ten times of COD release rate, generally.

(3) Reaeration Constant

Generally, a reaeration constant is between 0.1 and 0.9 1/day. We finally set 0.8 1/day through calibration tests.

(4) Saturated DO Concentration

We set 6.8 mg/l according to the observation data.

h) Dispersion Coefficient

Dispersion Coefficient is shown in Fig.2.3-5 before.

i) External Load

The present external loads through rivers and direct loads into the bay used for the model are shown in Table 2.3-5.

Regarding the direct loads, we treated only BOD loads in the model.

For the estimation of PO_4-P and O-P loads, we assumed the relation of PO_4-P/T-P=0.4 based on the result of the river survey shown in Fig.2.3-11, because we only calculated T-P loads for each river basically. O-P we calculated as the difference of T-P and PO_4-P.

j) Initial Value

The initial values for the distribution of concentration in each index were given with the concentrations observed.

Moreover, we practiced a pre-calculation using the above concentration for the period of 120 tidals and the result of the pre-calculation was used as an initial value for the final calculation.

Table 2.3-5(1) External Load used for Simulation in Dry Season in Present

RIVER INFLOW　　　　　　　　Dry Season in 1991

NO	NAME	I	J	Discharge (m3/s)	BOD (t/day)	COD (t/day)	PO4-P (t/day)	O-P (t/day)
River load								
1	B.-CHARITAS	46	38	0.93	1.96	1.61	0.072	0.108
2	CANAL CANTO DO RIO	43	39	0.73	1.54	1.27	0.056	0.084
3	B.-CATEDRAR	40	43	0.68	1.38	1.14	0.052	0.078
4	B.-NORTE CENTRO	40	47	0.77	1.61	1.33	0.060	0.090
5	RIO BOMBA	45	52	2.99	6.67	5.40	0.240	0.360
6	RIO IMBOASSU	52	63	2.48	4.99	4.04	0.176	0.264
Eastern Sub Total				8.58	18.15	14.79	0.656	0.984
7	B.-ITAOCA	52	70	0.58	1.18	0.98	0.044	0.066
8	RIO ALCANTARA	59	76	8.94	16.49	13.10	0.560	0.840
9	RIO CACERBU	60	81	20.89	11.70	12.19	0.344	0.516
10	RIO GUAPIMIRIN	59	87	23.79	3.41	8.01	0.084	0.126
11	CANAL DE MAGE	57	88	0.52	0.31	0.32	0.008	0.012
12	RIO RONCADOR	56	88	2.79	1.31	1.49	0.040	0.060
13	RIO IRIRI	49	90	0.75	0.39	0.42	0.012	0.018
14	RIO SURUI	44	87	1.60	0.50	0.69	0.016	0.024
Northeastern Sub Total				59.86	35.29	37.2	1.108	1.662
15	B.-MAUA	34	84	0.74	0.32	0.37	0.008	0.012
16	RIO ESTRELA	23	80	10.79	10.40	9.14	0.328	0.492
171	RIO IGUACU	17	76	20.68	25.86	21.34	0.820	1.230
172	RIO SARAPUI	17	76	16.15	35.84	28.19	1.248	1.872
18	B.-CABO DO BRITO	12	71	2.32	4.77	3.87	0.172	0.258
Northwestern Sub Total				50.68	77.19	62.91	2.576	3.864
19	RIO S.J.DE MERITI	9	63	22.26	53.31	42.02	1.884	2.826
20	RIO IRAJA	11	62	7.41	18.43	15.00	0.684	1.026
21	CANAL DO CUNHA	19	49	11.98	29.75	23.93	1.088	1.632
22	B.-S.CRISTOVAO	23	45	0.97	2.24	1.86	0.084	0.126
23	CANAL DO MANGUE	23	43	7.50	18.33	14.82	0.672	1.008
24	B.-BOTAFOGO	32	35	5.36	13.27	10.85	0.496	0.744
Western Sub Total				55.48	135.33	108.48	4.908	7.362
25	I.DO GAVANADOR	23	66	2.83	5.51	4.45	0.192	0.288
26	I.DO FUNDAO	18	52	0.20	0.19	0.18	0.008	0.012
27	I.DE PAQUETA	43	72	0.09	0.12	0.10	0.004	0.006
28	I.DO ENGENHO	43	56	0.19	0.42	0.36	0.016	0.024
29	I.DE S.CRUZ	41	51	0.10	0.18	0.15	0.008	0.012
Islands Sub Total				3.41	6.42	5.24	0.228	0.342
River load Total				178.01	272.38	228.62	9.476	14.214
Direct Load								
007		43	36	-	2.13	-	-	-
001		46	55	-	6.70	-	-	-
004		46	56	-	2.40	-	-	-
008		44	51	-	2.10	-	-	-
009		40	47	-	1.94	-	-	-
027		45	52	-	0.80	-	-	-
034		46	57	-	0.66	-	-	-
044		46	57	-	0.51	-	-	-
047		46	57	-	0.48	-	-	-
062		48	59	-	0.38	-	-	-
113		51	62	-	0.22	-	-	-
Eastern Sub Total				-	18.32	-	-	-
015		17	76	-	1.32	-	-	-
018		17	76	-	1.20	-	-	-
075		17	76	-	0.33	-	-	-
029		17	76	-	0.79	-	-	-
086		17	76	-	0.31	-	-	-
137		10	68	-	0.16	-	-	-
Northwestern Sub Total				-	4.11	-	-	-
030		11	62	-	0.72	-	-	-
042		11	62	-	0.52	-	-	-
051		32	36	-	0.45	-	-	-
Western Sub Total				-	1.69	-	-	-
Direct Load Sub Total				-	24.11	-	-	-
Total				178.01	296.49	228.62	9.476	14.214

Table 2.3-5(2) External Load used for Simulation in Rainy Season in Present

RIVER INFLOW — Rainy Season in 1991

NO	NAME	I	J	Discharge (m3/s)	BOD (t/day)	COD (t/day)	PO4-P (t/day)	O-P (t/day)
River load								
1	B.-CHARITAS	46	38	1.40	2.74	2.16	0.048	0.072
2	CANAL CANTO DO RIO	43	39	1.10	2.15	1.70	0.040	0.060
3	B.-CATEDRAR	40	43	1.03	1.92	1.53	0.036	0.054
4	B.-NORTE CENTRO	40	47	1.15	2.24	1.77	0.040	0.060
5	RIO BOMBA	45	52	4.52	9.34	7.26	0.168	0.252
6	RIO IMBOASSU	52	63	3.80	7.05	5.58	0.124	0.186
Eastern Sub Total				13.00	25.44	20.00	0.456	0.684
7	B.-ITAOCA	52	70	0.87	1.64	1.31	0.032	0.048
8	RIO ALCANTARA	59	76	14.01	23.66	18.91	0.400	0.600
9	RIO CACEREBU	60	81	34.45	17.91	22.38	0.292	0.438
10	RIO GUAPIMIRIN	59	87	40.93	5.93	17.94	0.124	0.186
11	CANAL DE MAGE	57	88	0.82	0.46	0.55	0.008	0.012
12	RIO RONCADOR	56	88	4.51	2.00	2.74	0.036	0.054
13	RIO IRIRI	49	90	1.18	0.58	0.75	0.012	0.018
14	RIO SURUI	44	87	2.59	0.77	1.36	0.012	0.018
Northeastern Sub Total				99.36	52.95	65.94	0.916	1.374
15	B.-MAUA	34	84	1.18	0.48	0.69	0.008	0.012
16	RIO ESTRELA	23	80	17.40	15.43	15.05	0.252	0.378
171	RIO IGUACU	17	76	33.34	38.08	33.82	0.616	0.924
172	RIO SARAPUI	17	76	25.06	50.96	39.24	0.880	1.320
18	B.-CABO DO BRITO	12	71	3.54	6.73	5.30	0.120	0.180
Northwestern Sub Total				80.52	111.68	94.10	1.876	2.814
19	RIO S.J.DE MERITI	9	63	34.28	75.35	57.33	1.320	1.980
20	RIO IRAJA	11	62	11.09	25.64	19.60	0.472	0.708
21	CANAL DO CUNHA	19	49	18.10	41.58	31.67	0.752	1.128
22	B.-S.CRISTOVAO	23	45	1.44	3.10	2.42	0.060	0.090
23	CANAL DO MANGUE	23	43	11.30	25.59	19.57	0.464	0.696
24	B.-BOTAFOGO	32	35	8.00	18.42	14.12	0.340	0.510
Western Sub Total				84.21	189.68	144.71	3.408	5.112
25	I.DO GAVANADOR	23	66	4.35	7.81	6.21	0.136	0.204
26	I.DO FUNDAO	18	52	0.30	0.28	0.27	0.004	0.006
27	I.DE PAQUETA	43	72	0.13	0.17	0.15	0.004	0.006
28	I.DO ENGENHO	43	56	0.27	0.58	0.46	0.012	0.018
29	I.DE S.CRUZ	41	51	0.15	0.25	0.21	0.004	0.006
Islands Sub Total				5.20	9.09	7.30	0.160	0.240
River load Total				282.29	388.84	332.05	6.816	10.224
Direct Load								
007		43	36	-	2.13	-	-	-
001		46	55	-	6.70	-	-	-
004		46	56	-	2.40	-	-	-
008		44	51	-	2.10	-	-	-
009		40	47	-	1.94	-	-	-
027		45	52	-	0.80	-	-	-
034		46	57	-	0.66	-	-	-
044		46	57	-	0.51	-	-	-
047		46	57	-	0.48	-	-	-
062		48	59	-	0.38	-	-	-
113		51	62	-	0.22	-	-	-
Eastern Sub Total				-	18.32	-	-	-
015		17	76	-	1.32	-	-	-
018		17	76	-	1.20	-	-	-
075		17	76	-	0.33	-	-	-
029		17	76	-	0.79	-	-	-
086		17	76	-	0.31	-	-	-
137		10	68	-	0.16	-	-	-
Northwestern Sub Total				-	4.11	-	-	-
030		11	62	-	0.72	-	-	-
042		11	62	-	0.52	-	-	-
051		32	36	-	0.45	-	-	-
Western Sub Total				-	1.69	-	-	-
Direct Load Sub Total				-	24.11	-	-	-
Total				282.29	412.95	332.05	6.816	10.224

Table 2.3-5(3) External Load used for Simulation in Present Annual Mean

RIVER INFLOW — Annual Mean value in 1991

NO	NAME	I	J	Discharge (m3/s)	BOD (t/day)	COD (t/day)	PO4-P (t/day)	O-P (t/day)
River load								
1	B.-CHARITAS	46	38	1.17	2.35	1.89	0.060	0.090
2	CANAL CANTO DO RIO	43	39	0.92	1.84	1.49	0.048	0.072
3	B.-CATEDRAR	40	43	0.86	1.65	1.33	0.044	0.066
4	B.-NORTE CENTRO	40	47	0.96	1.92	1.55	0.048	0.072
5	RIO BOMBA	45	52	3.75	8.00	6.33	0.204	0.306
6	RIO IMBOASSU	52	63	3.14	6.02	4.81	0.152	0.228
Eastern Sub Total				10.80	21.78	17.40	0.556	0.834
7	B.-ITAOCA	52	70	0.73	1.41	1.14	0.036	0.054
8	RIO ALCANTARA	59	76	11.48	20.07	16.01	0.480	0.720
9	RIO CACEREBU	60	81	27.67	14.80	17.28	0.320	0.480
10	RIO GUAPIMIRIN	59	87	32.36	4.67	12.97	0.104	0.156
11	CANAL DE MAGE	57	88	0.67	0.38	0.44	0.008	0.012
12	RIO RONCADOR	56	88	3.65	1.66	2.11	0.036	0.054
13	RIO IRIRI	49	90	0.97	0.49	0.59	0.012	0.018
14	RIO SURUI	44	87	2.09	0.63	1.02	0.016	0.024
Northeastern Sub Total				79.62	44.11	51.56	1.012	1.518
15	B.-MAUA	34	84	0.96	0.40	0.53	0.008	0.012
16	RIO ESTRELA	23	80	14.10	12.92	12.09	0.288	0.432
171	RIO IGUACU	17	76	27.01	31.97	27.58	0.720	1.080
172	RIO SARAPUI	17	76	20.61	43.40	33.72	1.064	1.596
18	B.-CABO DO BRITO	12	71	2.93	5.75	4.58	0.144	0.216
Northwestern Sub Total				65.61	94.44	78.50	2.224	3.336
19	RIO S.J.DE MERITI	9	63	28.27	64.33	49.68	1.604	2.406
20	RIO IRAJA	11	62	9.25	22.04	17.30	0.576	0.864
21	CANAL DO CUNHA	19	49	15.04	35.66	27.80	0.920	1.380
22	B.-S.CRISTOVAO	23	45	1.21	2.67	2.14	0.072	0.108
23	CANAL DO MANGUE	23	43	9.40	21.96	17.20	0.568	0.852
24	B.-BOTAFOGO	32	35	6.68	15.84	12.48	0.416	0.624
Western Sub Total				69.85	162.50	126.60	4.156	6.234
25	I.DO GAVANADOR	23	66	3.59	6.66	5.33	0.164	0.246
26	I.DO FUNDAO	18	52	0.25	0.23	0.22	0.004	0.006
27	I.DE PAQUETA	43	72	0.11	0.14	0.13	0.004	0.006
28	I.DO ENGENHO	43	56	0.23	0.50	0.41	0.012	0.018
29	I.DE S.CRUZ	41	51	0.13	0.22	0.18	0.004	0.006
Islands Sub Total				4.31	7.75	6.27	0.188	0.282
River load Total				230.19	330.58	280.33	8.136	12.204
Direct Load								
007		43	36	-	2.13	-	-	-
001		46	55	-	6.70	-	-	-
004		46	56	-	2.40	-	-	-
008		44	51	-	2.10	-	-	-
009		40	47	-	1.94	-	-	-
027		45	52	-	0.80	-	-	-
034		46	57	-	0.66	-	-	-
044		46	57	-	0.51	-	-	-
047		46	57	-	0.48	-	-	-
062		48	59	-	0.38	-	-	-
113		51	62	-	0.22	-	-	-
Eastern Sub Total				-	18.32	-	-	-
015		17	76	-	1.32	-	-	-
018		17	76	-	1.20	-	-	-
075		17	76	-	0.33	-	-	-
029		17	76	-	0.79	-	-	-
086		17	76	-	0.31	-	-	-
137		10	68	-	0.16	-	-	-
Northwestern Sub Total				-	4.11	-	-	-
030		11	62	-	0.72	-	-	-
042		11	62	-	0.52	-	-	-
051		32	36	-	0.45	-	-	-
Western Sub Total				-	1.69	-	-	-
Direct Load Sub Total				-	24.11	-	-	-
Total				230.19	354.69	280.33	8.136	12.204

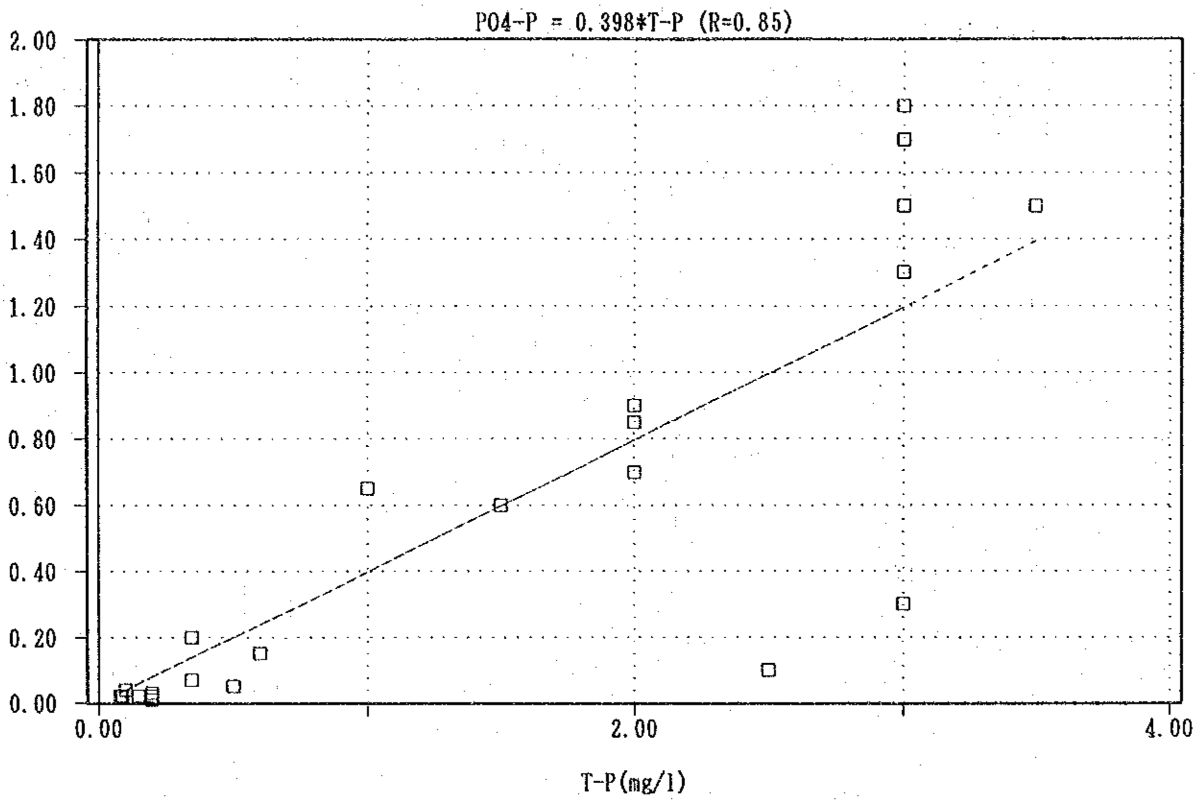

Fig. 2.3-11 Correlation between T-P and PO_4-P in River

k) Open Boundary Concentration

The concentration of each index at the open boundaries was given with the concentrations observed at the outside of the bay (St.1).

2.4 Verification Test of the Hydrodynamic Model

2.4.1 Results of Calculation

The tidal current simulation in the Guanabara Bay was carried out using a two-level model mentioned in the previous chapter. As representative distributions of the currents in the bay, current. As representative distributions of the currents in the bay, current maps for the flood and ebb of upper layer and lower layer in dry season, rainy season and annual mean value are shown in Fig.2.4-1. Residual current map are also shown in Fig.2.4-2. On these maps, the thickness of the upper layer is three (3) meters as mentioned before.

The distribution map of vertical velocity averaged for a tidal is shown in Fig.2.4-3.

According to the current map, the flow toward north and south is obvious in tidal current in the bay.

The maximum velocity is about 80cm/s at the baymouth and about 40cm/s at the center part of the bay and channel in the western area and 10~20cm/s at the inner part of the bay in flood stream and ebb stream.

According to the residual current map, there are several horizontal circulation especially near the baymouth and between island and island.

According to the vertical velocity map, the maximum vertical velocity is about 0.4mm/s and the area is near the baymouth and island.

The order of vertical velocity is much smaller than horizontal velocity.

Though we tried the calculation for three cases of dry season, rainy season and annual mean, the large difference of current pattern could not be found.

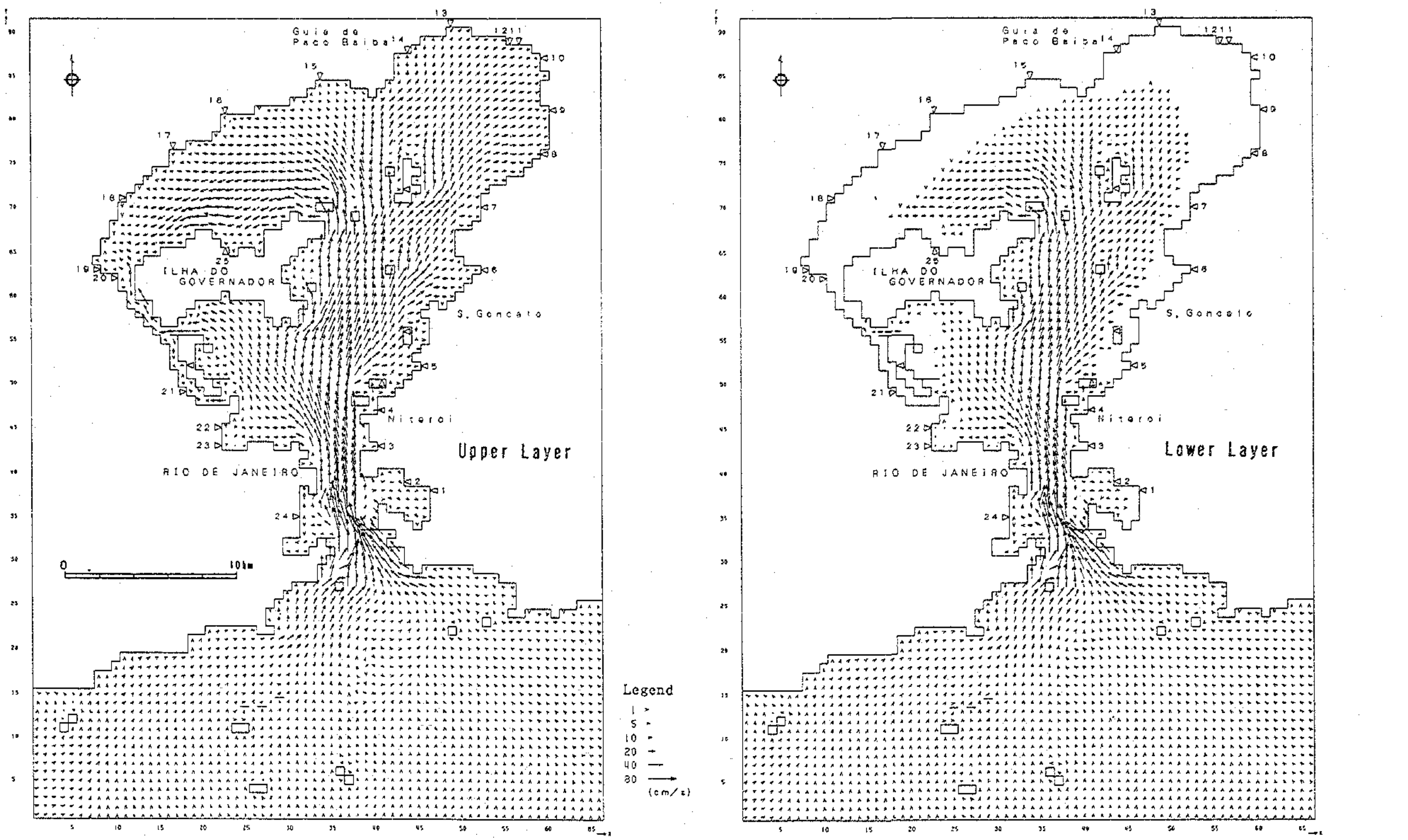

Fig. 2. 4-1(1) Calculated Tidal Current (Dry Season: Flood Stream)

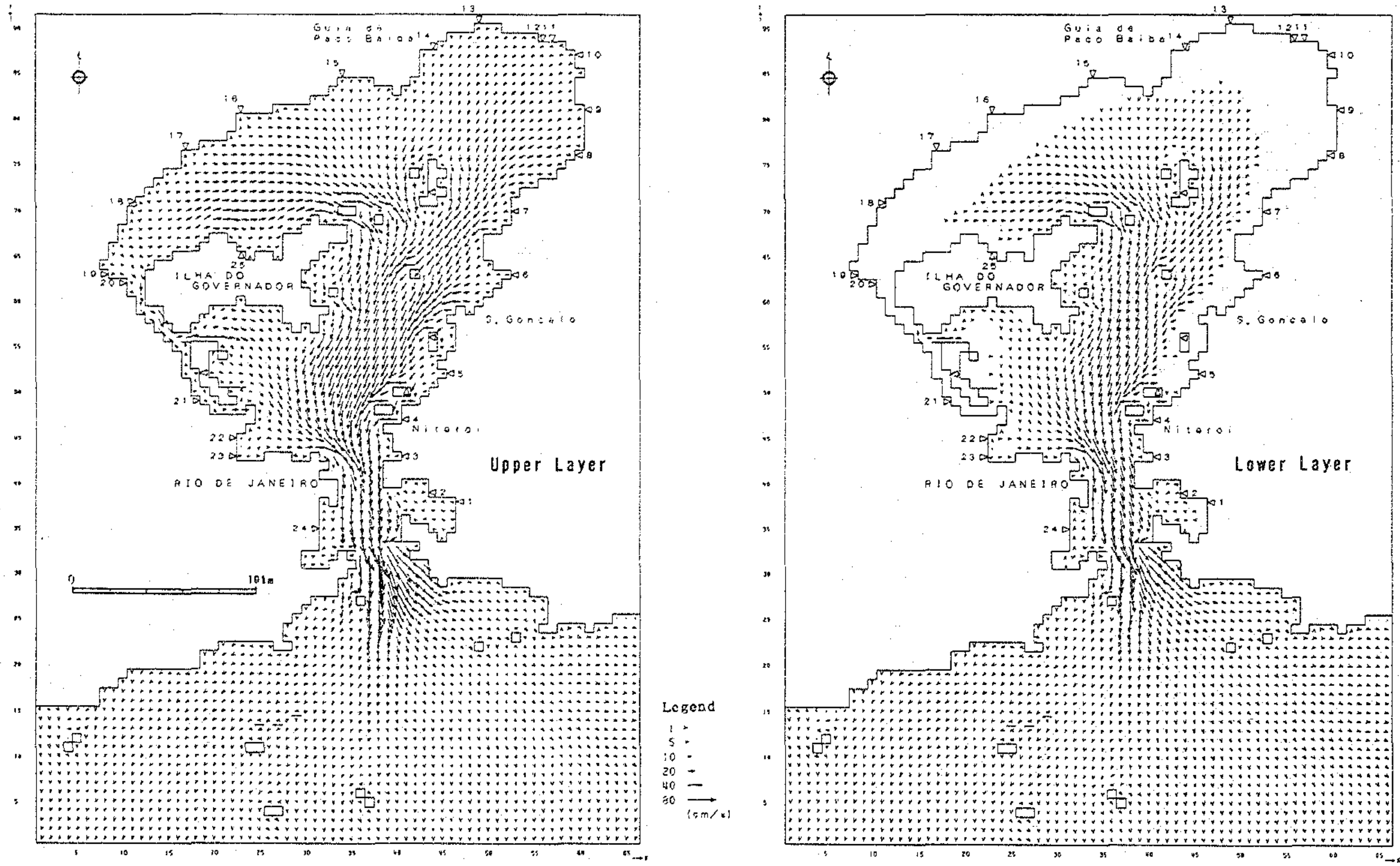

Fig. 2.4-1(2) Calculated Tidal Current (Dry Season: Ebb Stream)

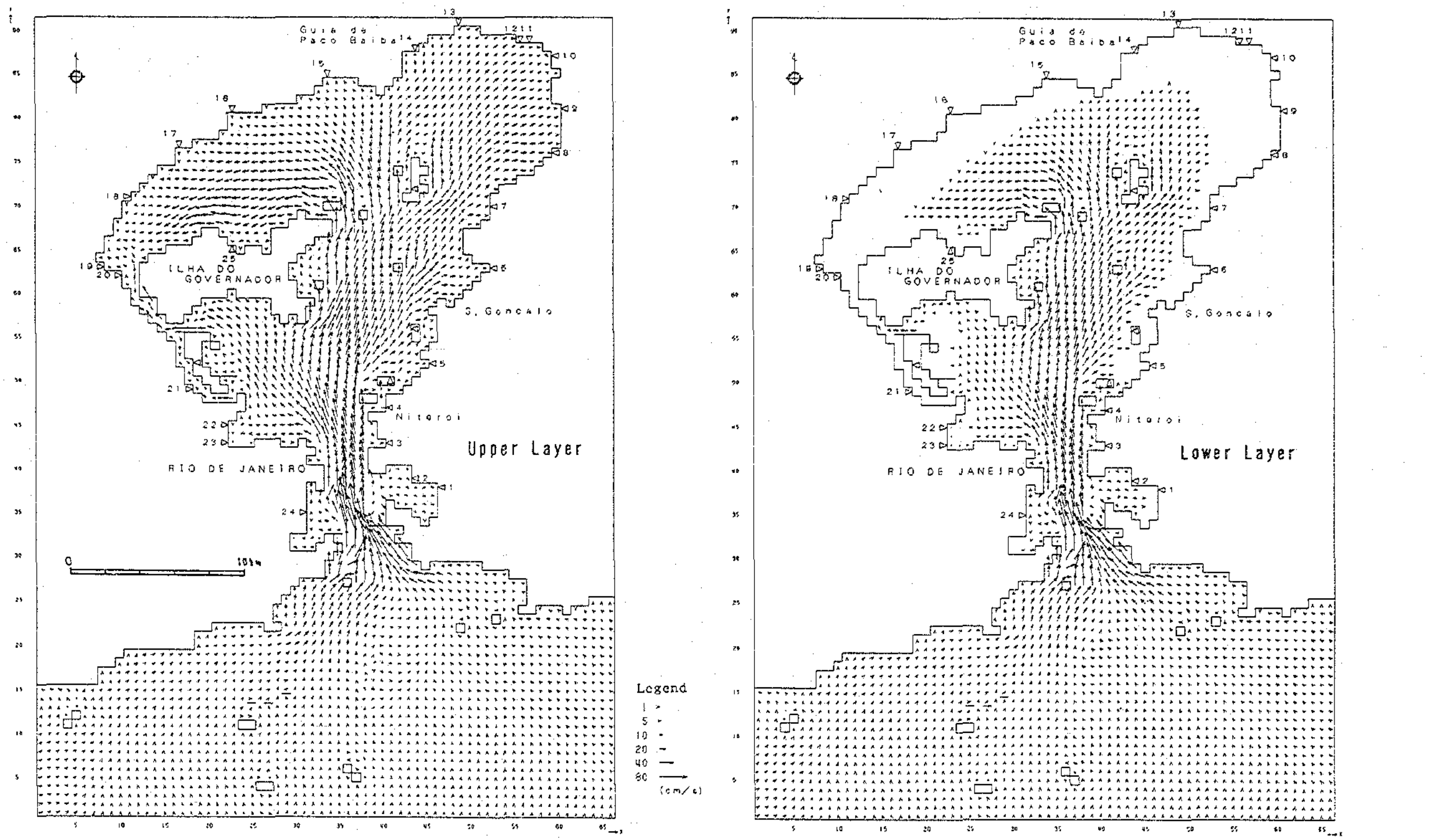

Fig. 2. 4-1(3) Calculated Tidal Current (Rainy Season:Flood Stream)

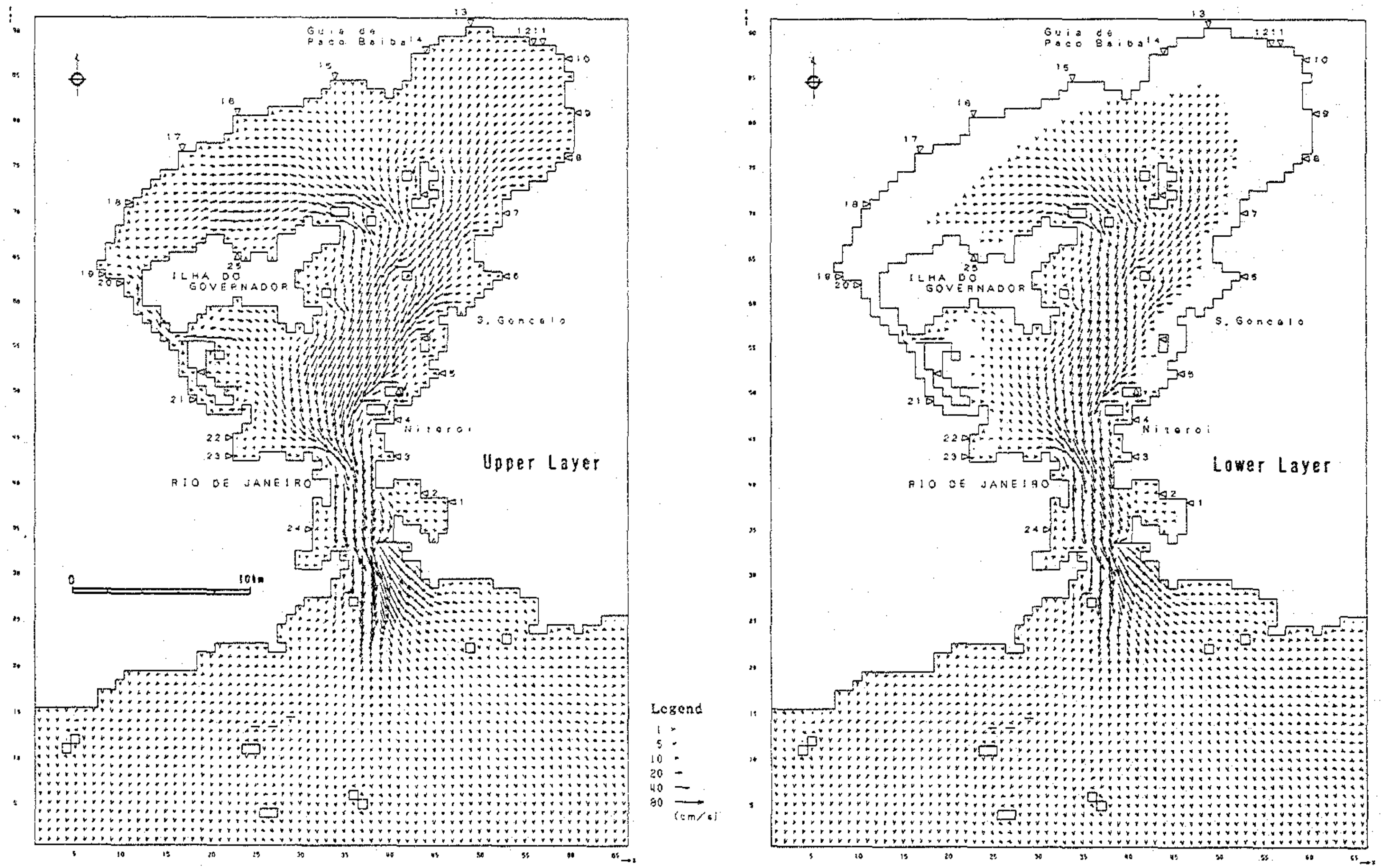

Fig. 2. 4-1 (4)   Calculated Tidal Current (Rainy Season:Ebb Stream)

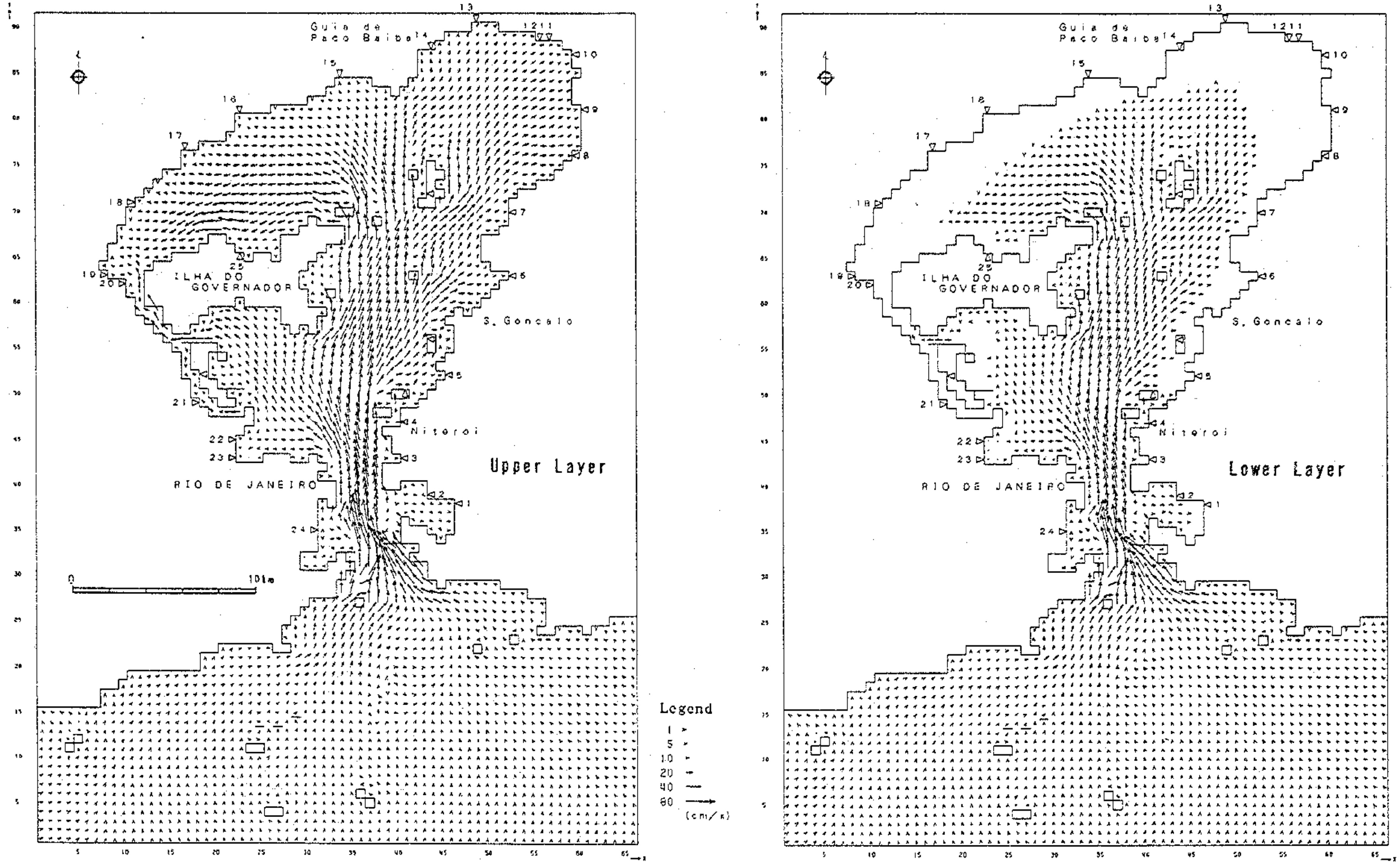

Fig. 2. 4-1 (5)　　Calculated Tidal Current (Annual Mean: Flood Stream)

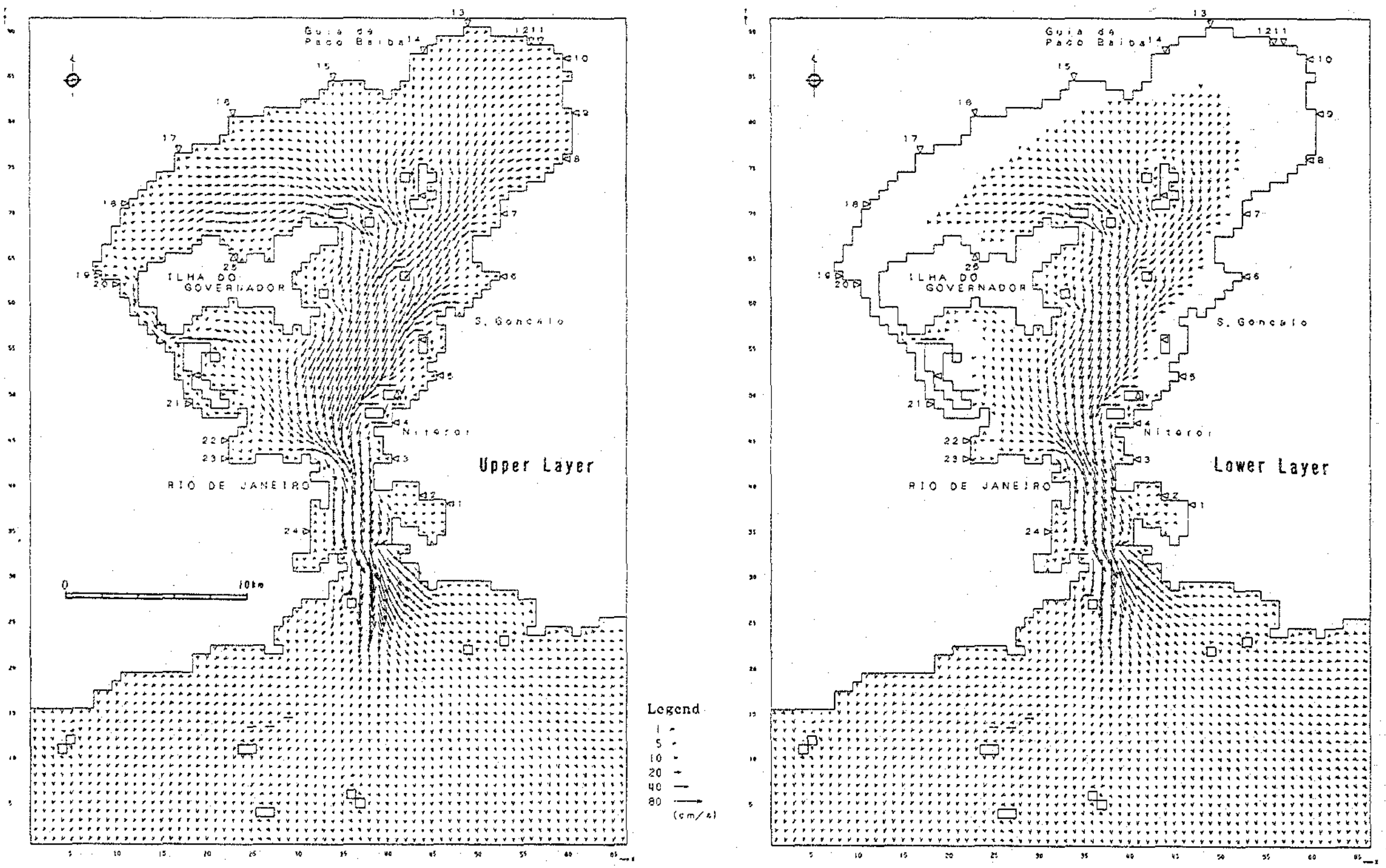

Fig. 2.4-1(6) Calculated Tidal Current (Annual Mean:Ebb Stream)

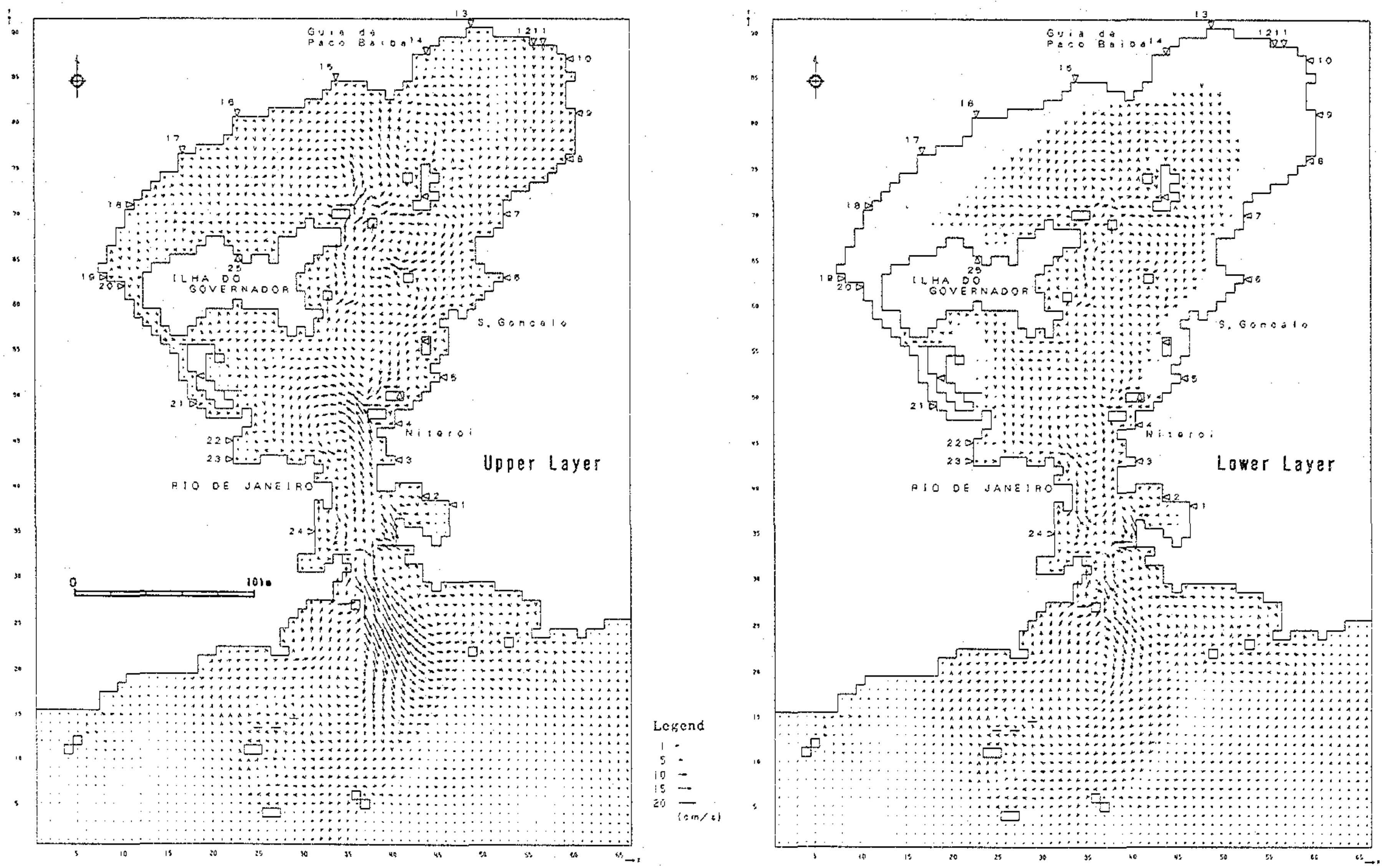

Fig. 2.4-2(1) Calculated Residual Current (Dry Season)

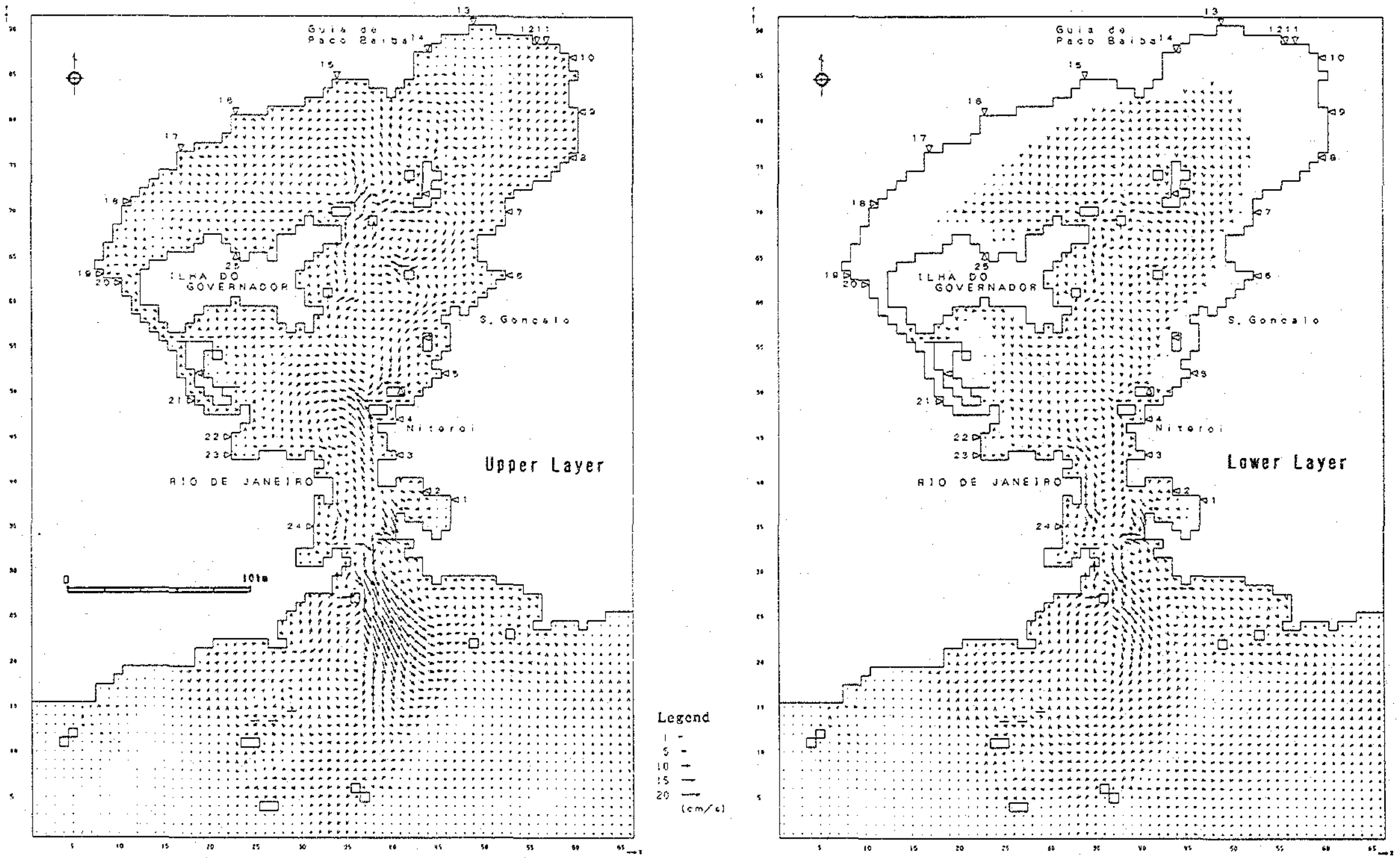

Fig. 2.4-2(2)　Calculated Residual Current (Rainy Season)

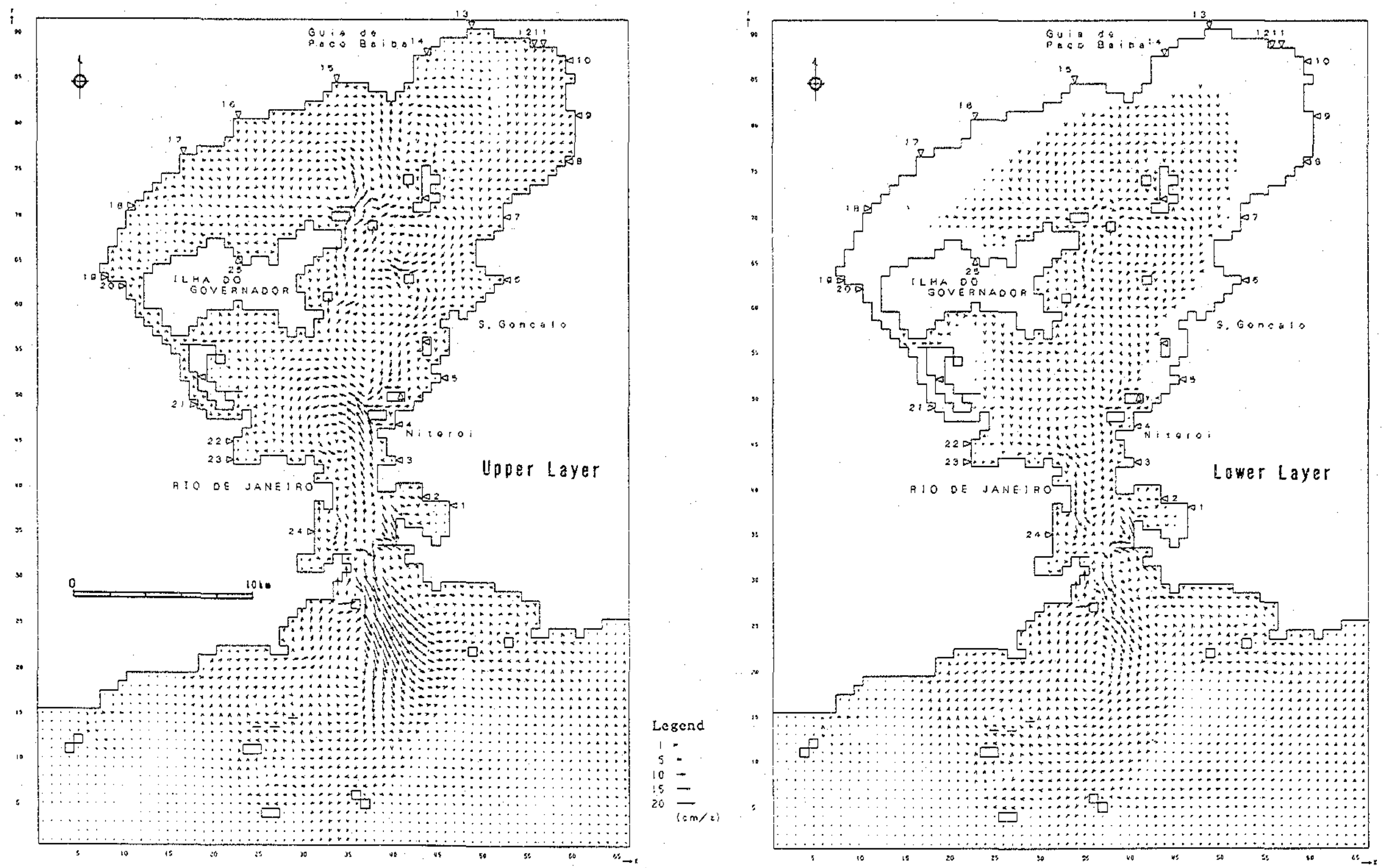

Fig. 2.4-2(3) Calculated Residual Current (Annual Mean)

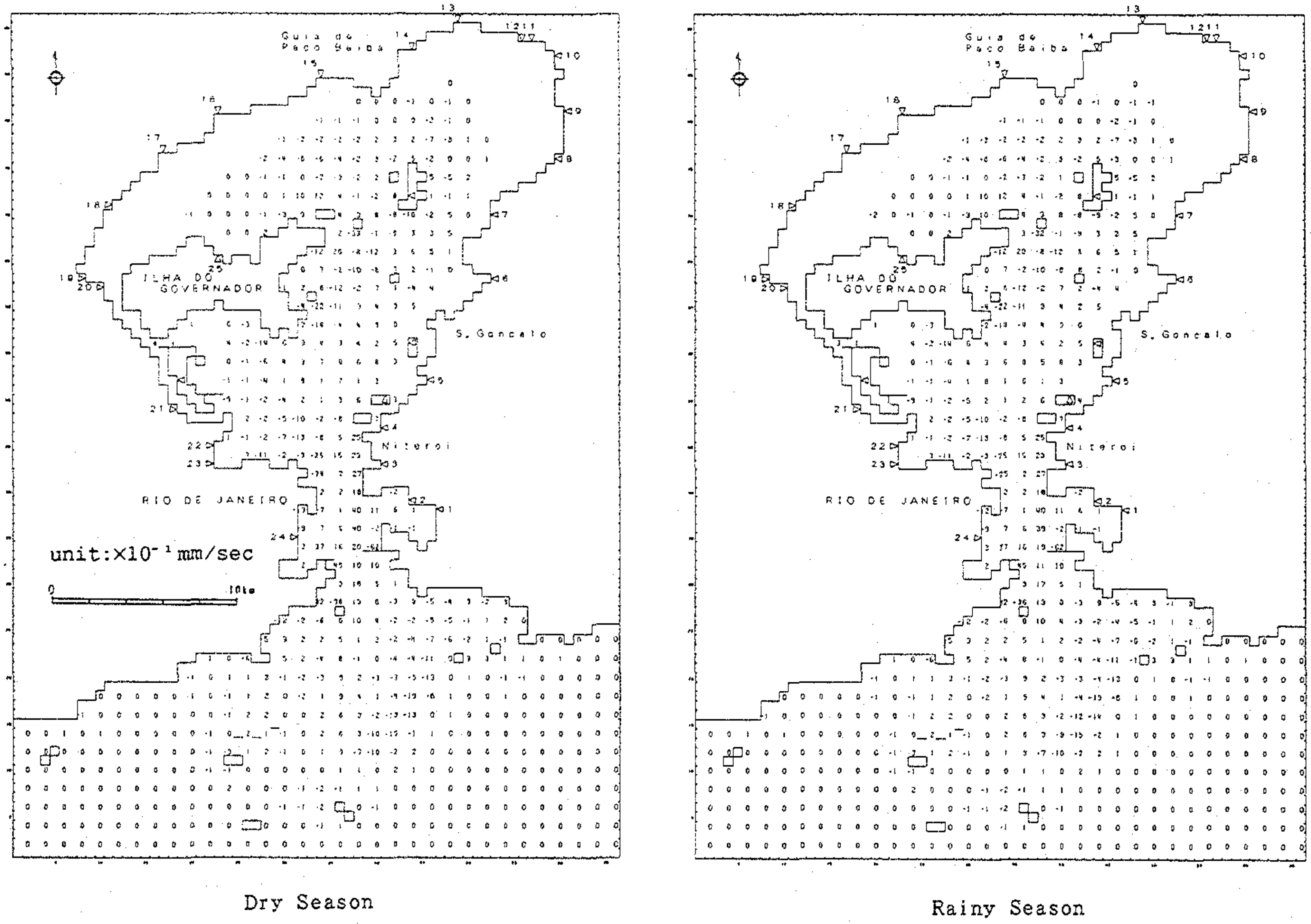

Fig. 2.4-3(1) Calculated Vertical Velocity Averaged for a Tidal

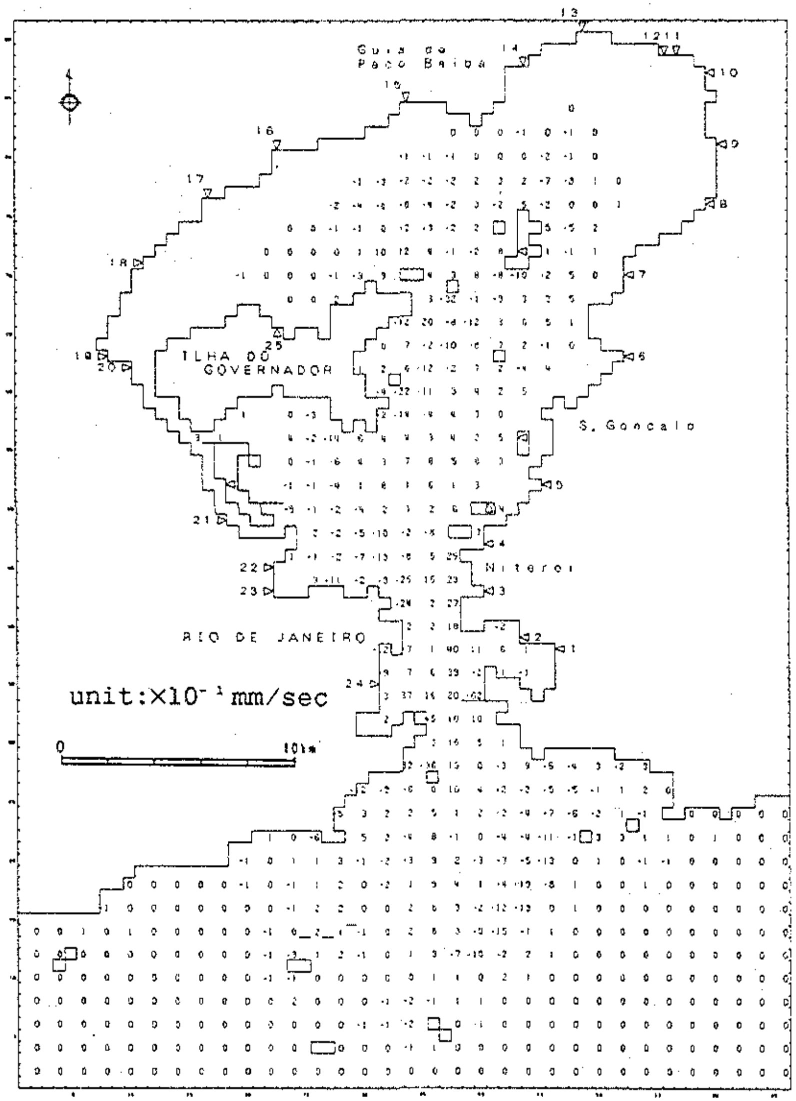

Fig. 2.4-3(2) Annual Mean

Calculated Vertical Velocity Averaged for a Tidal

2.4.2 Verification of the Hydrodynamic Model

In order to evaluate the verification of the hydrodynamic model, we showed two figures.
The first shows the comparison of the observed velocity and the calculated velocity at each point in the case of annual mean with tidal current ellipses in Fig.2.4-5.
The second is the comparison of the observed and calculated tidal curves at Ponta da Armacao and Ilha de Paqueta.

It will be said that calculated velocity and calculated tidal height totally agree with the observed one, though there are some differences between them, particularly in the upper layer of St.B and St.H about velocity.

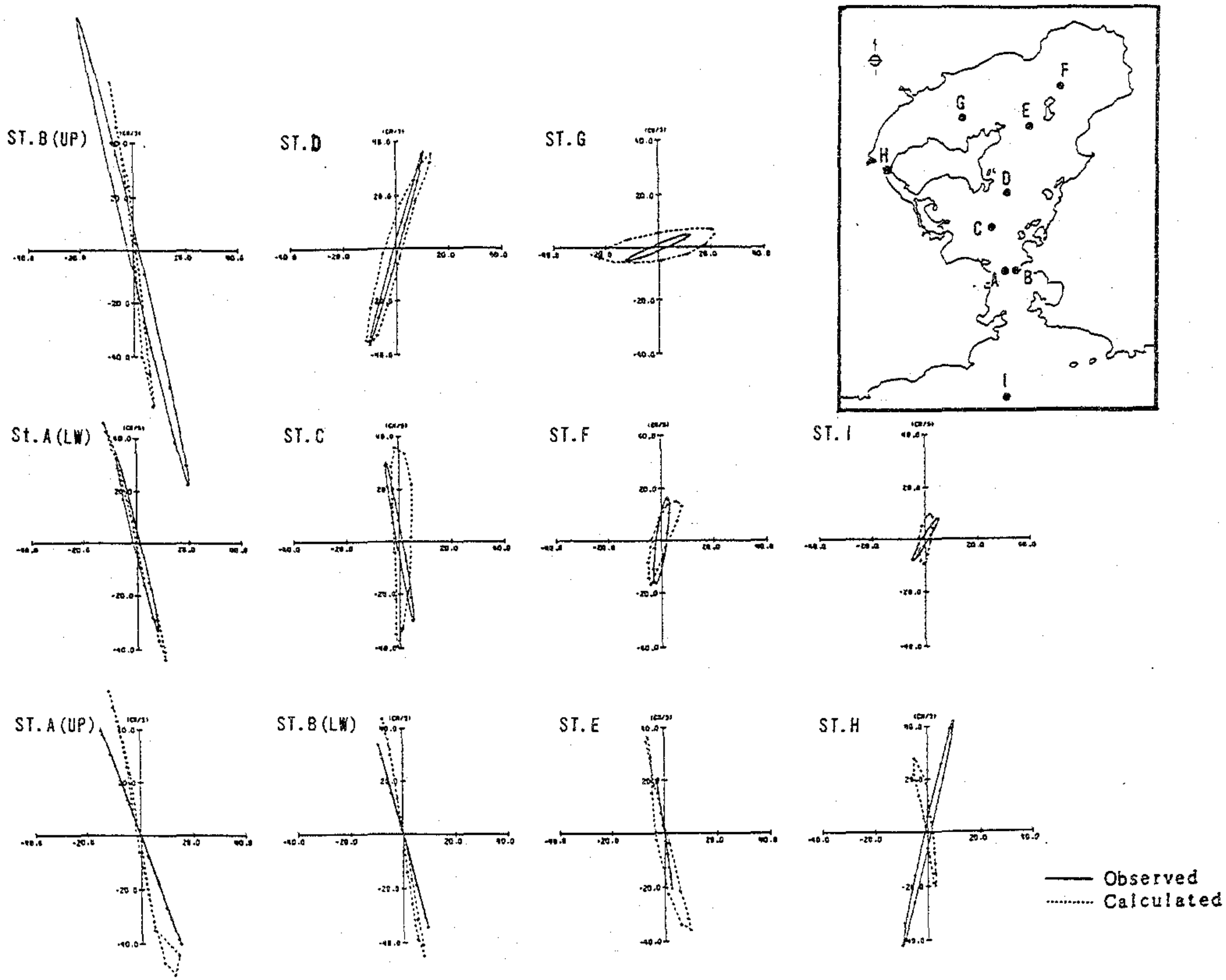

Fig. 2. 4-5 Comparison of Observed and Calculated Velocity by Tidal Current Ellipses (M_2+S_2)

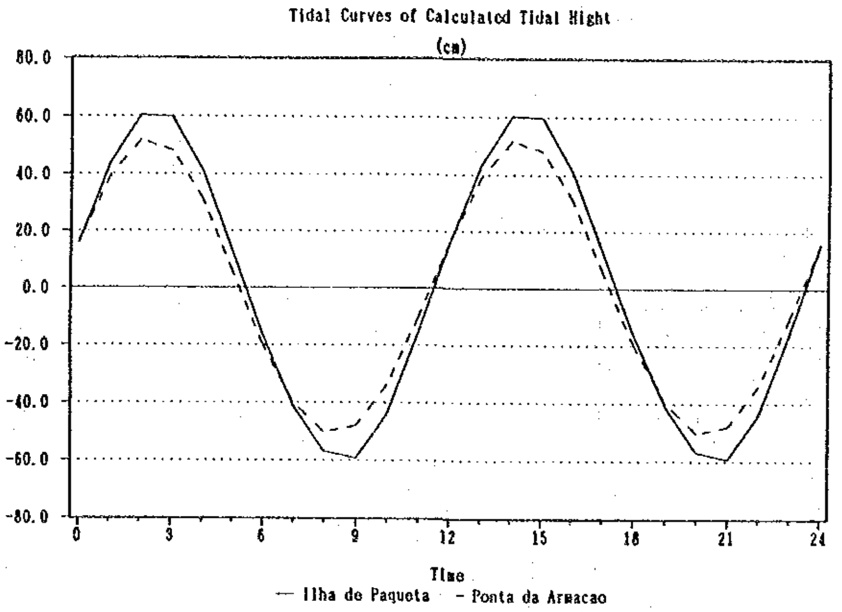

Calculated

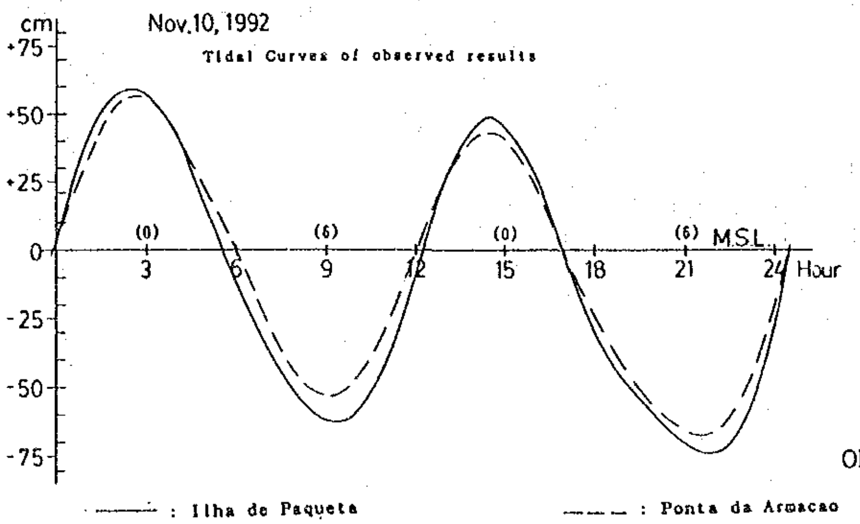

Observed

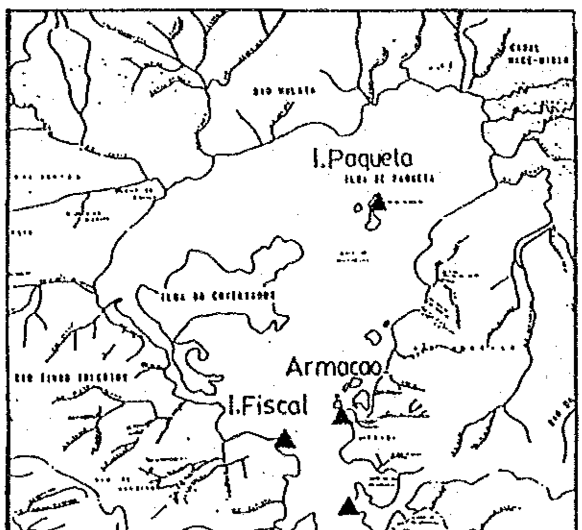

Fig. 2.4-6 **Comparison of Tidal Curves**

2.5 Verification Test of the Diffusion Model

2.5.1 Results of Calculation

The simulation for the distribution of salinity in the Guanabara Bay was carried out using a diffusion model mentioned in the previous chapter. Main purpose by this model was to determine the dispersion coefficient in the area concerned.

We tried some cases on an assumption of various dispersion coefficients and finally set the coefficient as shown in Fig.2.3-5.

Fig.2.5-1 shows the calculated distribution of salinity using the coefficient shown Fig.2.3-5 in both seasons.

Calculated salinity concentration is 17~20 in the inner part of western and eastern area and it is 24~30 in the area from inner part of center to baymouth in dry season.
On the other hand, it is 11~14 in the inner part of western and eastern area and in the area from control part to baymouth is 20~30 in rainy season.

2.5.2 Verification of Diffusion Model

Fig.2.5-2 shows the comparison of calculated and observed salinity. The calculated concentration is lower than the observed one in the inner part of the bay in dry season, particularly.
There was, however, large difference in the salinity value by the weather condition. Therefore, it is said that the distribution pattern is rather important in salinity.

On this aspect, it will be said that the distribution pattern of calculated value totally agrees with that of observed one, particularly in the rainy season.

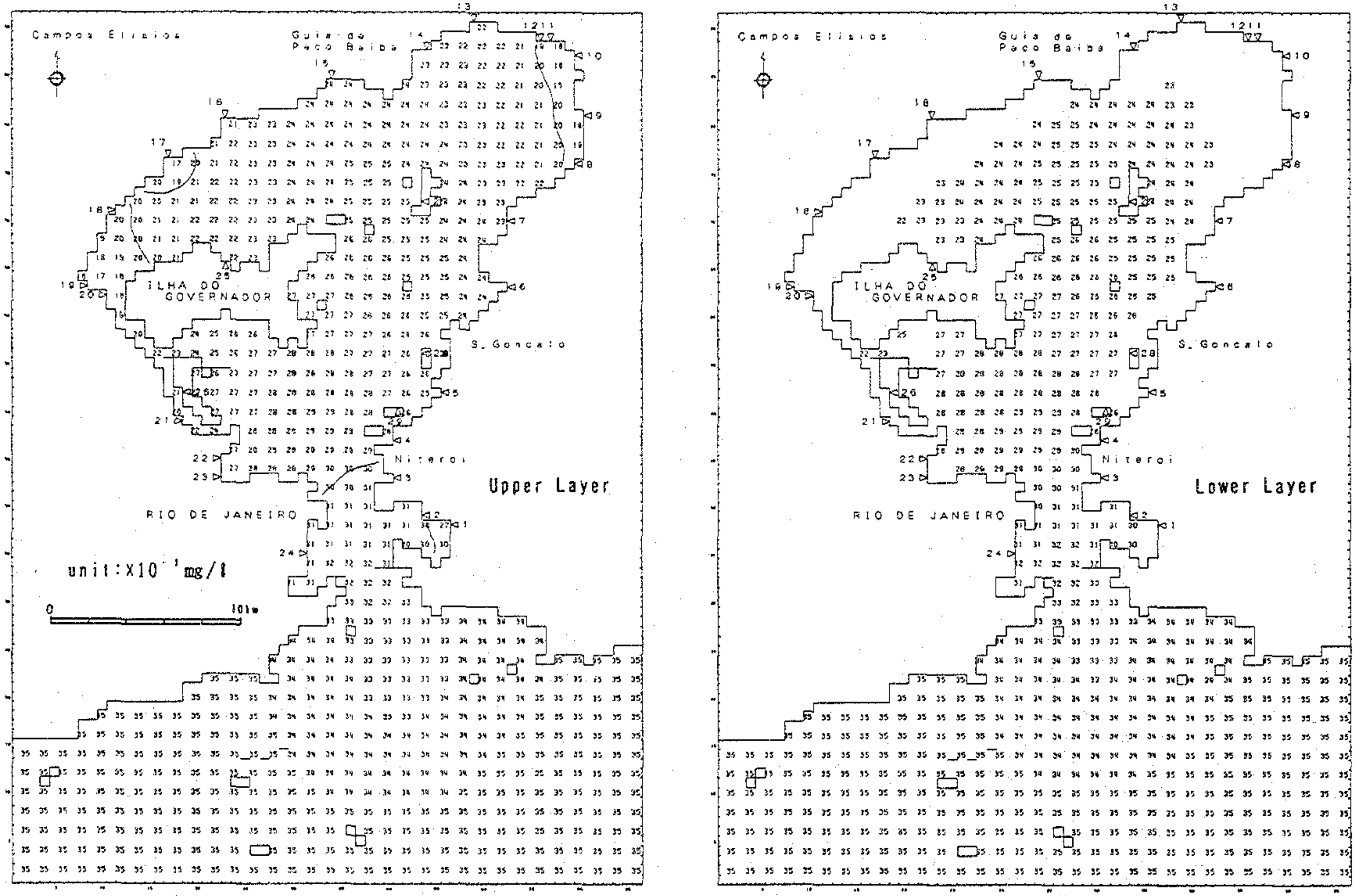

Fig. 2.5-1(1) Calculated Water Quality Distribution in Dry Season (Salinity)

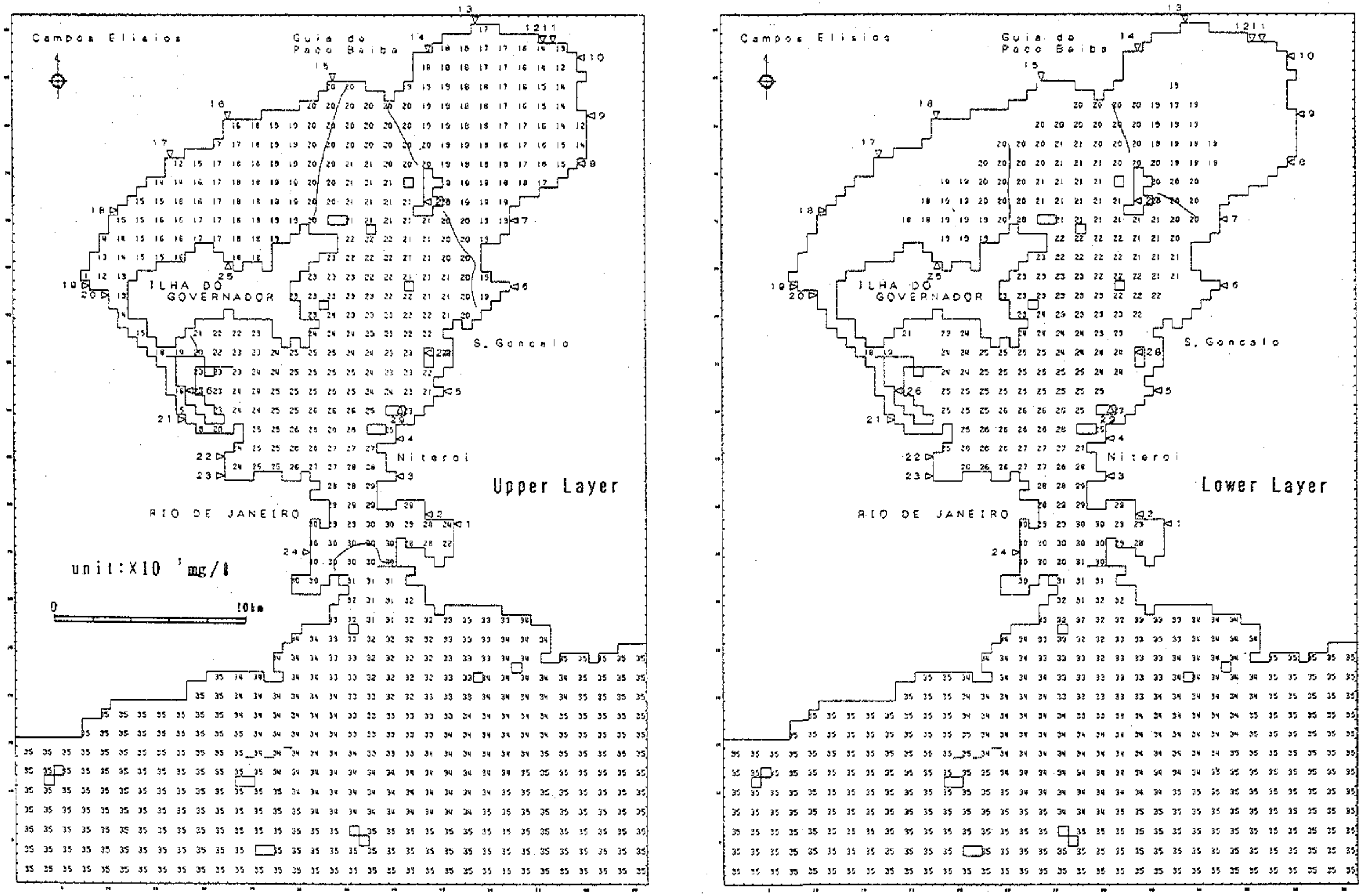

Fig. 2. 5-1(2) Calculated Water Quality Distribution in Rainy Season (Salinity)

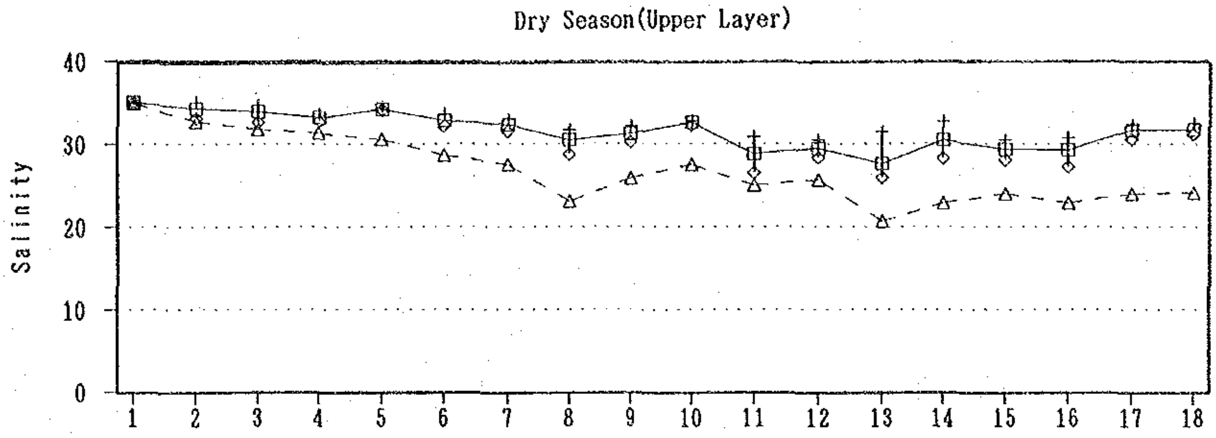

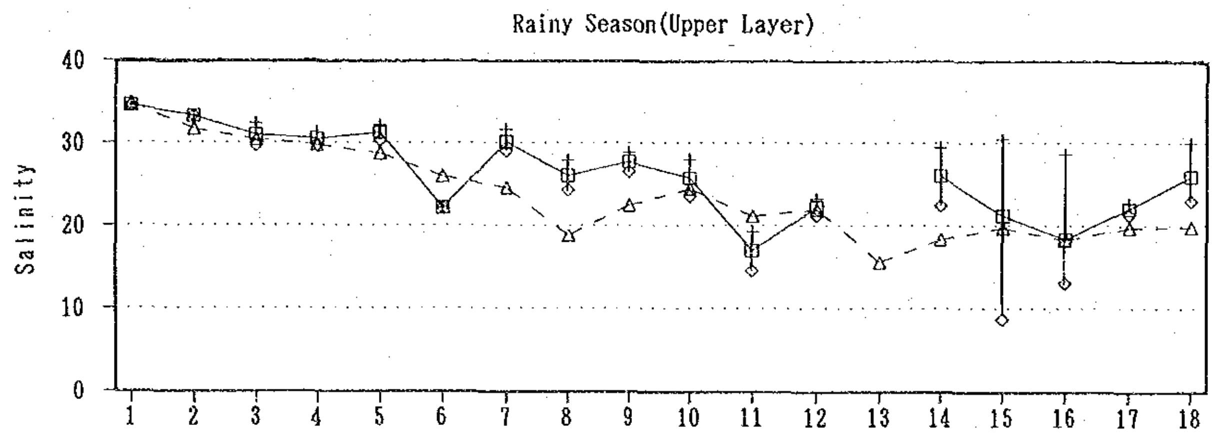

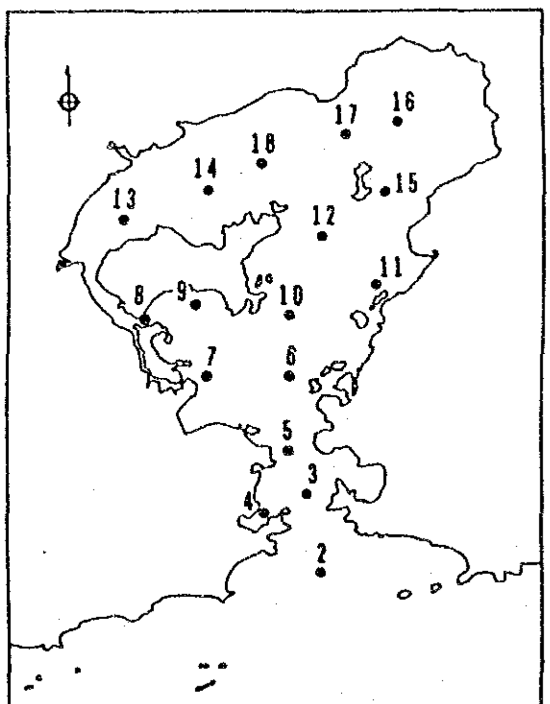

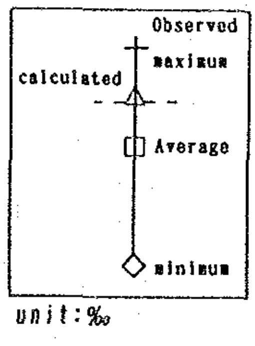

Fig. 2. 5-2 Comparison of Observed and Calculated Salinity

2.6 Verification Test of the Eutrophication Model

2.6.1 Results of Calculation

The simulation for the distribution of organic matters (COD and BOD), nutrient salts (O-P and PO_4-P) and DO in the Guanabara Bay was carried out using a two-level eutrophication model mentioned in the previous chapter.

The results of the calculation are shown in Fig.2.6-1 ~ Fig.2.6-3 as a mean concentration of one tidal for upper layer and lower layer of BOD, COD, PO_4-P, O-P, T-P and DO in dry season, rainy season and annual mean. Here, T-P means the sum of O-P and PO4-P concentration.

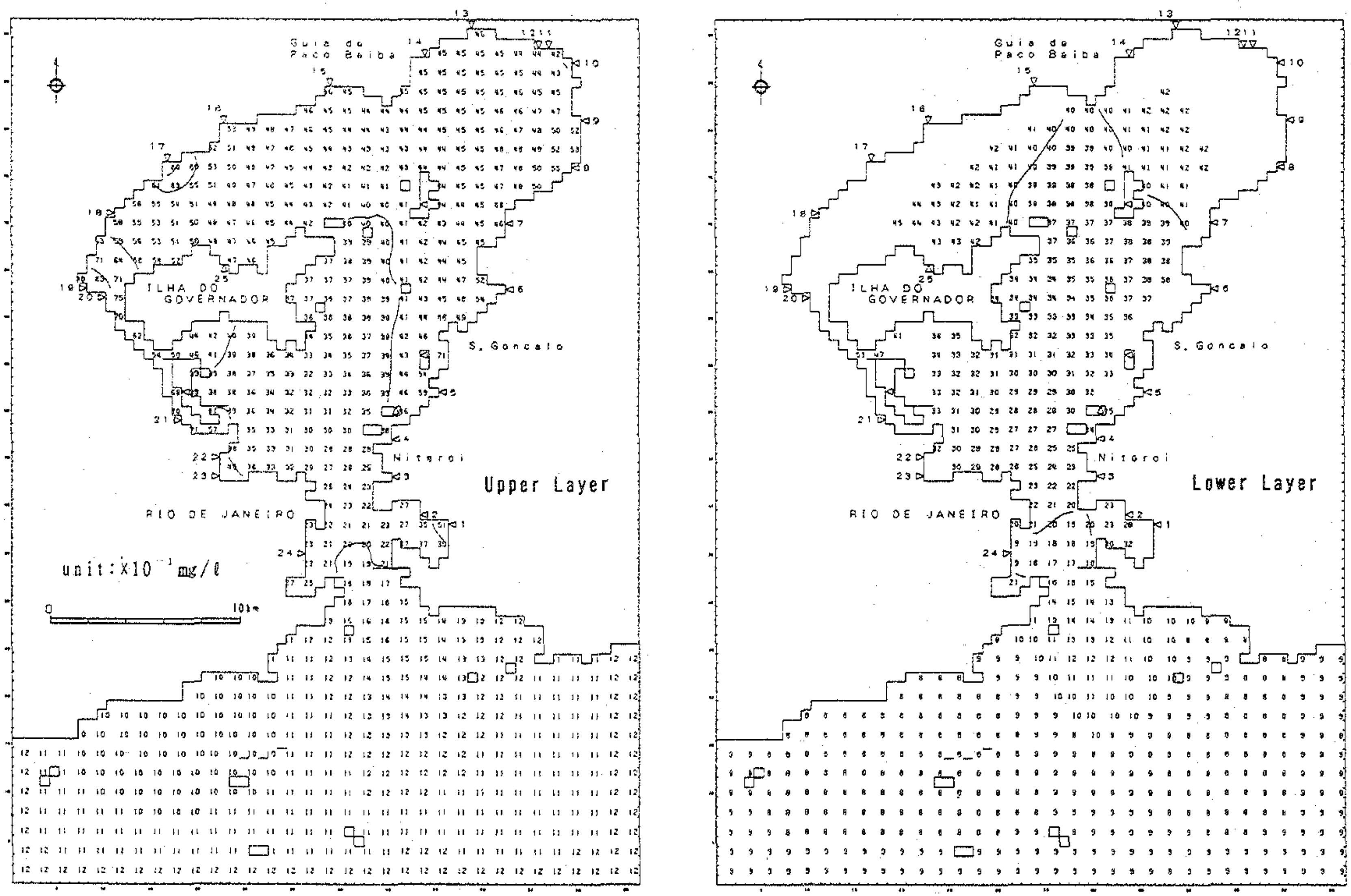

Fig. 2. 6-1(1) Calculated Water Quality Distribution in Dry Season (BOD)

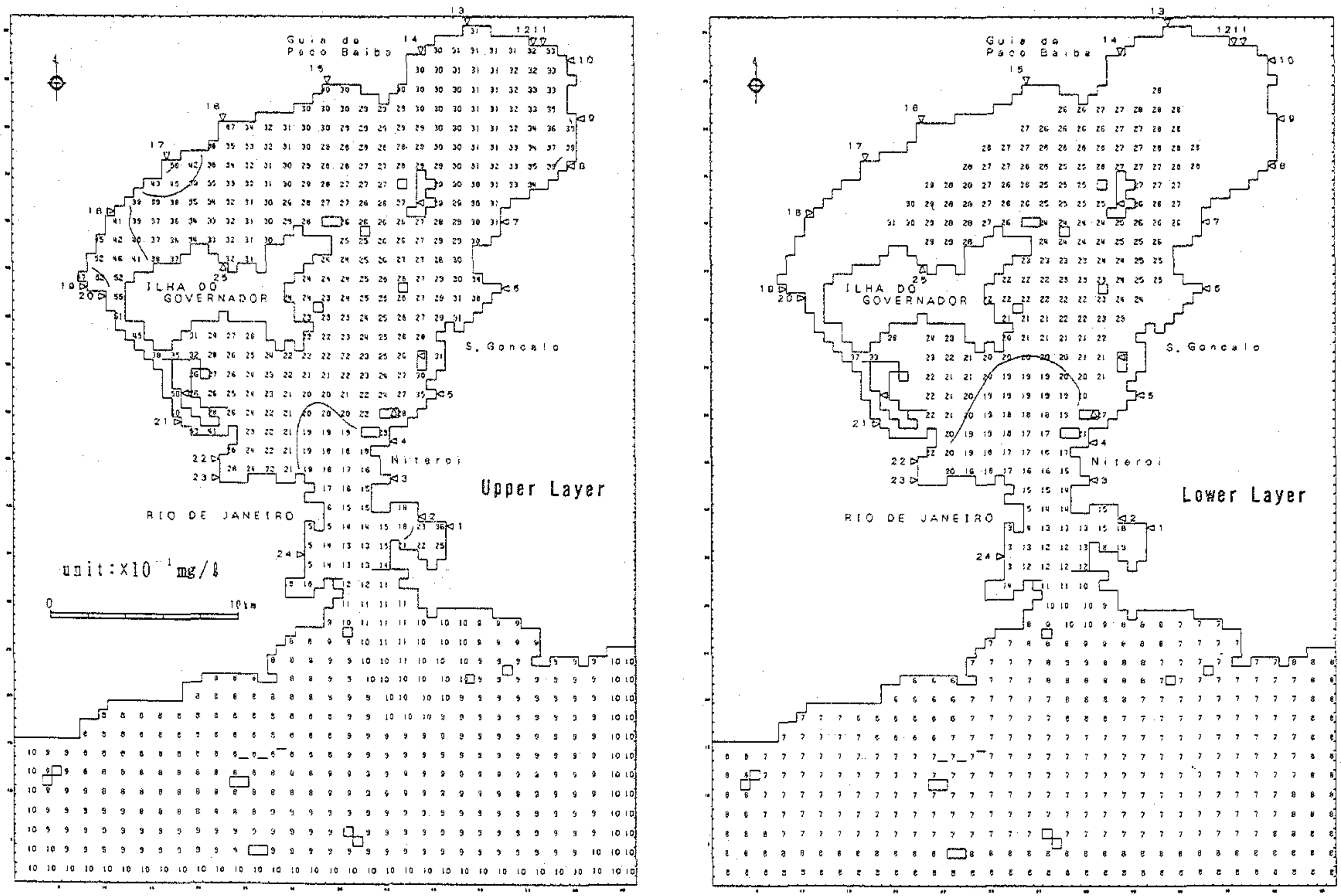

Fig. 2. 6-1(2) Calculated Water Quality Distribution in Dry Season (COD)

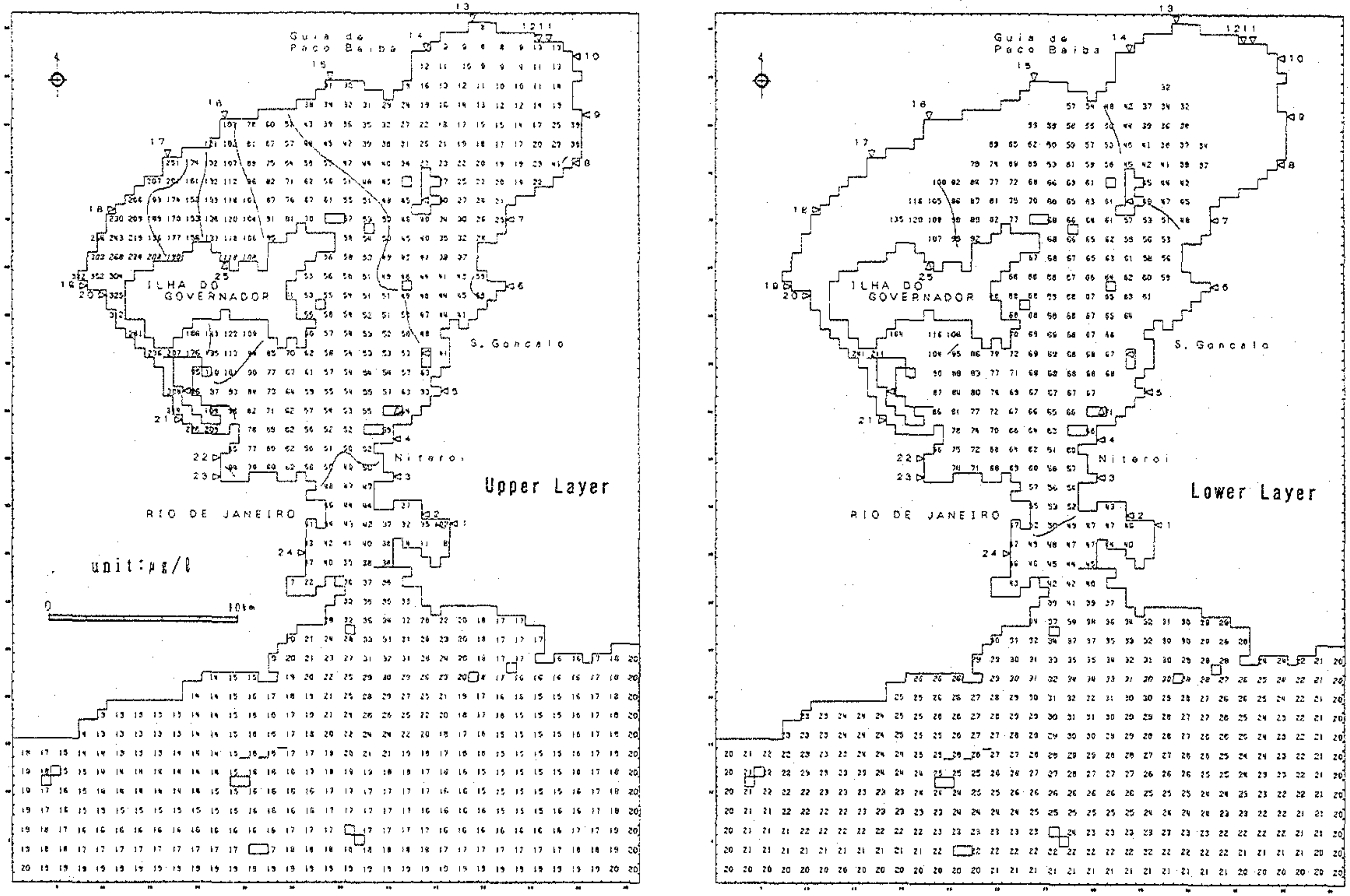

Fig. 2.6-1(3) Calculated Water Quality Distribution in Dry Season (PO_4-P)

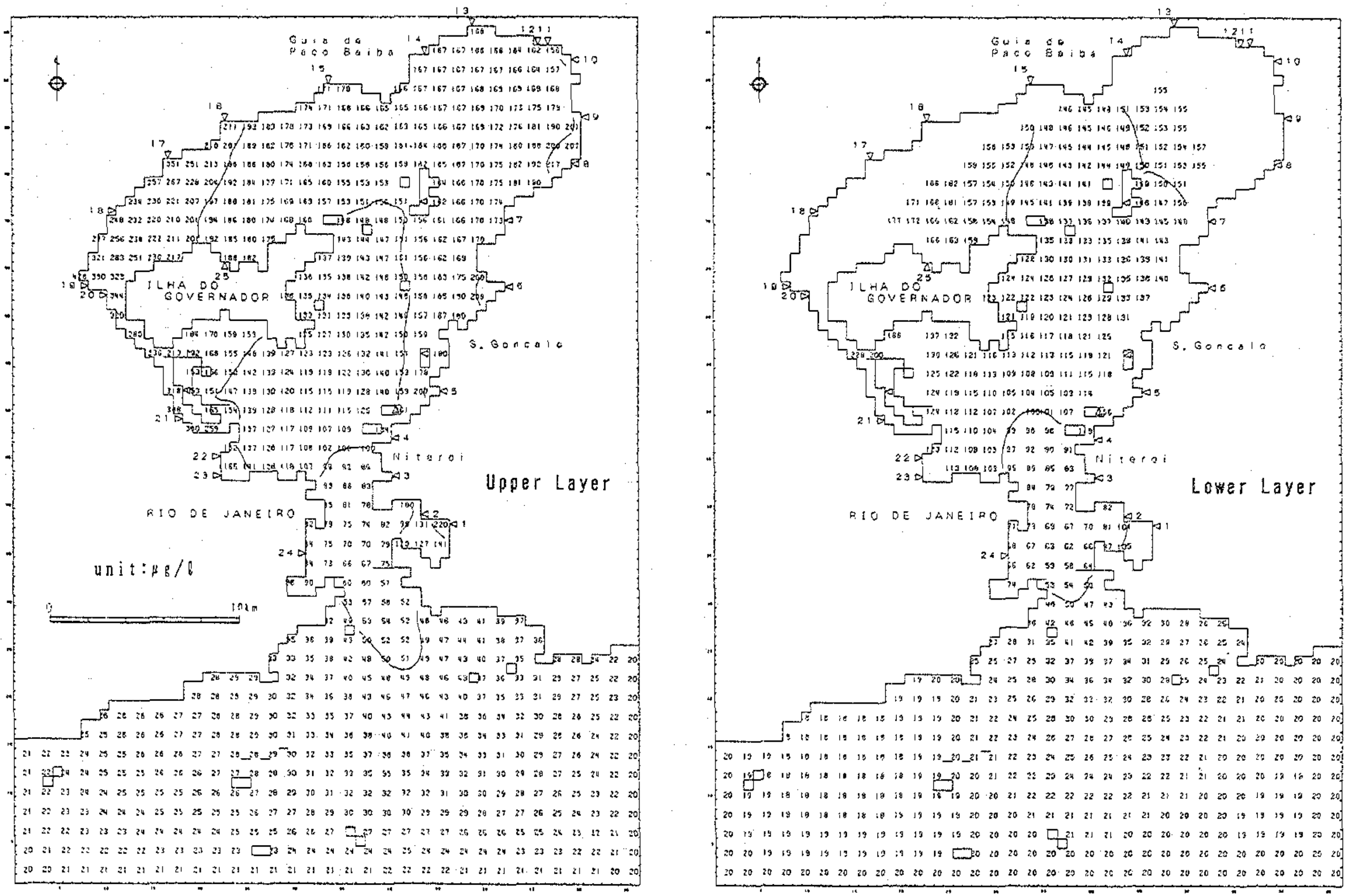

Fig. 2.6-1(4) Calculated Water Quality Distribution in Dry Season (O-P)

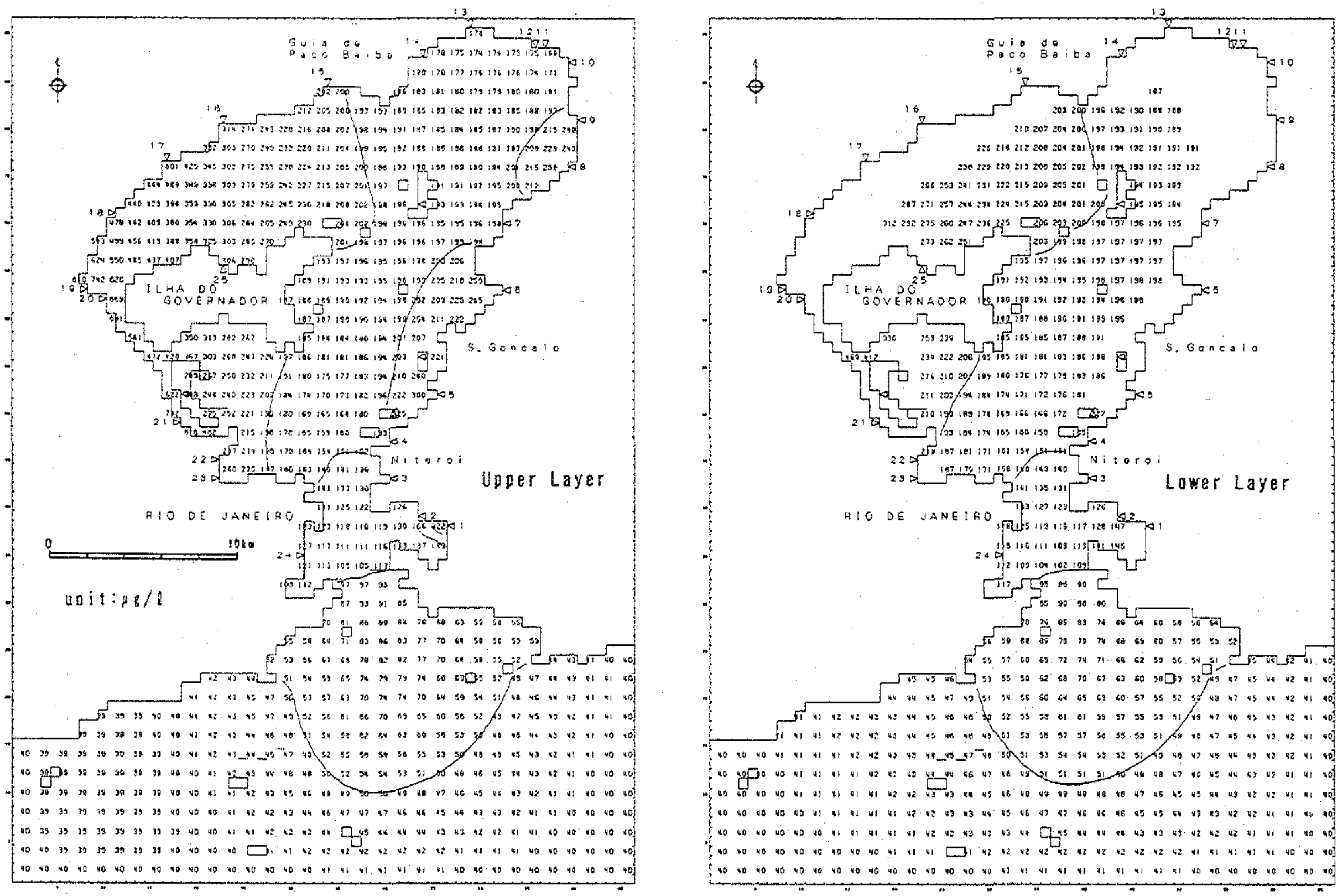

Fig. 2.6-1(5) Calculated Water Quality Distribution in Dry Season (T-P)

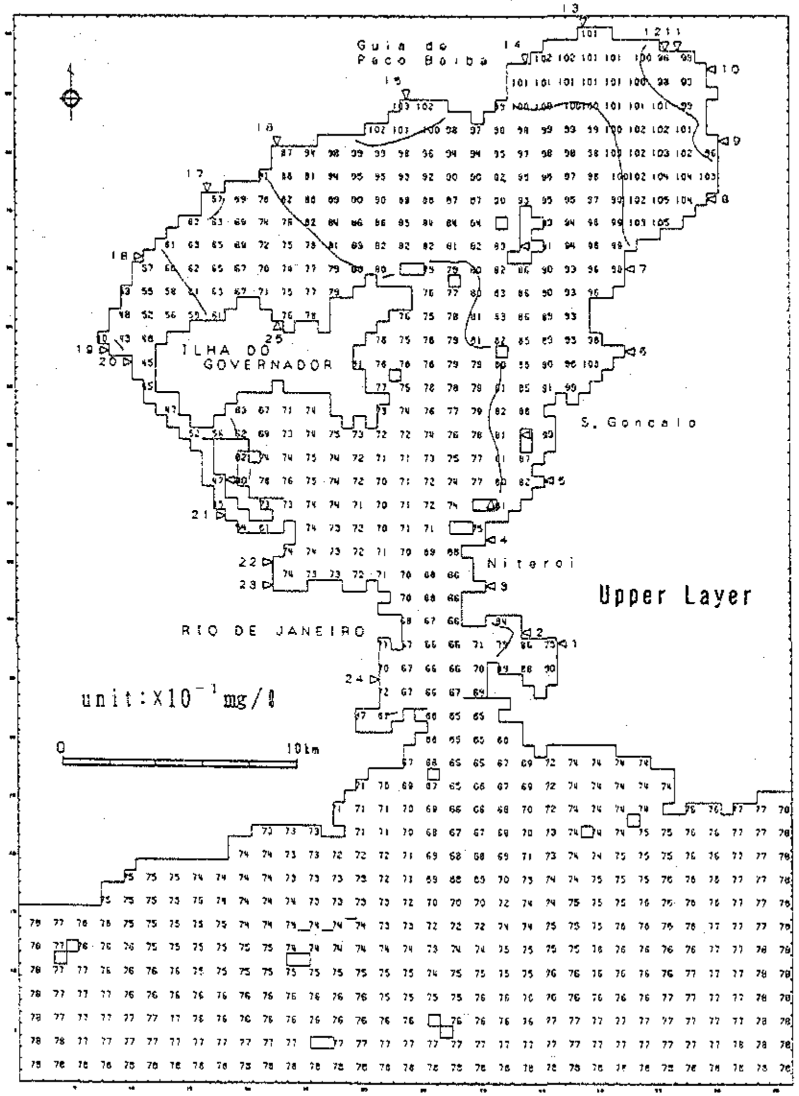

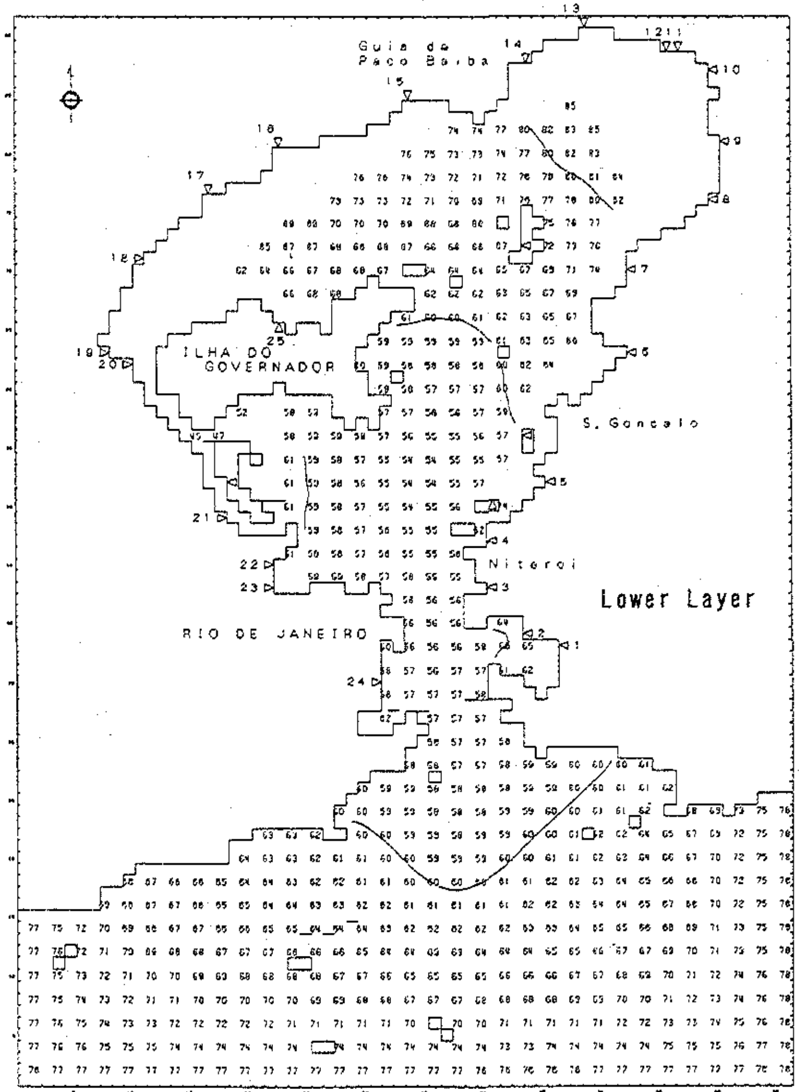

Fig. 2.6-1(6) Calculated Water Quality Distribution in Dry Season (DO)

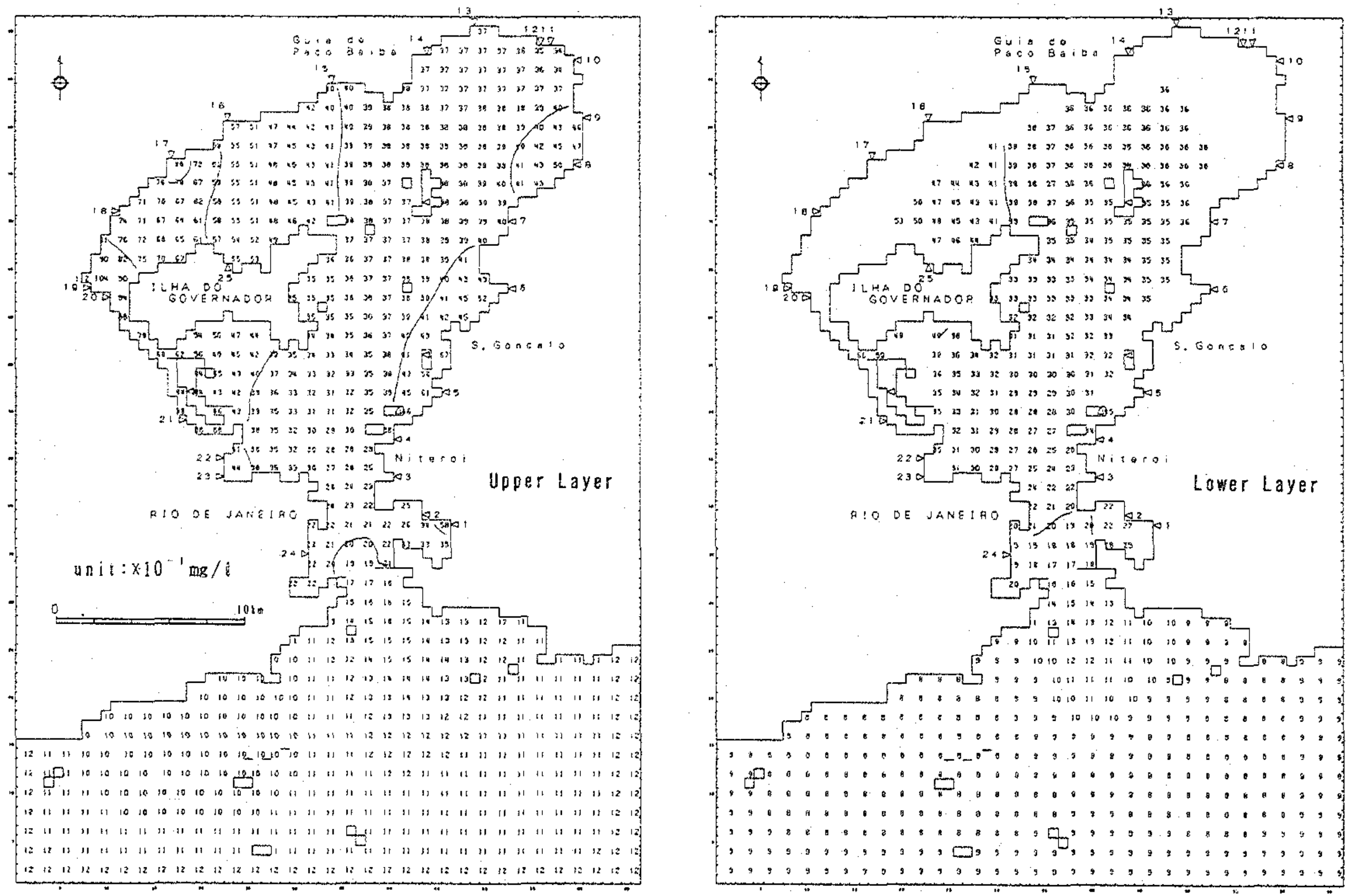

Fig. 2. 6-2(1) Calculated Water Quality Distribution in Rainy Season (BOD)

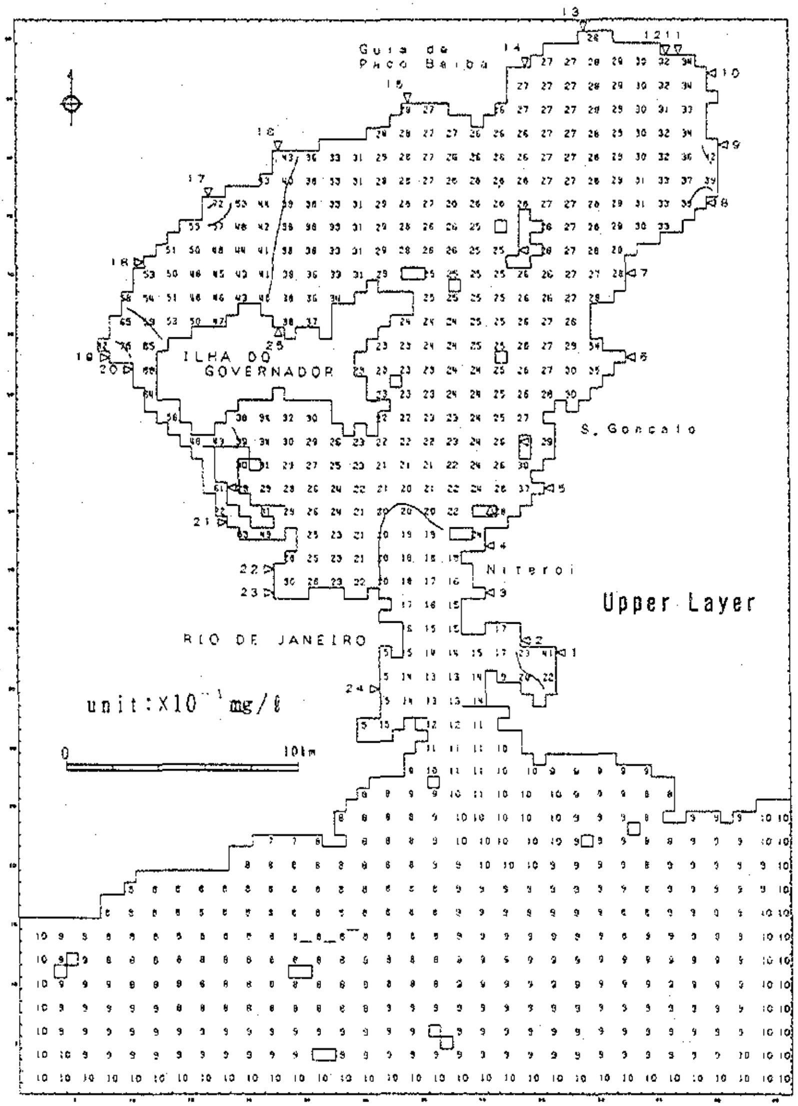

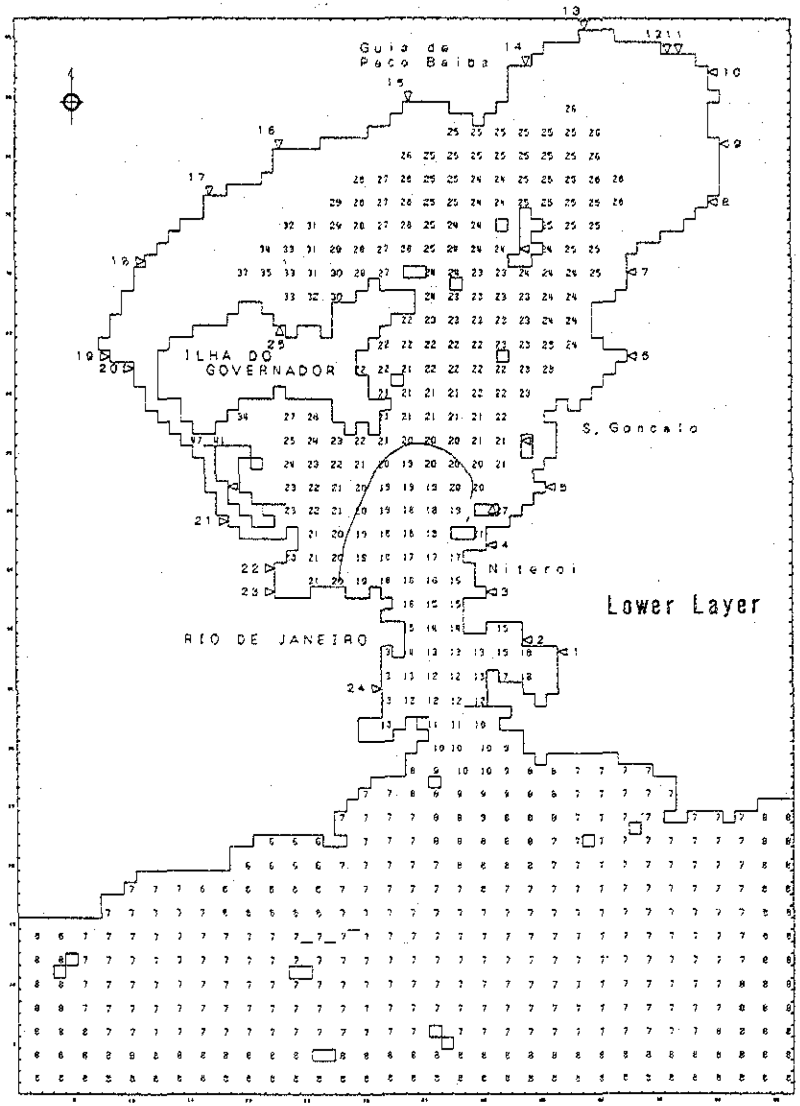

Fig. 2.6-2(2)   Calculated Water Quality Distribution in Rainy Season (COD)

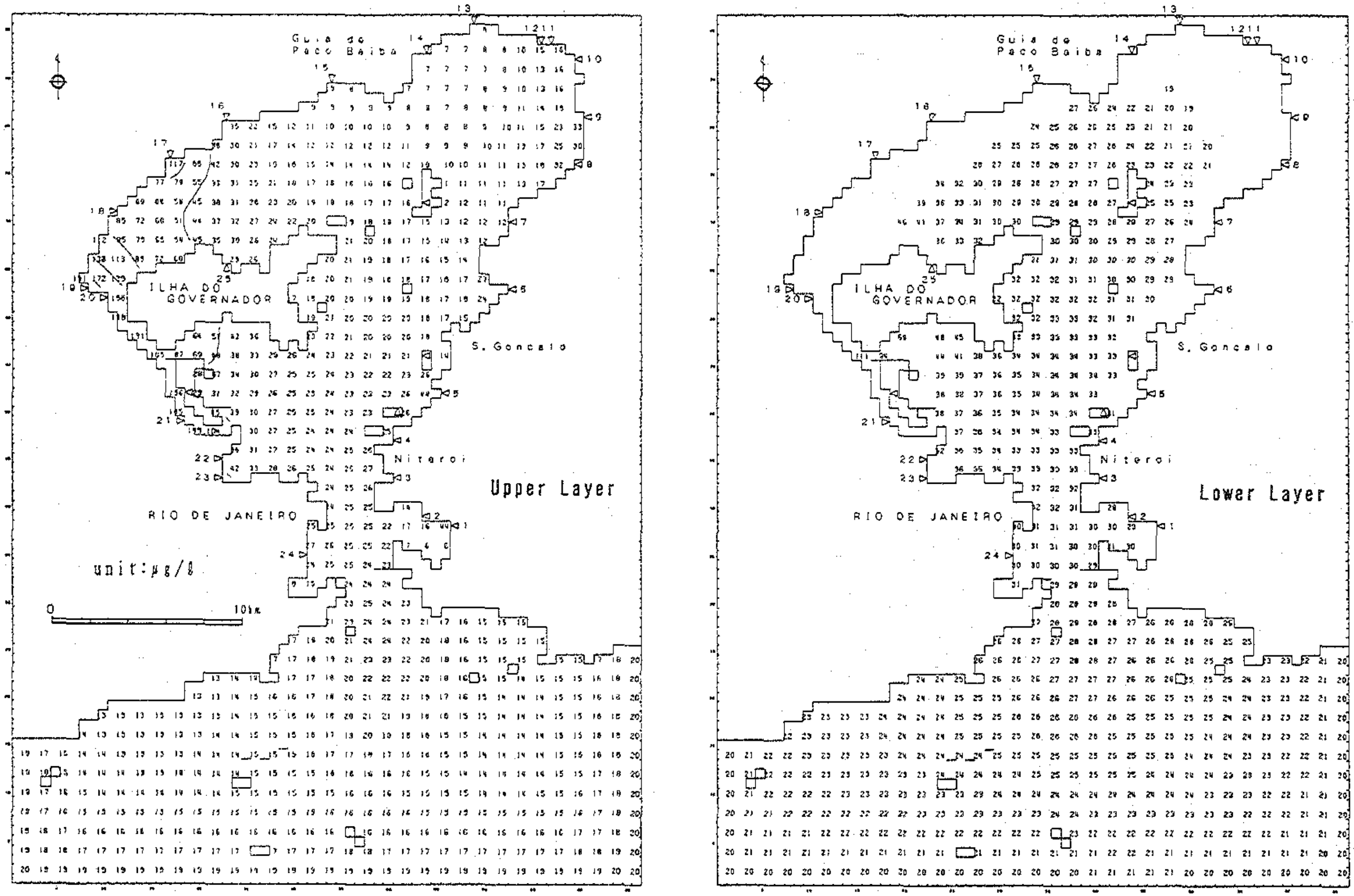

Fig. 2. 6-2(3) Calculated Water Quality Distribution in Rainy Season (PO_4-P)

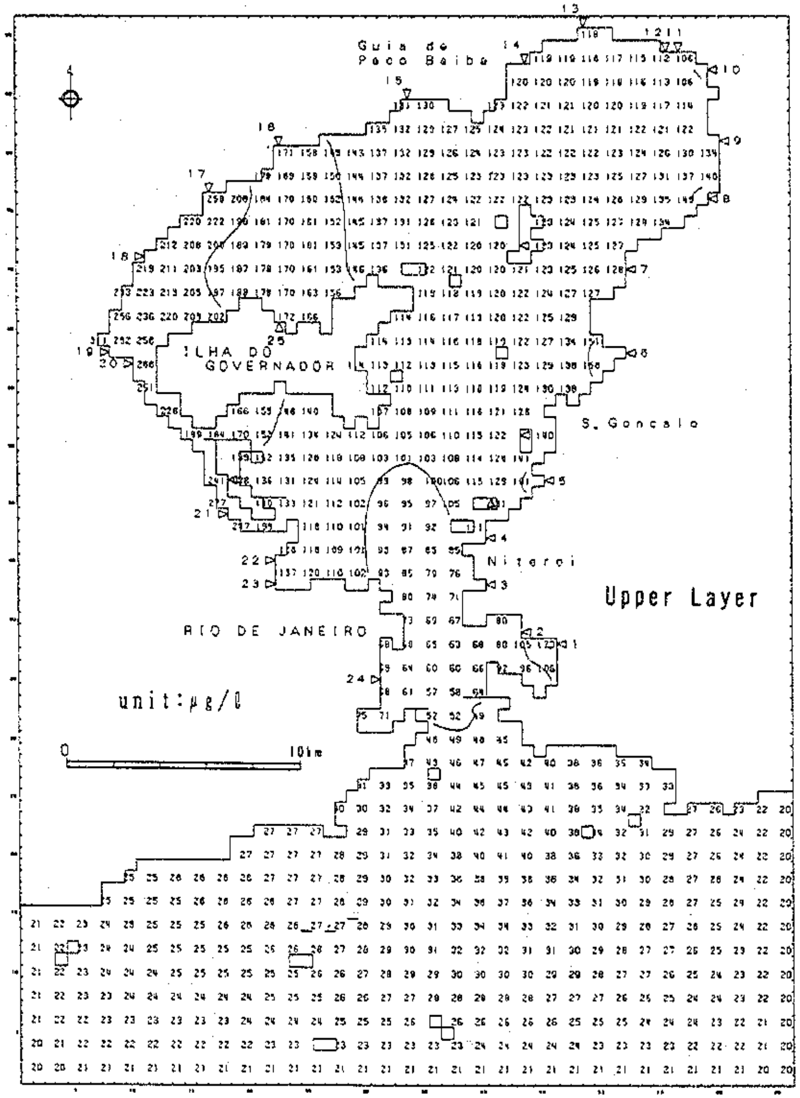

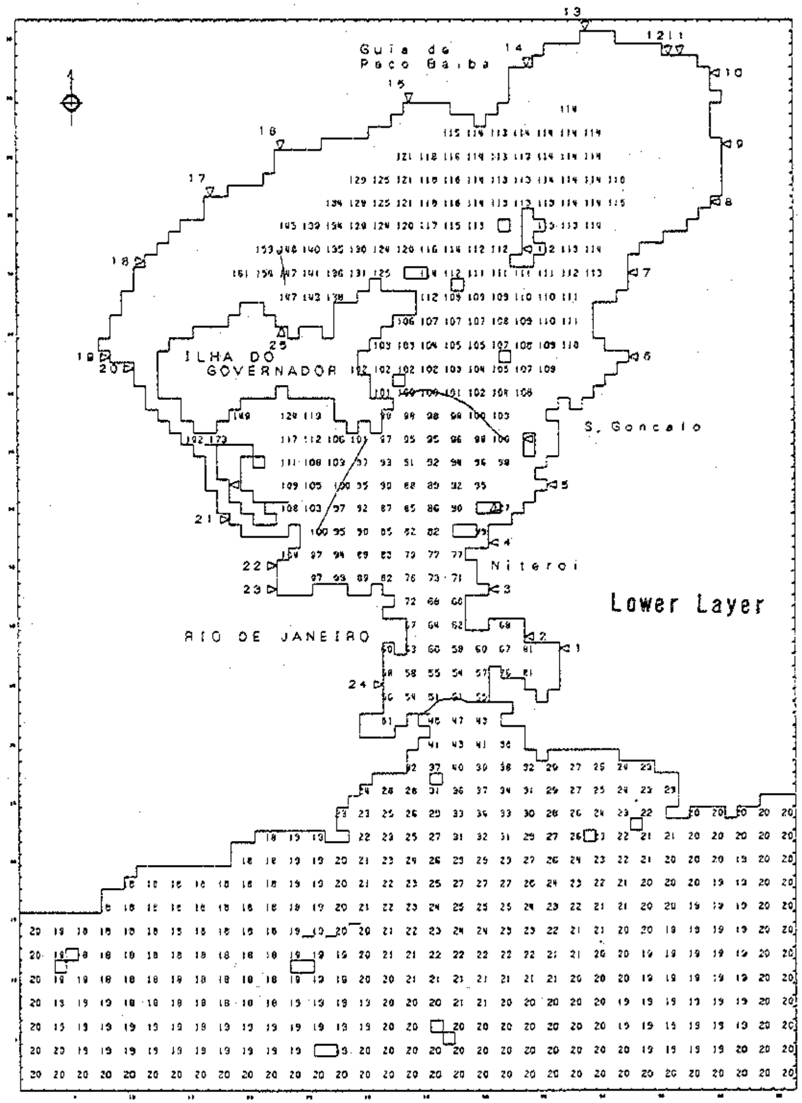

Fig. 2.6-2(4) Calculated Water Quality Distribution in Rainy Season (O-P)

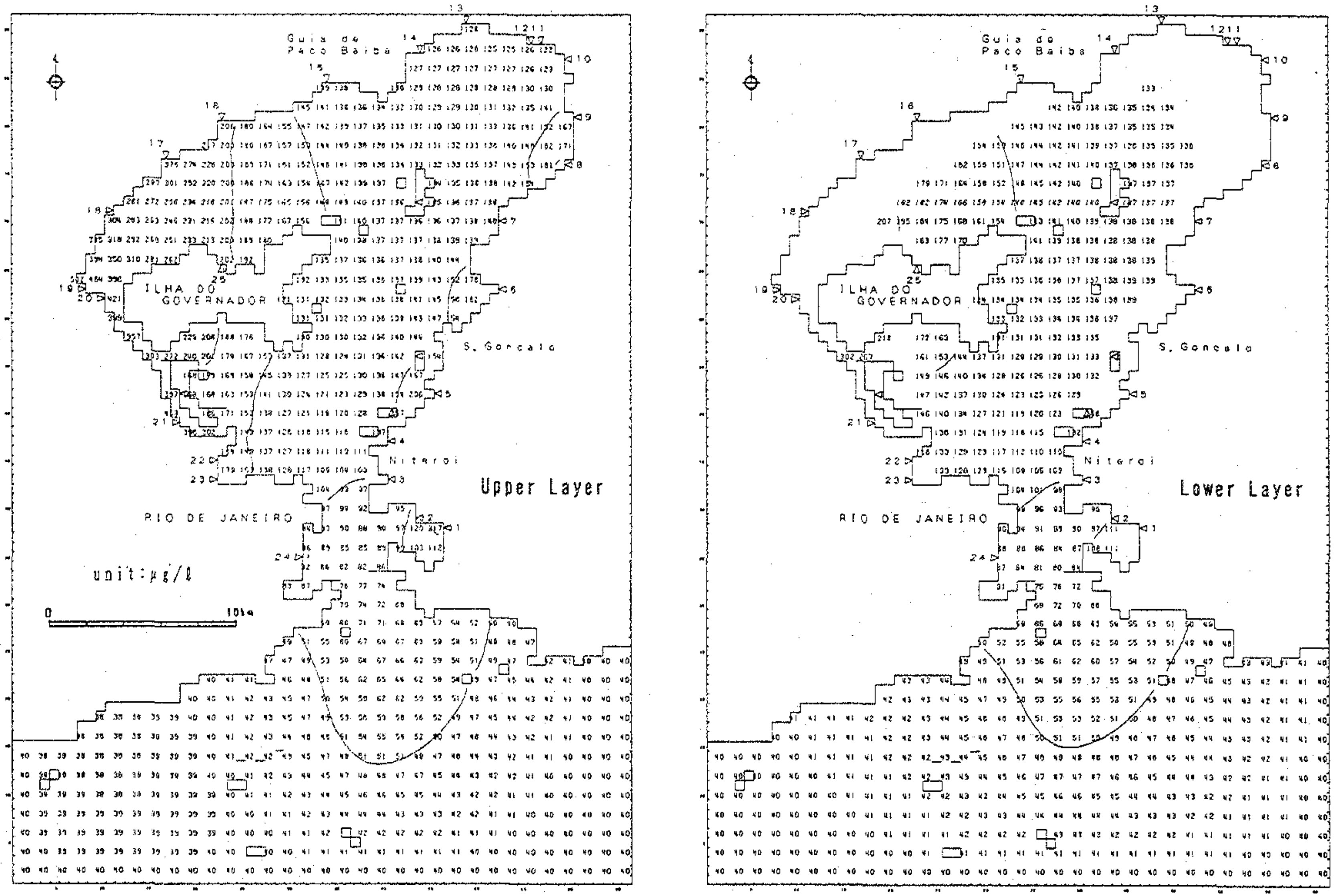

Fig. 2.6-2(5) Calculated Water Quality Distribution in Rainy Season (T-P)

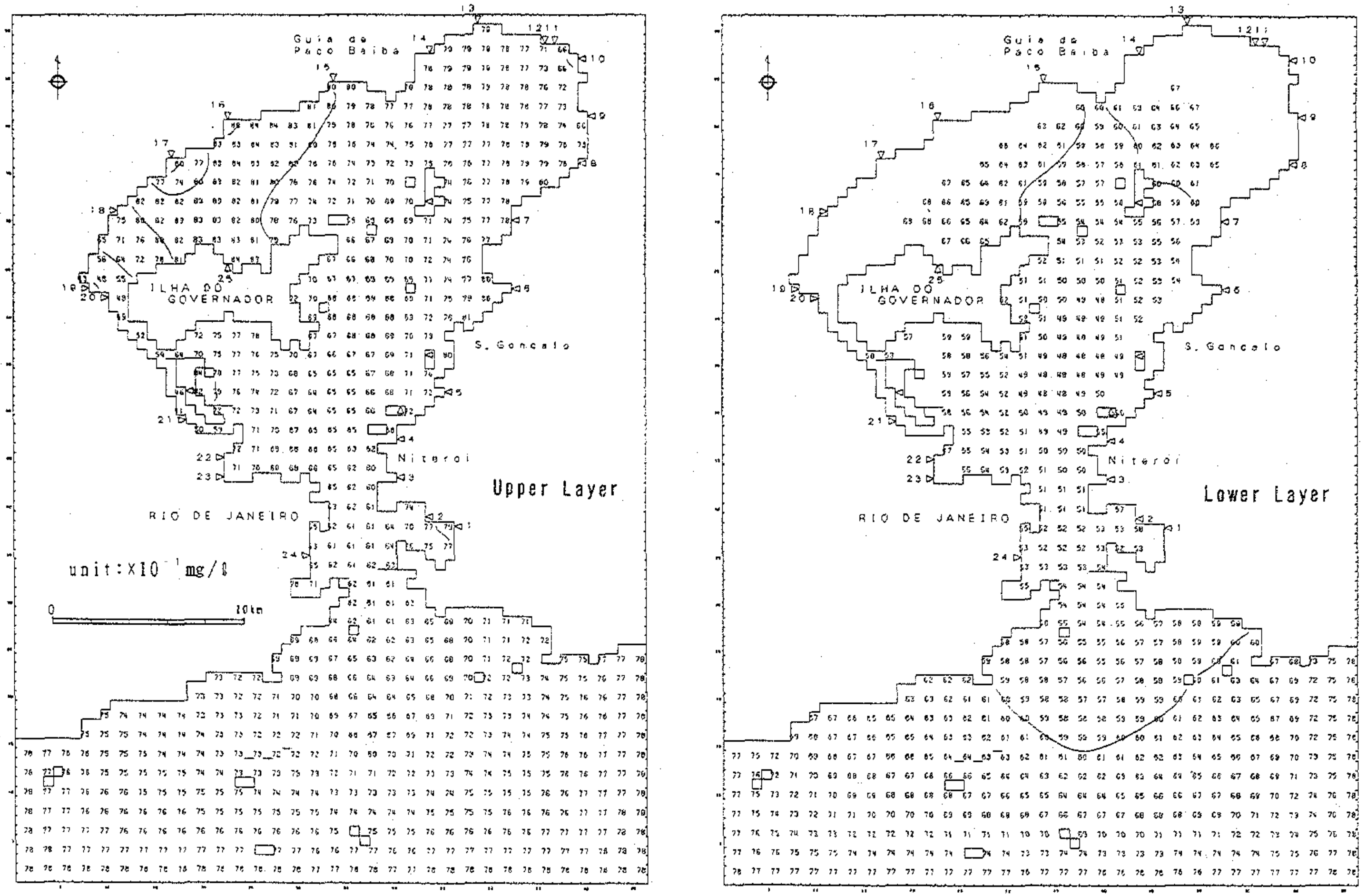

Fig. 2. 6-2(6) Calculated Water Quality Distribution in Rainy Season (DO)

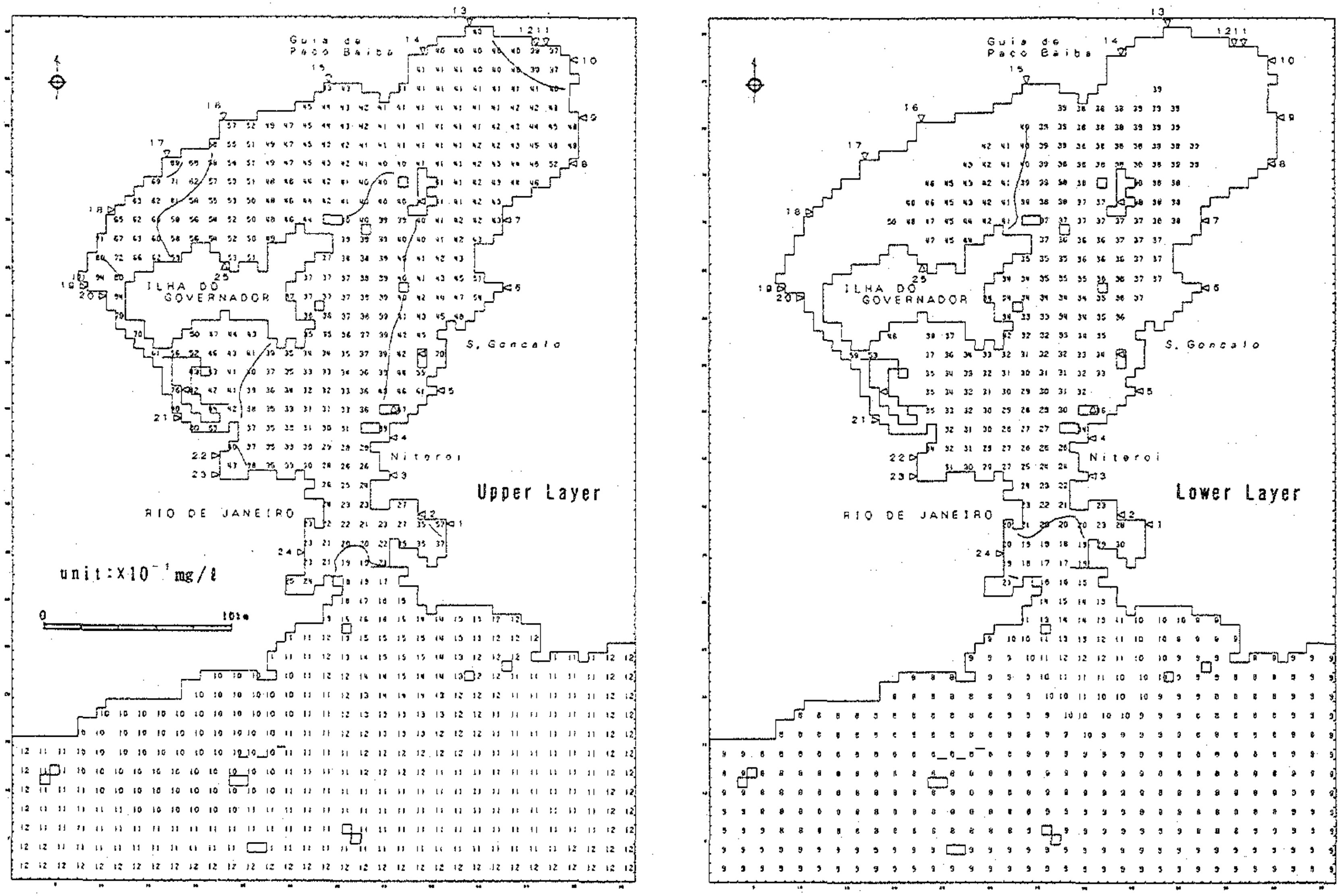

Fig. 2. 6-3(1) Calculated Water Quality Distribution of Annual Mean in 1991 (BOD)

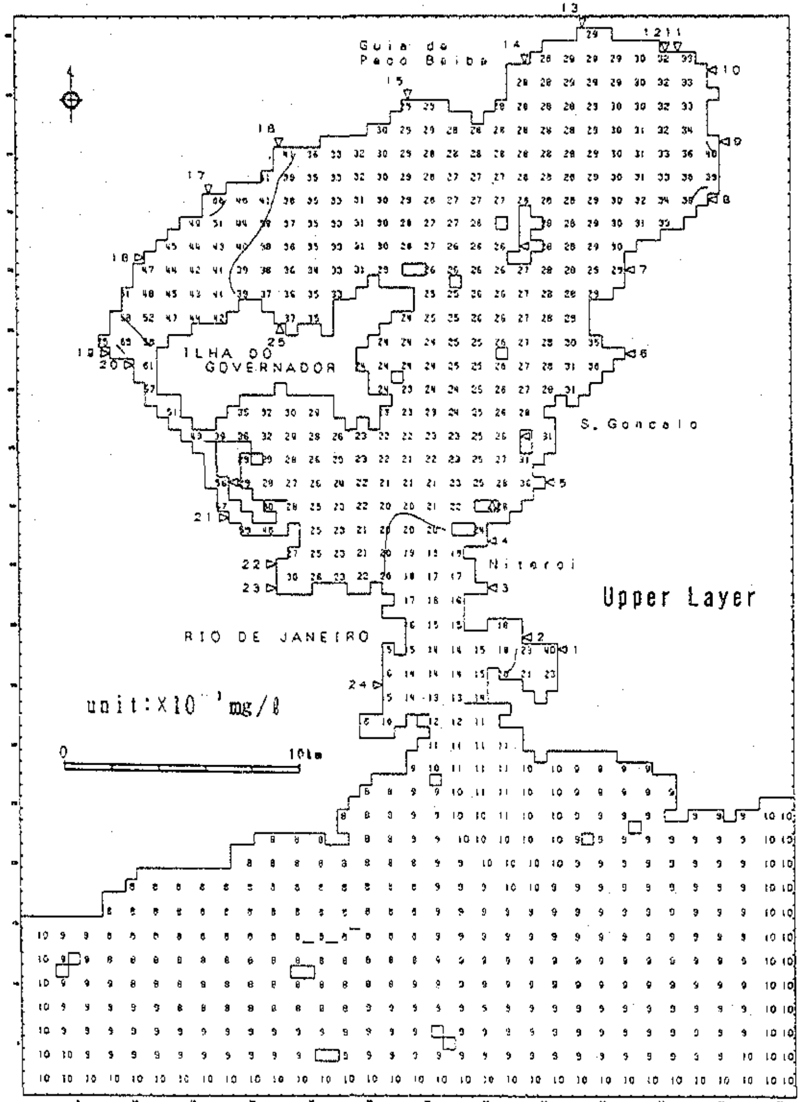

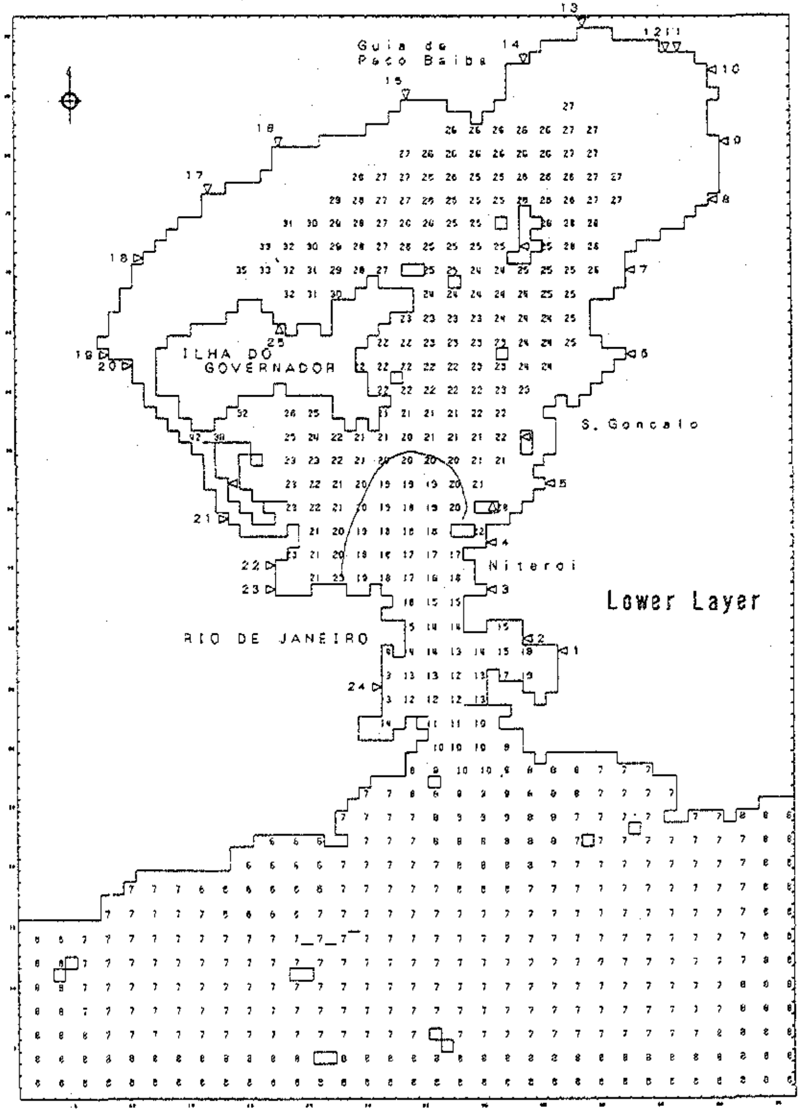

Fig. 2. 6-3(2)　Calculated Water Quality Distribution of Annual Mean in 1991 (COD)

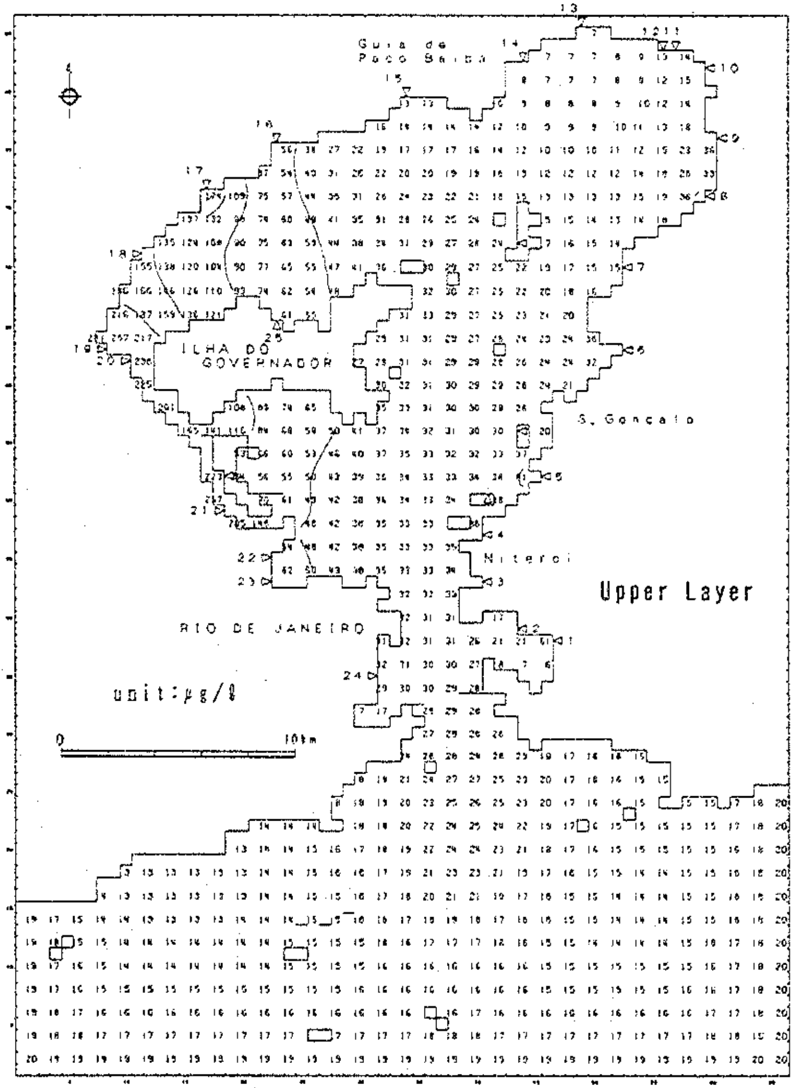

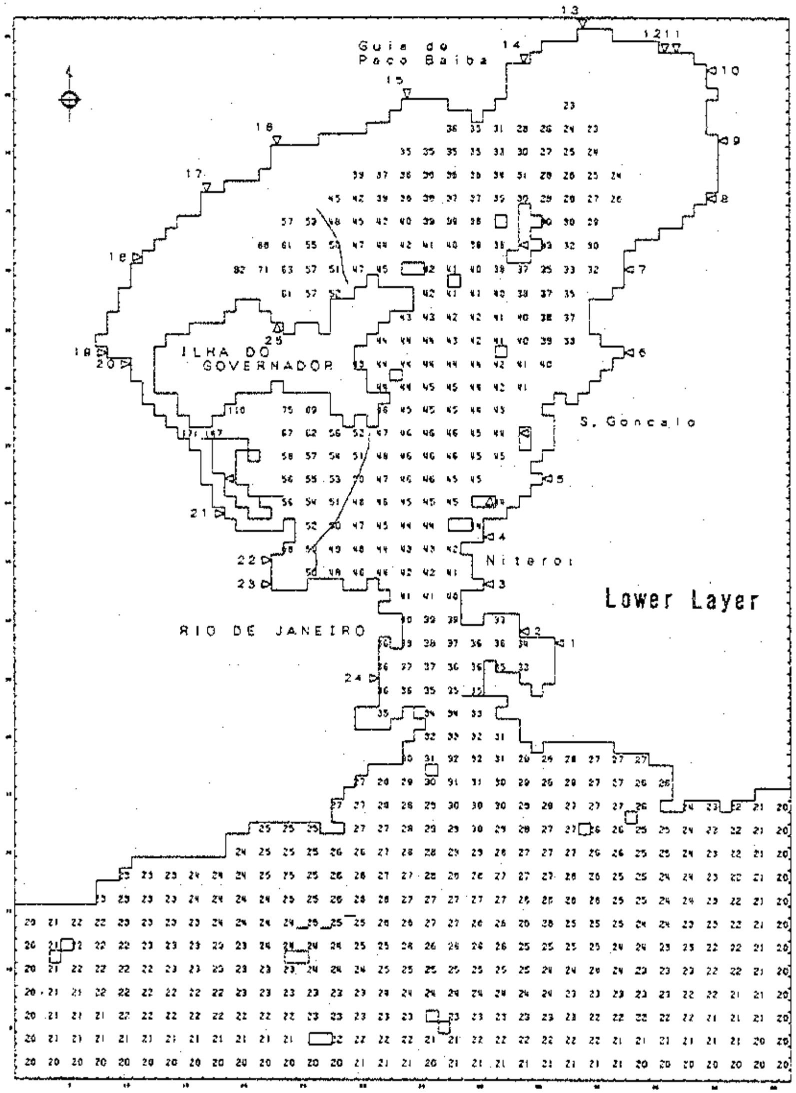

Fig. 2.6-3(3) Calculated Water Quality Distribution of Annual Mean in 1991 (PO_4-P)

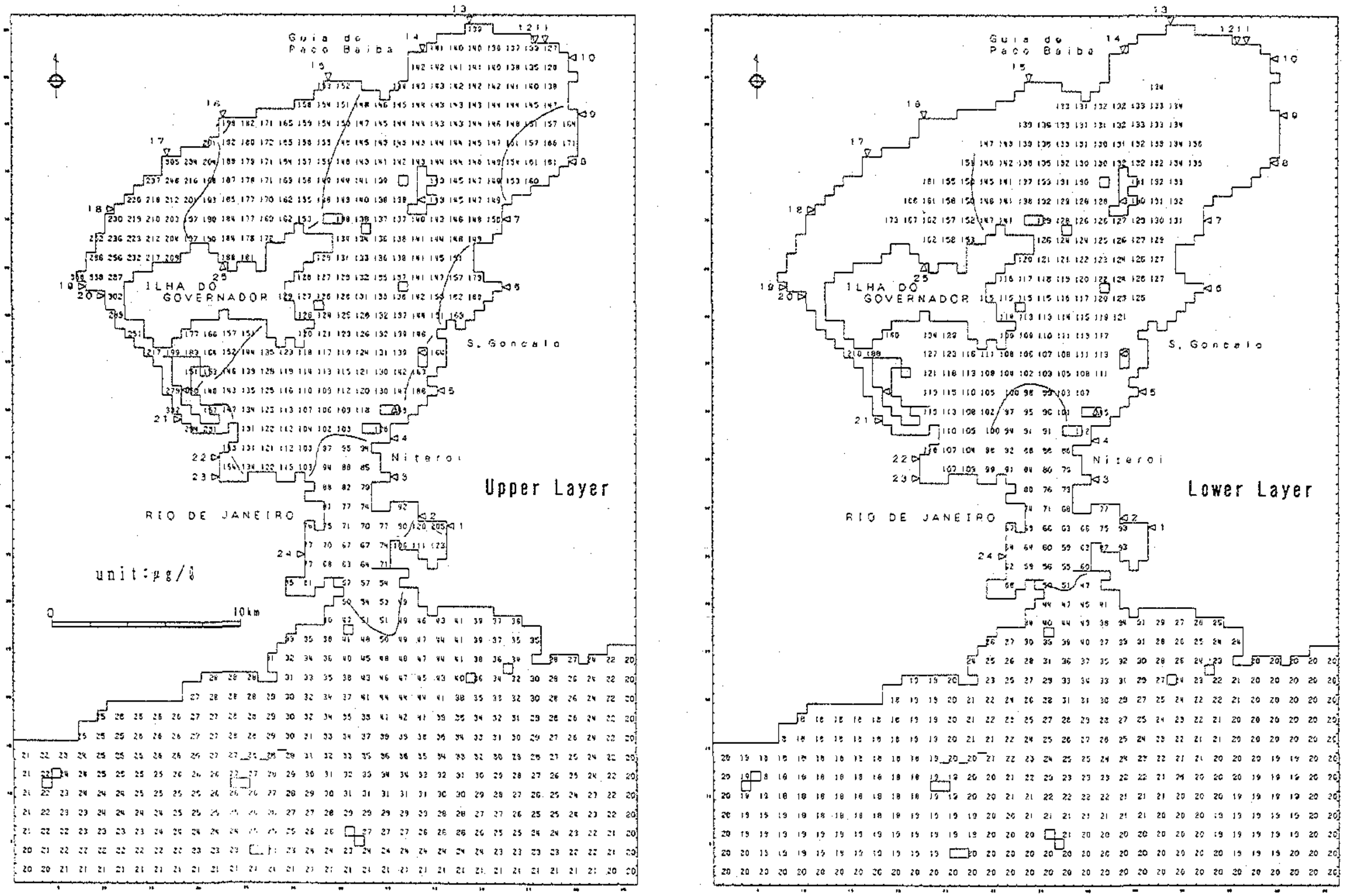

Fig. 2.6-3(4) Calculated Water Quality Distribution of Annual Mean in 1991 (O-P)

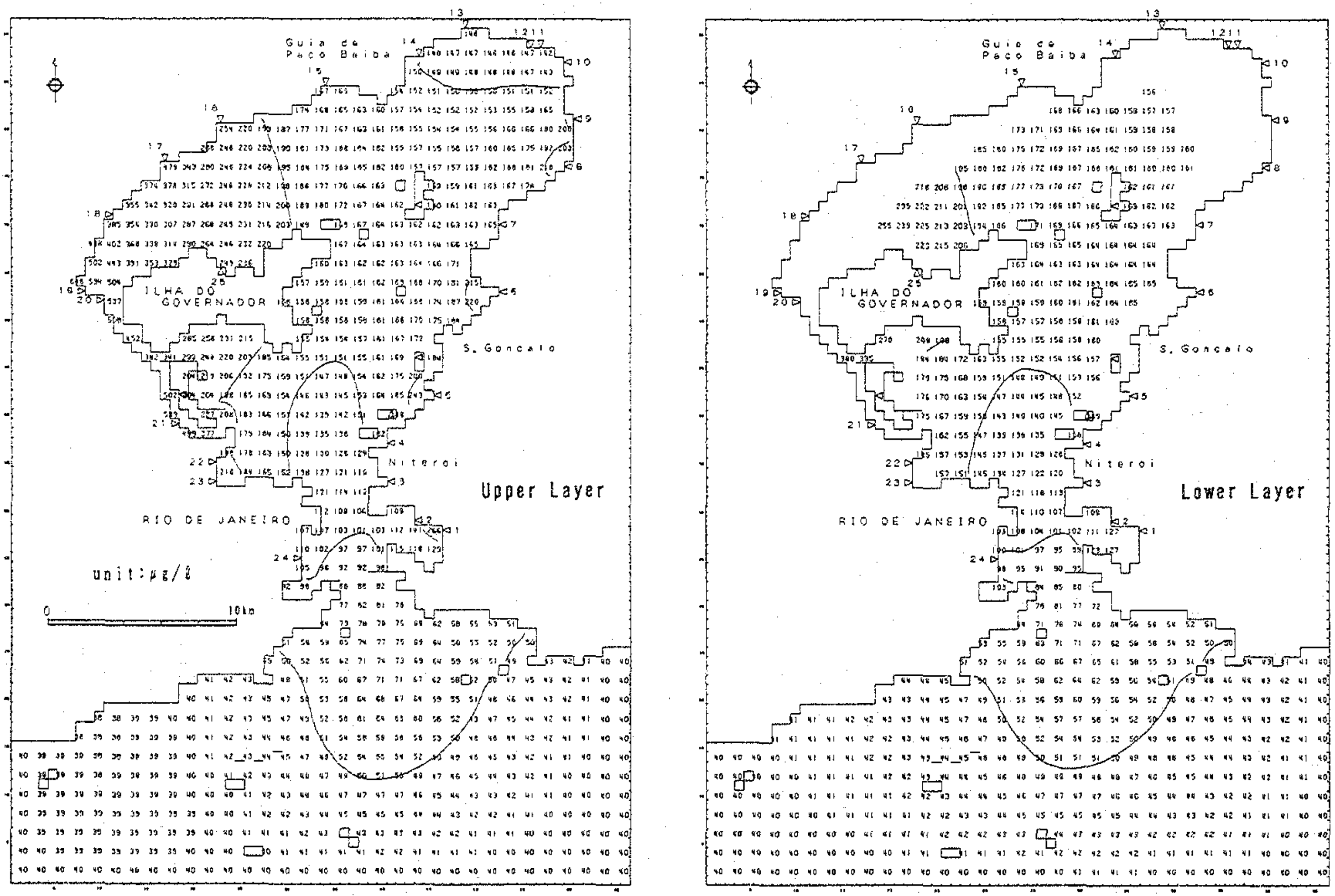

Fig. 2. 6-3(5) Calculated Water Quality Distribution of Annual Mean in 1991 (T-P)

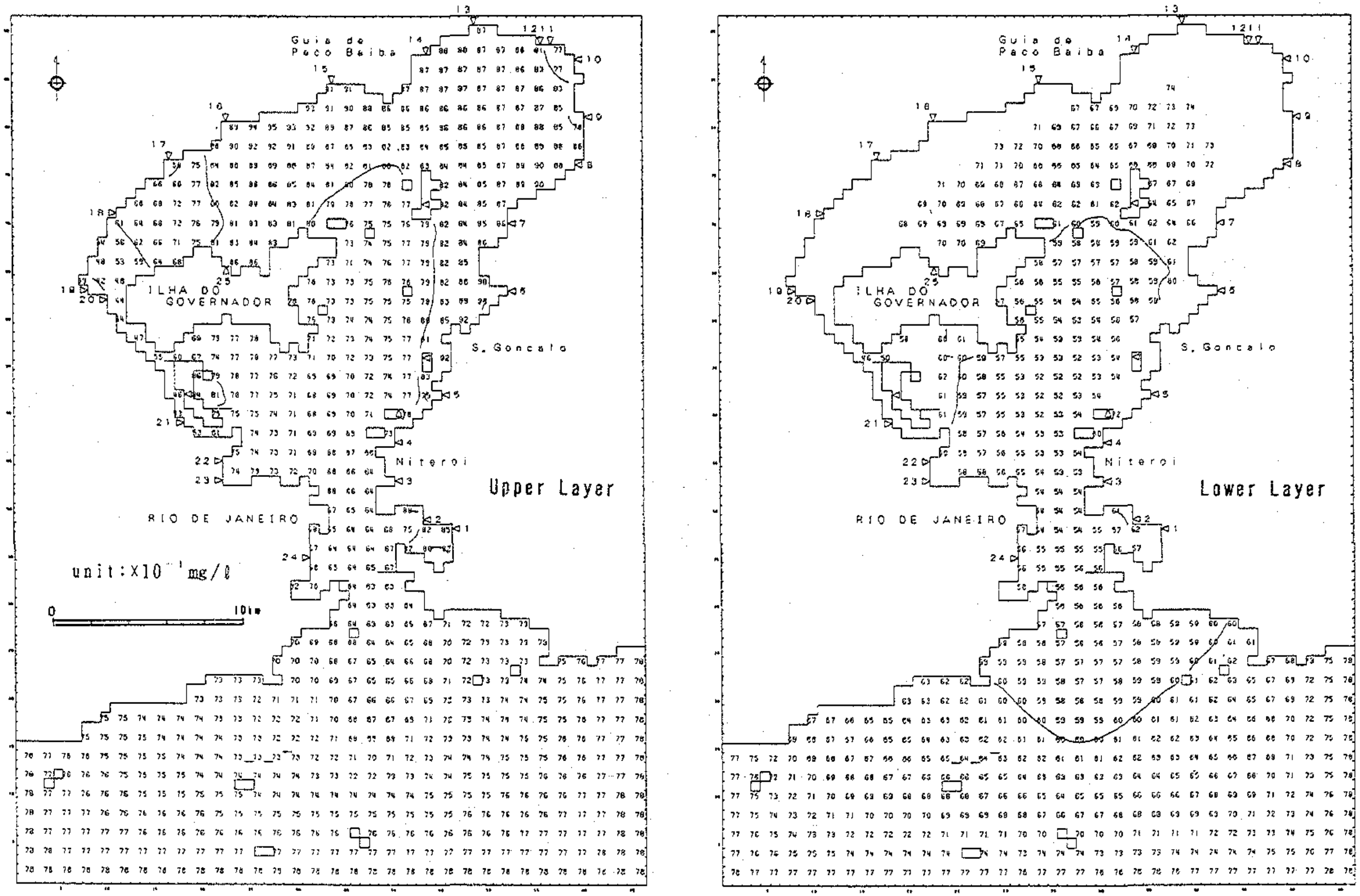

Fig. 2. 6-3(6) Calculated Water Quality Distribution of Annual Mean in 1991 (DO)

2.6.2 Verification of the Eutrophication Model

In order to evaluate the verification of the eutrophication model, we showed the comparison of the observed concentration and the calculated concentration at each station for each index in dry season, rainy season and annual mean value in Fig.2.6-4.

(1) Organic Matters (COD and BOD)
There are some differences at some points such as upper St.13 on dry season and lower on rainy season in COD. It will be said, however, that the calculated result agrees with the observed one to fully satisfactory degree.

(2) Dissolved Oxygen (DO)
The calculated values at St.7 to St.9 are larger than the observed ones. It will be said, however, that the calculated result totally agrees with the observed one.

(3) Nutrient Salts (O-P and PO_4-P)
Though the calculated values are larger than the observed ones in lower on dry season in PO_4-P and the calculated are larger than the observed as a whole in lower layer in all cases in O-P, the calculation result agrees with the observed values to satisfactory degree.

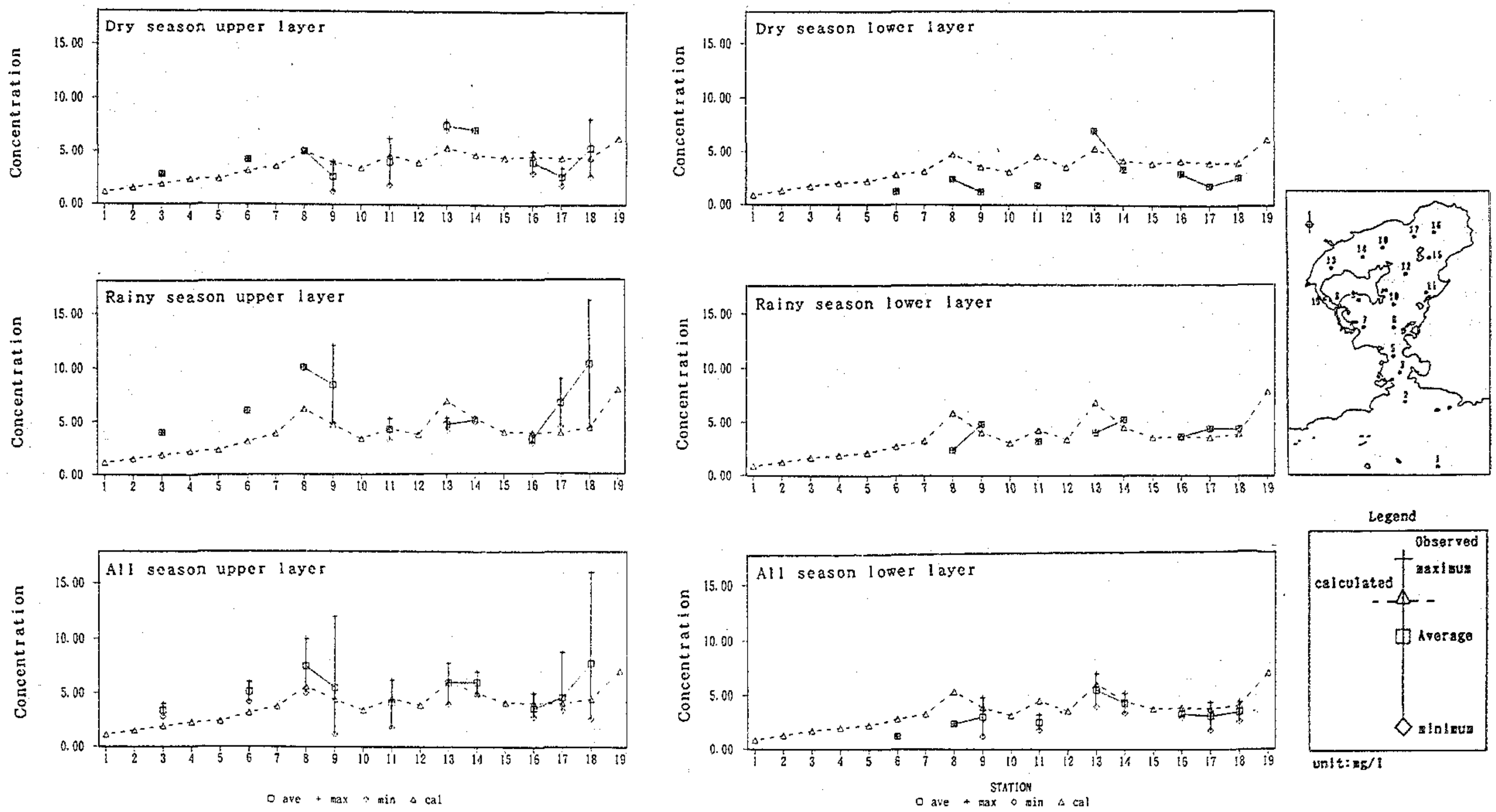

Fig. 2.6-4(1)　Comparison of Observed and Calculated BOD

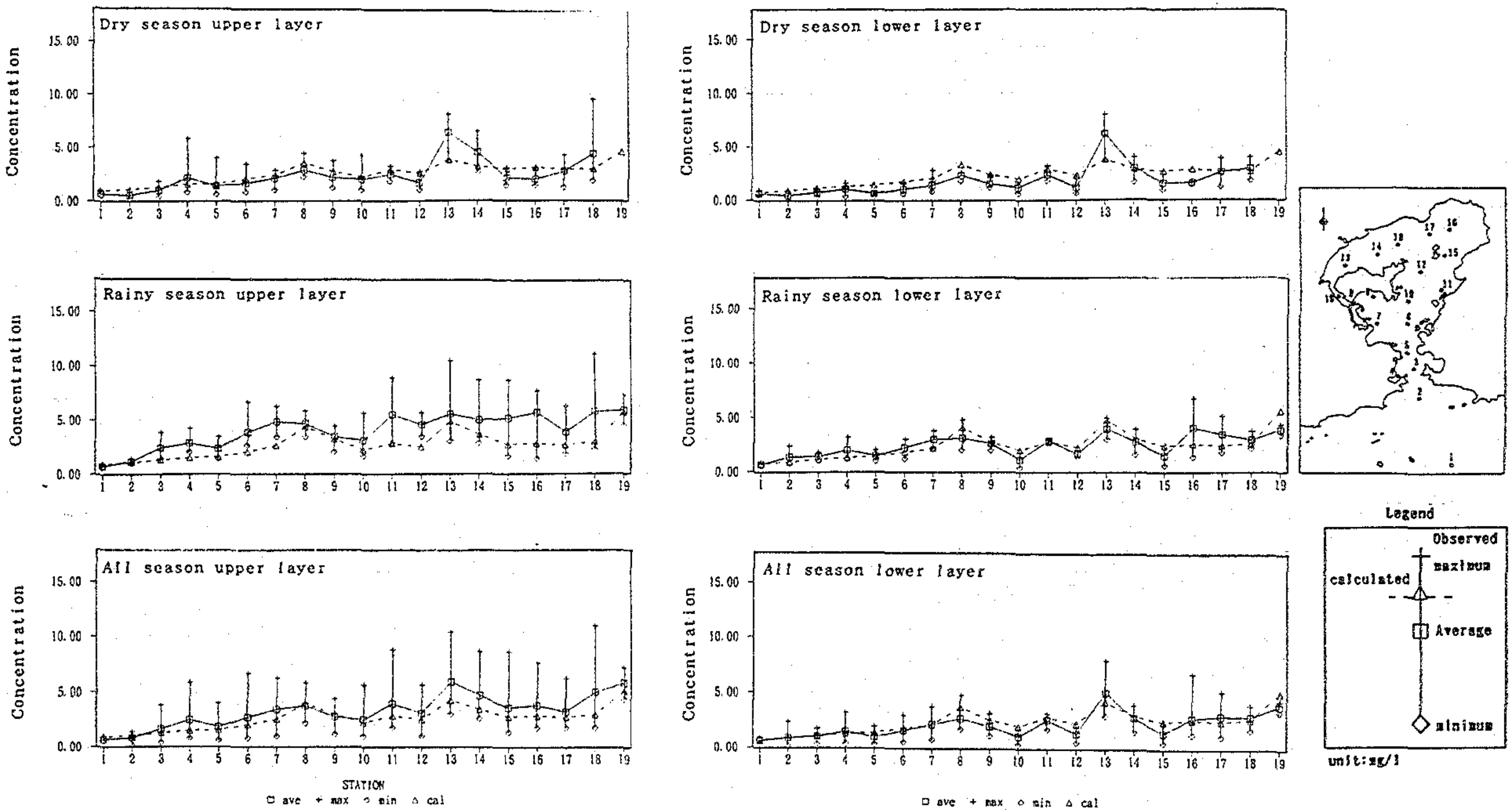

Fig. 2. 6-4(2) Comparison of Observed and Calculated COD

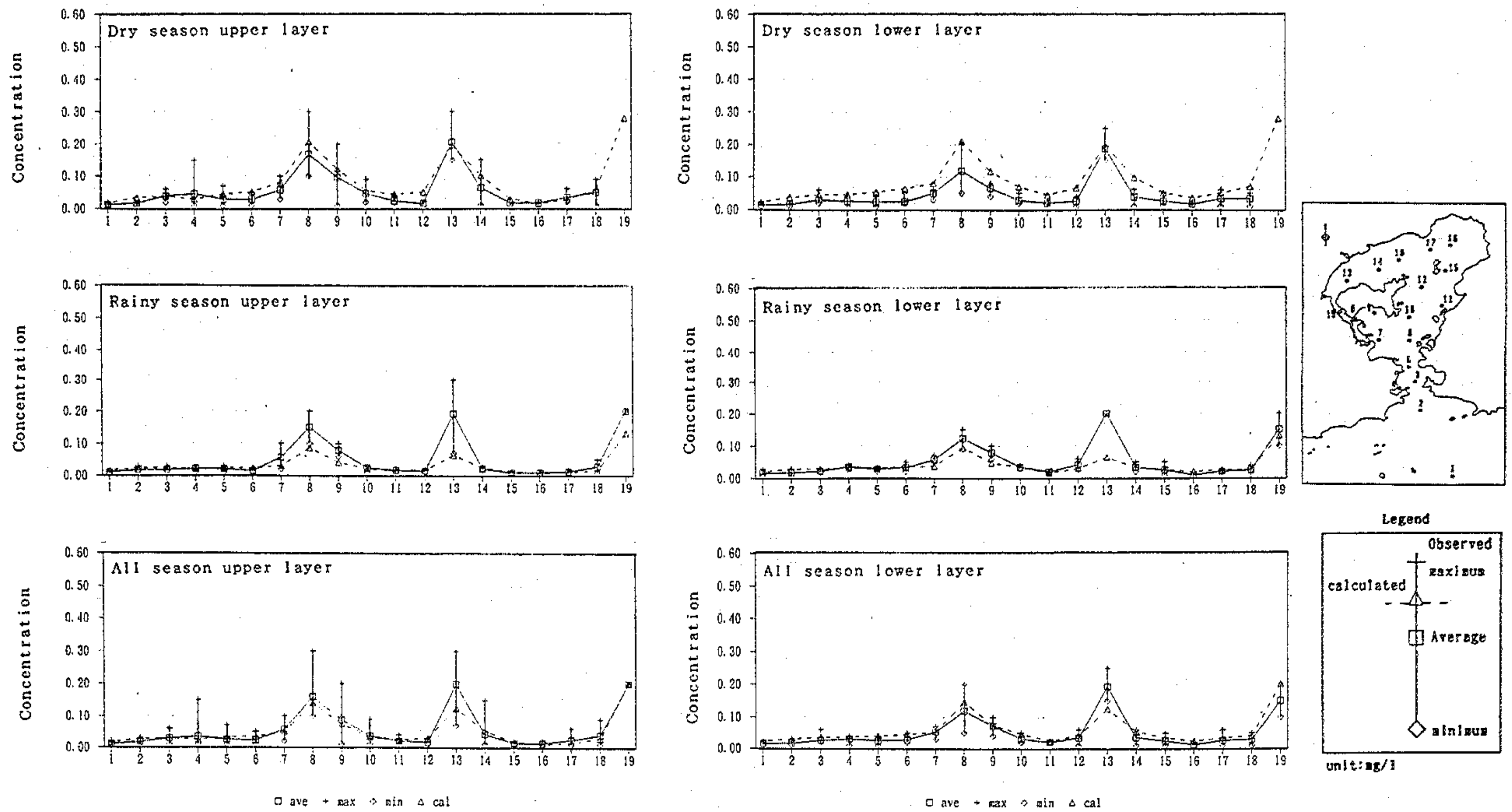

Fig. 2.6-4(3) Comparison of Observed and Calculated PO_4-P

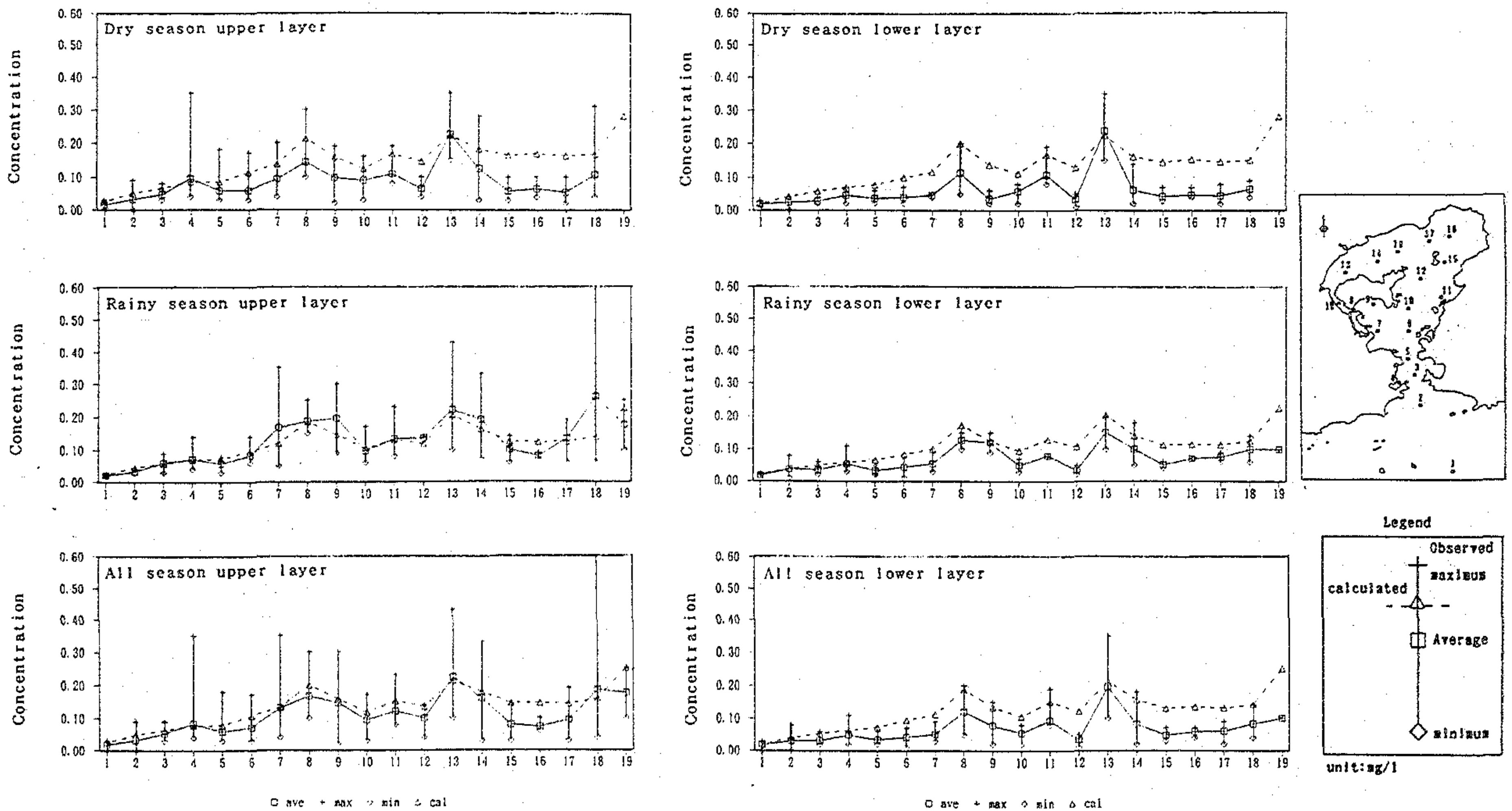

Fig. 2. 6-4 (4) Comparison of Observed and Calculated O-P

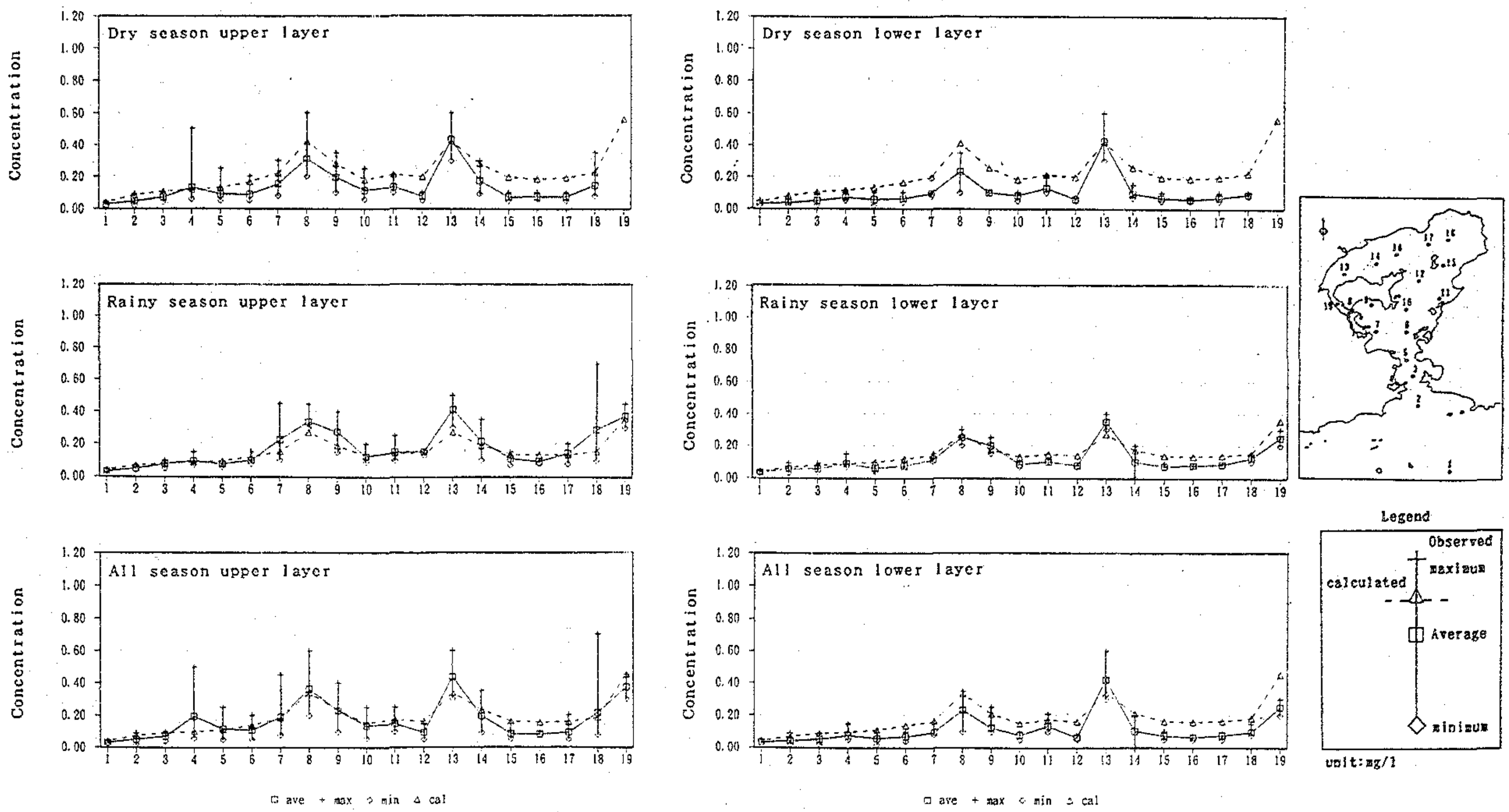

Fig. 2. 6-4(5) Comparison of Observed and Calculated T-P